Characterization of alcohol-containing dairy emulsions: Pseudo-ternary phase diagrams of sodium caseinate-oil-ethanol systems

by

Ginna Espinosa Martinez

A Thesis submitted to the Faculty of Graduate Studies of

The University of Manitoba

in partial fulfillment of the requirements of the degree of

MASTER OF SCIENCE

Department of Food Science

University of Manitoba

Winnipeg

I hereby declare that I am the sole author of this thesis.

I authorize the University of Manitoba to lend this thesis into other institutions or individuals for the purpose of scholarly research.

Ginna Espinosa Martinez

I further authorize the University of Manitoba to reproduce this thesis by photocopying or by other means, in total or in part, at the request of other institutions or individuals for the purpose of scholarly research.

Ginna Espinosa Martinez

Acknowledgement

To my advisor, Dr. Scanlon, thank you for your guidance and patience during the period of my master studies. Thank you for all the teachable meetings, this project would not have been possible without your support, I learn so much from you.

I would like to acknowledge to my committee members Dr. Fulcher and Dr. Cenkowski for sharing their knowledge over the course of my project.

I would also like to thank Michelle Stringer and other members of the Food Science department for their assistance during my studies.

I am grateful of the financial support from the Mexican *Becas MOB* Foundation and Dr. Scanlon.

I would like to thank to all my friends and family for their encouragement and support during the last two years.

Abstract

The physical properties and the stability of alcohol containing emulsions made with sodium caseinate using two types of oil, canola oil and coconut oil, were investigated. The region of emulsion stability was presented on ternary phase diagrams. Emulsion stability was limited to emulsion compositions in the range of sodium caseinate solutions between 32-68 %wt, oil contents between 10-53 %wt and ethanol concentrations from 8 to 32 %wt. The type of oil had a minor effect on emulsion stability, but stability was sensitive to ethanol content and casein/oil ratio. Emulsions were classified as Newtonian fluids, with high ethanol content (> 20 %wt) being low viscosity and those of low ethanol content (< 20 %wt) being of high viscosity. Analysis of emulsion droplet sizes showed that the presence of ethanol affected the average droplet size. From lipid oxidation determinations, there was no clear correlation between casein/oil ratio and concentration of lipid hydroperoxides

Table of Contents

List of Figures

List of Tables

1. Introduction

Dairy emulsions containing alcohol, cream, sugar, and flavors represent a type of alcoholic beverage called cream liqueurs. Since the development of those products during the 1980s, the stability and extension of their shelf life has been the subject of study. Creaming formation, serum separation at the bottom of the bottle, and formation of aggregates are the principal unstable behaviors investigated (Banks et al., 1981; Dickinson et al., 1989; Lynch & Mulvihill, 1997). Improvements in stability have been achieved by modification of the production process and cream liqueur formulation; for example, reduction of droplet size by high pressure homogenization, use of emulsifiers, and reduction of fat content (i.e., use of anhydrous milk fat instead of cream) (Dickinson et al., 1989b; Lynch & Mulvihill, 1997; Muir & Banks, 1986). A standard composition for these dairy products with at least 1 year of shelf life is 3% sodium caseinate, 15% milk fat, 14% ethanol and 20% sugar (Donnelly, 1987; Lynch & Mulvihill, 1997). Sodium caseinate has been reported as the emulsifier that shows the best performance for stabilizing emulsions containing alcohol due to its properties as water binder, viscosity enhancer, as well as its stability at high temperatures (Banks et al., 1981; Dalgleish & Law, 1988; Lynch & Mulvihill, 1997). Nevertheless, it is also documented that the functional properties of sodium caseinate are affected by the content of calcium ions and ethanol in the aqueous phase (Agboola & Dalgleish, 1996; Horne, 1987; Radford et al., 2004).

The use of milk fat in cream liqueur is a source of variability because milk fat contains a wide range of unsaturated and saturated fatty acids that governs its interactions with other ingredients (Marangoni & Lencki, 1998). Milk fat contains three melting point fractions: low, medium, and high. Long chain saturated fatty acids are present in the high melting fraction; short chains and unsaturated fatty acids in the low melting fraction, and both long

and short chains are present in the medium fraction (Marangoni & Lencki, 1998). The differences in composition might represent a factor to consider in the formulation of cream liqueur; variations in the solid fat content, in combination with process conditions such as preheating steps, may influence the presence of fat crystals in the fat globules which directly affects the stability of the emulsion due to partial coalescence (Fredrick et al., 2010).

The respective influences of sodium caseinate, fat and ethanol in a continuous phase represents a complex matrix. In this respect, the representation of the influence of one component (e.g., ethanol) on the behavior of a mixture of the other components (e.g., sodium caseinate, water and oil) at different concentrations can be characterized by the use of phase diagrams. Conceptually, phase diagrams are charts used to show the conditions at which the existence of phases can occur due to the relationships between the states of components (Predel et al., 2004). The lines that mark the conditions of equilibrium at which phases can co-exist are called equilibrium lines or phase boundaries. These diagrams can be used to represent the equilibrium of a single component (e.g., pressure-temperature diagrams of water) or multiple components under different conditions (e.g., protein-protein systems as a function of concentration). For a mixture of more than three components, it is convenient to describe the behavior of components on a phase triangle as a pseudo-ternary system where the ratio of two components remains constant (Predel et al., 2004). Figure 1.1 shows a representation of a ternary mixture, where components are A, B and C, and where each corner of the equilateral triangle represents a 100% component concentration (i.e., as pure component). As well, each side of the triangle represents a binary system. For example, for components A and C, the 100% point of C represents the 0% point of A and conversely, increments in the concentration of A represent a reduction in the concentration of C. Mixtures lying on this

line are binary, which means that the concentration of the third (B) component is equal to 0%. The point Q represents a composition with the three components mixed. In this case, the composition of each component corresponds to the parallel lines to each side of the triangle, such that the overall composition is equal to 100%. Thus, the point Q represents 30% A, 20%B and 50% C.

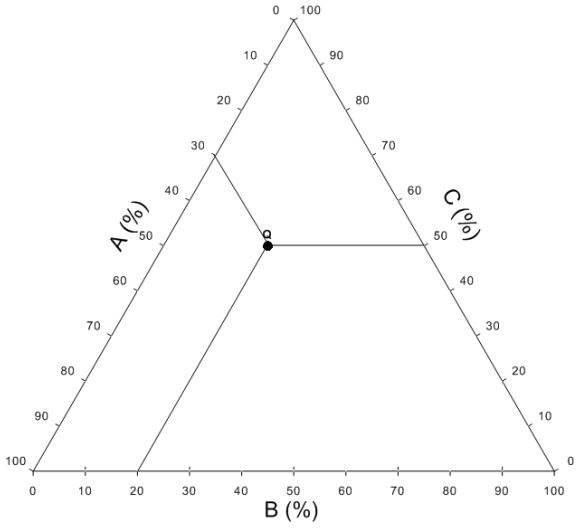

Figure 1.1 Model of ternary phase diagram where point Q represents a specific composition where the three components are mixed.

Previous studies on emulsions containing alcohol and sodium caseinate have focused mainly on the mechanisms promoting physical instability (i.e., flocculation, phase separation, creaming) (Dickinson & Golding, 1997; Dickinson & Woskett, 1988; Mezdour et al., 2006); the influence of protein concentration on the rheological behavior of casein stabilized emulsions (Bouchoux et al., 2009; Dickinson, 2001; Radford et al., 2004), and the interfacial oil-water layer composition (Dickinson, 2001; Euston & Hirst, 1999; Fang & Dalgleish, 1993). As well, these studies have been performed mainly with the use of nonfood grade oils (e.g., n-tetradecane) as the oil phase. There is less research about how

the three components, alcohol, food grade oil, and protein, interact in the continuous phase under a wide range of concentrations. Therefore, for this study, the complete range of a ternary phase diagram was evaluated using two types of food grade oil: canola and coconut oil. Those oils had been selected because they have different fatty acid profiles. Coconut oil is rich in saturated fatty acids while canola oil is mainly composed of unsaturated fatty acids (Chaiyasit et al., 2007). In others words, they represent the two predominant fractions (high and low) of fatty acids present in milk fat.

The objective of this study was to establish the complete phase diagram for the pseudo-ternary systems: sodium caseinate-ethanol-canola oil, a predominantly unsaturated oil, and the system sodium caseinate-ethanol-coconut oil, a predominantly saturated oil. After identifying the regions of emulsion stability, a characterization of this region by the determination of its rheological behavior, droplet size distribution and lipid oxidation was conducted. The characterization of the emulsion behavior in the stable region is used to explore and describe the main mechanisms affecting emulsion stability; special attention is given to the influence of ethanol on emulsion destabilization.

2. Literature Review

2.1 Casein

Casein is a milk protein fraction. Milk proteins are distributed in ~80% casein and ~20% whey protein fractions (Horne & Davidson, 1986). The principal fractions of whey protein are α-lactalbumin, β- lactoglobulin, bovine serum albumin, and immunoglobulins. Casein is mainly constituted by α_{s1}-,α_{s2}-, β- and κ-casein (Horne, 2006; Robson & Dalgleish,1987). Casein fractions are widely used in the food industry as emulsifiers.

2.1.1. Casein Structure

Casein is considered as a phosphoprotein due to its phosphoseryl residues. It is divided into four main fractions: α_{s1}-,α_{s2}-, β- and κ-casein in weight ratios of 4:1:4:1 (Farrer & Lips, 1999; Robson & Dalgleish, 1987). The major fractions are α_{s1}-, and β-casein. Casein proteins are also considered a non-globular protein with around 200 residues, including proline which inhibits the formation of tertiary structure. The absence of cysteine in α_{s1}-, and β- casein minimizes intramolecular crosslinks due to no formation of disulfide bonds and enhances the stability of α_{s1}- and β- casein at high temperature. The k-casein fraction contains only one phosphate residue in its amino acid sequence and this is responsible for the interactions with other casein fractions (Horne, 1998).

In solution, casein exhibits a flexible lineal conformation. As a monomer, α_{s1} and β- casein have a net negative charge at neutral pH (Dickinson, 1999). Although α_{s1} casein and β-casein have a similar structure, the arrangement of α_{s1}-casein in solution is less organized than of β-casein which affects its behavior at the interfacial layer in oil-in-water emulsions (Dickinson, 2001) (see section 2.2.4.1). As monomers, β- and κ-casein form soap-like micelles whereas α_{s1}- casein exhibits an open and more rigid aggregate structure as shown in Figure 2.1 (Farrer & Lips, 1999).

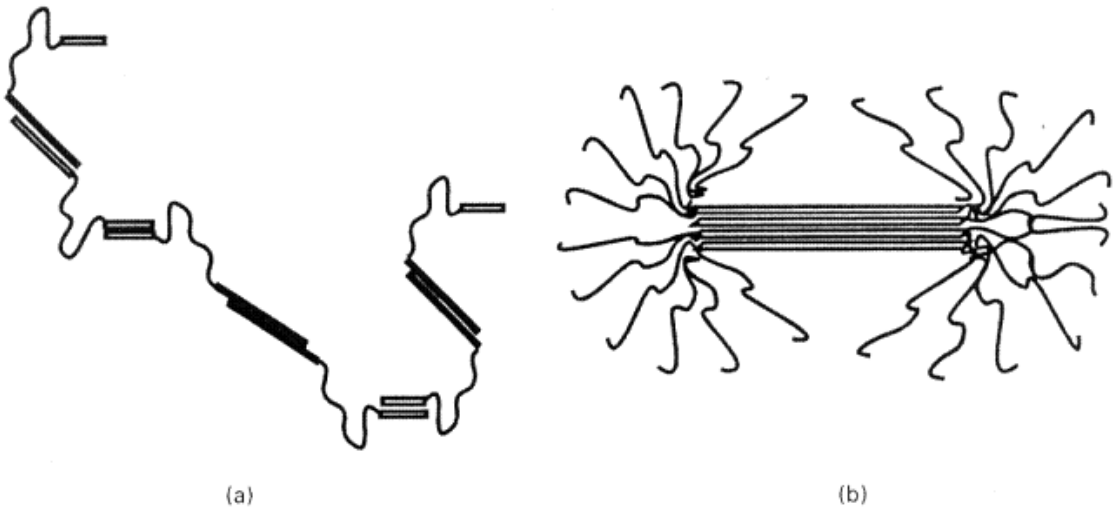

Figure 2.1 Schematic representation of (a) α_{s1} casein and (b) β casein, rectangular bars represent the hydrophobic regions of the protein. (Adapted from International Dairy Journal, v. 8, D.S. Horne, Casein interactions: Casting light on the black boxes, the structure in dairy products, p.172, Copyright (1998), with permission from Elsevier).

2.1.2. Casein Model

Several publications define casein micelles as associations of α- and β- casein stabilized by a layer of κ-casein with the micelle having a radius of 100 nm (Dalgleish & Law, 1988; De Kruif, 1999; Dickinson, 1999; Horne, 1998). The self association of casein fractions that determinate micelle formation has been the objective of various studies, and in this matter two models are the most prominent. The submicelle model described micelle formation as the result of the hydrophobic and electrostatics interactions. Hydrophobic interactions determine that casein proteins aggregate into subunits (15-20 molecules) and then those subunits interact with each other to create a micelle. Subunits rich in κ-casein stay on the micelle surface while subunits with low concentration of κ-casein stay on the internal side of the micelle (Figure 2.2) (Horne, 2006). Horne (2006) points out that the variation in the

density of k-casein on the surface is not well explained by this model. The other model extensively mentioned in the literature is the Holt model or the hairy micelle model, shown in Figure 2.3. It refers to casein micelles as a network joined by calcium phosphate groups; the growth in size is due to the crosslinking between subunits and the steric configuration of the casein (loop formation). This model suggests that α_{s1} and β casein crosslinkages lead structure formation and that κ-casein is located mainly as an external layer where tails that are negatively charged protrude into the surrounding solvent which would limit the interaction between the hydrophobic regions of the casein micelle with other adjacent micelles. The tails give to the casein micelle a charged hairy layer providing electrostatic stabilization to the casein micelle and minimizing casein aggregation. This hairy layer can be considered as a polyelectrolyte layer because it carries negatively charged groups that can be ionized by alterations in the quality of surrounding solvent (i.e., pH and ionic strength) that will affect the surface charge of the casein micelle and its electrostatic and steric stabilization (De Kruif, 1999; Holt & Horne, 1996). The growth in size of the casein micelles is also restricted by the hairy layer; once the hydrophobic region of the κ-casein interacts with other casein molecules no further increase can occur because the charged hairs of κ-casein cause micelles to repel each other (Horne, 1998). Therefore, if some destabilization behavior or change in medium conditions, such as acidification, heating or ionic strength, affects or disrupts the hairy layer, casein micelles lose their electrostatic and steric stabilization and start aggregating (De Kruif, 1999; Horne, 2006).

The hairy model has been shown to be a valid model for casein micelles present in either fresh milk or in dispersed forms like sodium caseinate (De Kruif, 1999; Dickinson, 1997).

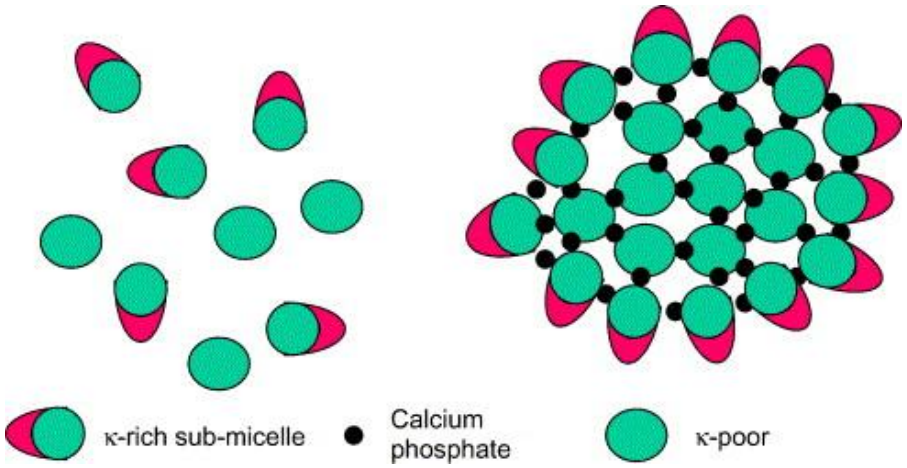

Figure 2.2 The submicelle model of the casein micelle (Adapted from Journal Current Opinion in Colloidal and Interface Science, v. 11, D.S. Horne, Casein micelle structure: Models and muddles, p.149 Copyright (2006), with permission from Elsevier).

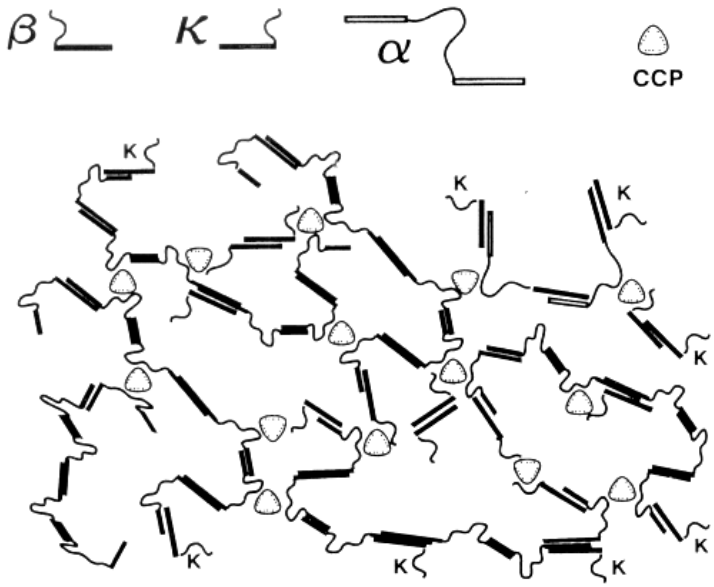

Figure 2.3 Model of casein micelle. Rectangular bars represents hydrophobic regions, loops represents hydrophilic regions with linkage by interaction of phosphoserine groups with colloidal calcium phosphate clusters (CCP), β-, α_{s}- and κ- casein fractions are represented in the model as indicated at the top of the figure. (Adapted from International Dairy Journal, v. 8, D.S. Horne, Casein Interactions: Casting light on the black boxes, the structure in dairy products, p.174 Copyright (1998), with permission from Elsevier).

2.1.3. Casein Micelle Interactions

A well accepted approach for describing casein interactions is by considering casein as a hydrophobic colloid of adhesive spheres where electrostatic repulsion and hydrophobic interaction governs its self-association as well as its behavior under unstable conditions such as low pH or rennet treatments (De Kruif, 1999; Horne, 1998). Thus, the interaction energy of individual caseins (i.e., α-, β-, and κ-casein) or their aggregates (i.e., casein micelles) is expressed as the sum of their electrostatic and hydrophobic interactions (Horne, 1998).

Electrostatic interactions between casein fractions occur when surface charge segments of the protein come close to each other causing an electrostatic repulsion. The distribution of the charges on the surface is sensitive to variation in aqueous composition, for example the presence of polyvalent ions such as Ca^{+2} and PO_4^{+3} affects the magnitude of the interaction, because ions modify the charge density of the protein, increasing the electrostatic attraction within segments inducing aggregation (Horne,1998). Altering the ionic strength of the medium by the presence of salt (e.g., NaCl) induces an electrostatic screening (Na^+ stays at the surface of COO^- group) and consequently the repulsion interaction decreases (McClements, 2004). On the other hand, hydrophobic interaction occurs when non-polar groups of protein tend to associate with each other as a response at attempting to minimize their contact with water molecules. The strength of the interaction is highly dependent on solvent conditions. Hydrophobic and electrostatic interactions govern the degree of aggregation of caseins. For example, a decrease in electrostatic repulsion enhances the interaction between casein fractions and it would increase the size of the casein micelle, in contrast, an increase in the pH of the medium increases the charge of the casein fractions affecting the electrostatic repulsion and therefore limiting the growth of the casein micelle (Horne, 1998). Hydrophobic interactions

have been also related with the collapse of the brush of κ-casein and as a consequence with alteration of the overall steric stabilization of the casein micelle. As was mentioned early, the κ-casein fraction contains phosphoserine residues that enhance its capacity to form ionic links with other segments of the casein micelle. In others words, the charged segment (C-terminal) of κ-casein interacts with the surface of other casein fractions restricting its growth, while the hydrophobic segment (N-terminal) forms ionic links to the rest of the micelle (De Kruif, 1999; Horne, 1998). This implies that a collapse of the hairy layer governs the steric stability of casein as well as its capacity to form gels (De Kruif, 1999).

2.1.4. Composition of Sodium Caseinate

Sodium caseinate is produced by acidification of milk at pH 4.6, the pH that is close to the iso-electric point of the casein, thus it causes the precipitation of the casein fraction and its dissociation from the calcium phosphate clusters. Then the precipitate is redissolved by increasing the pH up to neutrality. Sodium hydroxide or calcium carbonate are frequently used as alkali for increasing the pH, so that based on the counterion used, the product is called sodium caseinate or calcium caseinate (Dalgleish & Law, 1988; Pitkowski et al., 2008; Robson & Dalgleish, 1987). For industrial uses, it can be spray or roller-dried. The main fractions of sodium caseinate are α_{s1} and β- casein. Dalgleish & Law (1988) evaluated the differences between sodium caseinate and native casein and found that the acidification process and heat treatment during the drying stage may affect some phosphoseryl groups and decrease the sensitivity of the interactions of casein micelles with calcium ions when it is in the continuous phase.

Sodium caseinate in water solutions at neutral pH and high ionic strength (>100 mM) have a major fraction with a hydrodynamic radius of ~ 11 nm containing around 15 casein molecules (mainly attached to each other by hydrophobic interactions) and a small fraction

with a larger hydrodynamic radius of ~80nm (Pitkowski et al., 2008). Therefore, sodium caseinate in water solution can be described as a mixture of the individual casein molecules associating into differently sized micelles: spherical casein micelles of larger hydrodynamic radius, in equilibrium with spherical casein micelles of smaller hydrodynamic radius (also called casein submicelles) (Dickinson, 1999). The extent of aggregation in sodium caseinate is less marked than in fresh milk, because when casein is separated from fresh milk by precipitation, the aggregated structure of casein micelles is affected (Euston & Hirst, 1999; Robson & Dalgleish, 1987).

2.1.5. Rheological Behavior of Casein Suspensions

Casein solutions behave as polymer solutions where casein micelles are surrounded by solvent molecules (Bouchoux et al., 2009; Pitkowski et al., 2008). The rheological behavior of caseinate suspensions is concentration dependent. In the dilute regime (low volume fraction) the micelles have enough space to stay separate and the interaction is minimal. As concentration increases (high volume fraction) more casein micelles get closer for a given solution volume, so that the system becomes concentrated. In this regime, the interactions between casein micelles increase and the behavior of the solution starts changing from a liquid state to a solid state; at this point, casein solutions behave as a highly concentrated dispersion of casein micelles (Bouchoux et al, 2009; Dahbi et al, 2010; Pitkowski et al., 2008).

Sodium caseinate follows Newtonian behavior at concentrations below 100 g L^{-1} in the shear rate range of 10^{-1} to 10^{3} s^{-1}. In this regime, the viscosity is independent of the shear rate, which is also in agreement with the hard sphere model of casein where in the dilute regime micelles move mainly due to Brownian motion. At high concentrations (> 100 g L^{-1}),

behavior changes to shear thinning behavior until the maximum concentration as a liquid (c_{max}~178 g L^{-1}) is reached where the solutions turn to soft gels (Bouchoux et al., 2009).

The increment in the relative viscosity (n_r) as concentration increases is described by the equations (Bouchoux et al., 2009):

$$n_r = \left(1 - \frac{\varphi}{\varphi_{max}}\right)^{-2} \quad \text{or} \quad n_r = \left(1 - \frac{c}{c_{max}}\right)^{-2} \tag{1}$$

where φ represents casein volume fraction, c represents casein concentration and c_{max} a maximum concentration at which casein solutions move to a solid behavior. For a hard sphere model, a φ_{max} = 0.64 is considered for monodisperse spheres while φ_{max} = 0.78 is considered for a polydisperse dispersion. From casein dispersions, the literature reported that equation 1 describes the initial increment in viscosity when c_{max} is in the range of ~ 130-140 g L^{-1} which corresponds to a φ ~ 0.64 (Bouchoux et al., 2009; Pitkowski et al., 2008). Above this concentration when the casein volume fraction is close to φ ~ 0.78 the viscosity increments follow a power law behavior and hyperentanglement behavior has been observed because the formation of bonds between micelles at high concentrations produces a major resistance to deformation (Bouchoux et al., 2009). The concentration dependence of casein viscosity is also related with configuration changes in casein micelles from a hard sphere model into a soft solid model. The soft solid model refers to a casein dispersion approaching a close packing regime where the development of a soft gel network is started reflecting the formation of weak chains of micelle like aggregates (Bouchoux et al., 2009).

2.1.6. Effect of Ethanol on Casein Dispersions

The behavior of casein proteins in ethanol has been the subject of study due to the technological applications in preparation of cream liqueurs. Several attempts have been made to understand how the presence of ethanol in the aqueous phase affects the stability of cream liqueurs. The principal finding is that ethanol induces a collapse of the k-casein hairy layer affecting the steric stabilization of casein micelles (Horne, 1985; Horne & Davidson, 1986; Horne & Muir, 1990). As a result, a decrease in the hydrodynamic radius of the casein occurs that is proportional to the alcohol content (Horne & Davidson, 1986). The addition of alcohol to casein dispersions gradually induces aggregation of casein micelles. Some studies reported that ethanol concentrations above 10 %vol led to discernible changes in protein structure and reduction in hydrodynamic radius that caused negative effects on the functional properties of casein such as its efficiency as an emulsifier because casein micelles exposed to ethanol are more sensitive to precipitation (Horne & Davidson, 1986; Radford et al., 2004). In addition, casein in solutions containing ethanol is reported to adopt an α helix structure which reduces the contact between the amino acid groups and the solvent, hereby promoting protein-protein interaction (Dickinson & Woskett, 1988; Radford et al., 2004).

Horne and co-workers (Horne, 1984; Horne, 1987; Horne & Davidson, 1986) studied the effect of ethanol on casein micelles when the pH of the solution was adjusted to different values and when calcium was added. The stability of casein micelles towards aggregation decreased as Ca^{+2} was added (up to 20 mM) into solutions containing ethanol. It was also reported that addition of calcium and ethanol into skim milk lead to precipitation of calcium phosphate and therefore micelle destabilization was enhanced. Therefore, addition of calcium and ethanol each separately, or in combination, into casein solutions affects the

steric stabilization of casein micelles (Horne, 1984; Horne, 1987; Horne & Davidson, 1986).

2.1.6.1. Effect on Solvent Quality

Considering for a moment, the ethanol-water hydration process where there is a competition for bonding formation between solvent-solvent, solute-solute and solute-solvent. Ethanol-water interaction can be described as a minor formation of H-bond and a high rearrangement of solvent that leads to changes in water structure around the carboxyl side, and a second hydration on the hydroxyl group (Noskow et al., 2005). The result is a change in structural configuration of the ethanol-water mixtures that goes from an ethanol molecule surrounded by water molecules at low ethanol concentration (at this point there is an excess of H-bonding surrounding the ethanol molecules) to a high density of ethanol molecules at high ethanol concentrations, where water molecules are less available to form H-bonding in the region near to the ethanol molecules (Noskow et al., 2005).The ethanol-water hydration process produces changes in the dielectric constant (ε) of the mixture, decreasing from ~80 (pure water) to ~24 (pure ethanol), so that ethanol concentrations govern the changes in the dielectric constant (Mezdour et al., 2006).

The surface tension and viscosity are also changing as a function of the fractions of water and ethanol. The viscosity shows a non-linear dependence on concentration for ethanol and water mixtures. At a temperature of 20°C, viscosity increases from 1.004 mPa·s (0 %wt ethanol) to a maximum value of 2.980 mPa·s (46 %wt ethanol) and then it decreases to 1.202 mPa·s (100 %w ethanol) (Belda et al., 2004). The surface tension decreases with increasing ethanol fraction and also it is sensitive to temperature changes; it goes from 72.01 mN m^{-1} (0 %wt ethanol) to 21.82 mN m^{-1} (100 %wt ethanol) at 25°C (Vasquez et al., 1995). There is therefore a clear change in solvent quality due to the addition of ethanol.

2.1.6.2. Effect on Steric Stabilization

Studies conducted in casein suspensions to characterize the influence of ethanol on casein micelles have found that ethanol progressively reduces the hydrodynamic radius of casein micelles until a point where the changes in solvent polarity produce a rapid increment in the hydrodynamic radius and consequently casein aggregation is promoted (Figure 2.4) (Horne, 1985; Horne & Davidson, 1986). The reduction in the hydrodynamic radius represents a collapse in the casein hairy layer and as consequence a loss in its steric stability.

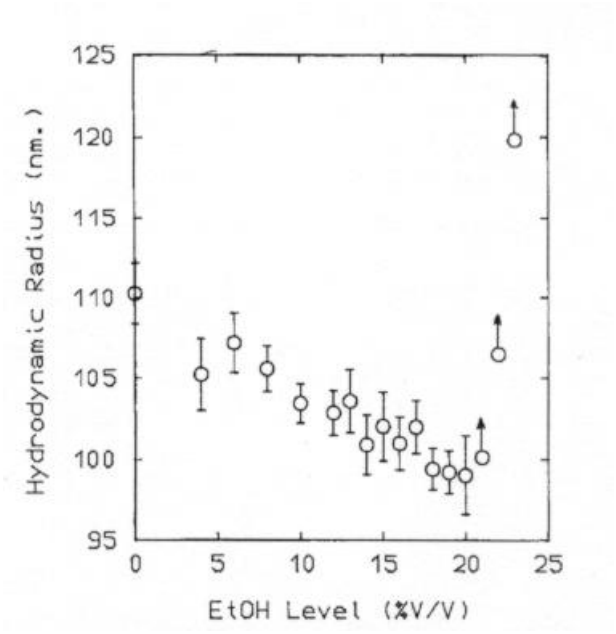

Figure 2.4 Influence of ethanol on the apparent hydrodynamic radius of casein micelles. Casein micelles are formed by hydration of skim milk powder in buffer solution at neutral pH (Adapted from Colloid & Polymer Science, v. 264, D. Horne & C.M. Davidson, The effect of environmental conditions on the steric stabilization of casein micelles, p.729 Copyright (1986) with permission from Springer). The arrow denotes progressively increasing of hydrodynamic radius.

Horne (1985) suggested two possible mechanisms to explain the reduction in the hydrodynamic radius: (i) casein micelles are dissociated into submicelles, (ii) there is a compaction of the hairy layer into the casein micelle. A first approach to evaluate the acceptability of these mechanisms was to observe if the presence of ethanol produced a reduction in casein molecular weight by turbidity measurement and protein content in the continuous phase over a wide range of alcoholic solution (up to 20 %v/v). No changes in turbidity of casein dispersions and protein levels in the continuous phase led to the conclusion that the reduction in hydrodynamic radius is not directly related either with a dissociation of casein or a reduction in molecular weight. In an attempt to explain the destabilization of casein micelles when they are exposed to ethanol, Horne & Davidson (1986) established a term called barrier thickness as the difference between the hydrodynamic radius of casein micelles measured in ethanol-free casein solutions versus the minimum hydrodynamic radius measured when casein micelles are exposed to ethanol solutions. The minimum hydrodynamic radius of casein represents the hydrodynamic radius of casein before aggregation occurs. Therefore it is associated with a critical level of ethanol required to cause the reduction of the casein micelle radius. This trend is shown in Figure 2.4, it can be seen that a minimum hydrodynamic radius of ~ 100 nm is reached at an ethanol level of 20 % v/v. The minimum radius is also called the core radius because it represented the radius at which the hairy layer will completely collapse.

The barrier thickness is sensitive to variations in environmental conditions such as pH, calcium content, and ionic strength. With respect to pH, Pierre (1989) pointed out that addition of ethanol into casein solutions induces a shift in the pH of the solvent that was dependent on the amount of ethanol added. Since electrostatic interactions between micelles are also sensitive to pH variations, as pH of the casein solution increases (pH range 6.0 to 7.5) electrostatic stabilization is favored so that more ethanol is required to

cause a collapse of the hairy layer. The range of pH 6.0 to 7.5 for casein solutions is close to the pK value of the casein phosphate groups. Therefore under this pH range, the electrostatic repulsion within the casein micelles prevents collapse of casein hairy layers and therefore more ethanol is required to destabilize the micelles (Horne & Davidson, 1986; Pierre, 1989). As a result, casein micelles became less compacted meaning that the thickness of the hydrodynamic barrier increases (Horne & Davidson, 1986). The resulting stability of the casein micelles also represented less cross-linking between adjacent casein micelles due to the electrostatic repulsion (Horne & Davidson, 1986; Pierre, 1989).

Regarding calcium content, as ethanol and Ca^{+2} increase in the casein solution, casein micelles are less stable towards aggregation because calcium and ethanol leads to precipitation of calcium phosphate (Horne, 1987). Horne and co-workers (Horne, 1985; Horne, 1987; Horne & Davidson, 1986) concluded that as the thickness of the barrier increases more ethanol is needed to induce hair collapse. A thicker barrier would therefore lead to a stable casein solution even at high ethanol concentration. In contrast, thinner barriers are more resistant to collapse; nevertheless they required less ethanol to reduce the hairy layer thickness to that of the core radius. The mechanism proposed by Horne is also supported by later studies (Donnelly, 1987; O'Kennedy, 2001; Pierre, 1989) where the influence and dependence of casein steric stability to a wide range of ethanol content, under different environmental conditions (i.e., ionic strength and calcium content) was reported. It was concluded that reduction in steric stabilization of casein micelles and ethanol content are directly related.

2.2 Emulsions

An emulsion is defined as a system composed of two immiscible liquids, one dispersed in the other (McClements, 2004). Oil and water are the two components most widely used, thus the emulsion composition can be oil in water (O/W), or water in oil (W/O). Since they are non-miscible liquids, energy barriers between molecules are high and interactions between them are weak which results in an unstable thermodynamic system, and they will tend to separate and form two layers; one rich in oil and one rich in water. Therefore, adding a third ingredient with amphiphilic characteristics, such as proteins, gums or carbohydrates, enhances interactions between the two phases improving the stability of the system (McClements, 2004). The energy input due to the presence of emulsifiers or due to homogenization overcomes the energy barriers (ΔG^*) associated with the mixture of two immiscible liquids (oil and water). This energy input causes the system to move from an unstable thermodynamic state to a thermodynamically stable state, until the system experiences another energy input that pushes it to move to a different energy level (McClements, 2004).

When emulsifiers are added into oil-in-water emulsions, emulsifier molecules bind to the oil droplet surface while other emulsifier molecules may remain in the continuous phase. If the emulsifier shows high affinity to the droplet surface, then hydrophobic interaction between emulsifier and oil are favorable. In contrast, a low affinity emulsifier preferably remains in the continuous phase (McClements, 2004). The free energy associated with the change in the thermodynamic state during emulsion formation is given by (McClements, 2004):

$$\Delta G_{formation} = \gamma \Delta A - T \Delta S_{configuration} \quad (2)$$

where γ is the interfacial tension, ∆A is the change in oil-water interfacial area, ∆S the entropy of configuration which indicates the changes in the oil and water arrangement during emulsion formation. The increase in contact area (∆A) multiplied by the interfacial tension has a positive sign because during emulsion formation, homogenization increases the contact area between oil and water; changes in the entropy term are negative because the arrangements of the oil and water phases after emulsion formation (addition of emulsifier) are favorable versus the possible arrangements of oil and water phases without emulsifier. The overall free energy of formation is dominated by the magnitude of the first term of equation 2 so that the free energy has a positive sign which is thermodynamically unfavorable (McClements, 2004). Therefore the free energy during emulsion formation does not give information about emulsion stability. Emulsion stability is related to kinetic stability because it describes the changes in emulsion characteristics over time.

2.2.1. Emulsion Formation

Oil-water systems are converted into emulsions by applying mechanical energy; hence oil disperses into water forming small droplets. The mechanical energy is applied using homogenizers. Based on the type of homogenizer, and the process conditions (i.e., feed rate, temperature and number of passes) the mixture (O/W) can be exposed to several turbulent fields which have a direct effect on droplet collision and droplet size distribution (McClements, 2004; Mohan & Narsimhan, 1997).

During homogenization two physical processes may take place: droplet disruption and droplet coalescence (McClements, 2004). Droplet disruption refers to the deformation of the droplet causing a change in its shape or breaking it up into smaller droplets, while droplet coalescence refers to the formation of large droplets during homogenization due to droplet-droplet collisions. The pressure applied during homogenization may be large

enough to avoid the joining of small droplets into larger ones in order to minimize droplet coalescence. When an emulsifier is added into the system, the interfacial tension between oil and water is reduced and the pressure required to break up the droplets is lessened (McClements, 2004; Mohan & Narsimhan, 1997).

Other important factors affecting emulsion formation are: the oil content, emulsifier concentration and emulsifier efficiency. Oil concentration is frequently reported as oil volume fraction (ϕ). It expresses the concentration of oil droplets per volume of emulsion $V_{oil} / V_{emulsion}$. This ratio can be described in terms of the dispersed and continuous volume fractions by the following equation (McClements, 2004):

$$\phi = \frac{\phi \rho_C}{\phi \rho_c + \rho_{oil}(1-\phi)} \quad (3)$$

where ρ_c and ρ_{oil} are densities of the continuous and oil phase, respectively.

2.2.2. Droplet Size Distribution

The droplet size is a useful parameter in emulsion characterization because changes in the droplet size can be related to the development of unstable behaviors. There are different ways to analyze the droplet sizes of emulsions. Static light scattering is widely used because it allows analyses of emulsion with droplet diameters between 20 nm and 2000 μm (MasterSizer 2000 user manual). The mean diameter of droplets in an emulsion is determined under the view that an emulsion behaves as a polydisperse system (i.e., the emulsion is composed of a range of droplet sizes) and that droplets tend to be spherical because this shape is thermodynamically favorable. A convenient form to represent the size distribution is a histogram where each bar represents a size class (McClements,

2004). The two mean diameters widely used are: surface-average mean diameter, d_{32}, equation 4, and volume fraction mean diameter, d_{43}, equation 5.

$$d_{32} = \frac{\sum n_i d_i^3}{\sum n_i d_i^2} \quad (4)$$

$$d_{43} = \frac{\sum n_i \, d_i^4}{\sum n_i \, d_i^3} \quad (5)$$

where n_i represents the number of droplets in a given size class and d_i the respective diameter.

The mean diameter is sensitive to variation in homogenization process, emulsion formation, type of emulsifier, and oil concentration. Once the mean diameter is known for a given oil volume fraction (ϕ) it is possible to calculate the surface area (A_N) of the droplets in contact with the continuous phase by the following equation (McClements, 2004):

$$A_N = \frac{6\phi}{d_{32}} \quad (6)$$

Equation 6 shows that small droplet sizes give high surface areas, so that formation of small oil droplets during homogenization allows more emulsifier to be in contact with the oil phase. As was mentioned earlier, the concentration of emulsifier also affects droplet size. It must be enough to cover droplet surfaces to avoid coalescence; likewise, the rate at which emulsifier is adsorbed on the droplet influences its efficacy and surface coverage (Γ, expressed in mg m^{-2}) (McClements, 2004; Mohan & Narsimhan, 1997). Considering a polydispersed emulsion with a given oil and emulsifier concentration the maximum surface area that the emulsifier covers is directly related with the mean volume droplet size (McClements, 2004). In an ideal alcohol-free sodium caseinate stabilized emulsion with a

ϕ of 0.3 the surface coverage reported is 3 mg m^{-2} (Dickinson & Golding, 1997b; Fang & Dalgleish, 1993).

2.2.3. Time Dependent Destabilization Behaviors

As was mentioned earlier, emulsions are an unfavorable thermodynamic system; however they can achieve long term stability because they can reach a stable kinetic state. To understand emulsion stability over time it is convenient to view an emulsion as a dynamic system where droplet interactions play an important role in the development of destabilization behaviors (McClements, 2004).

2.2.3.1 Gravitational Separation

Gravitational separation refers to the phase separation that may occur over time due to the differences in densities between the oil and continuous phase. Oil droplets will tend to move upward while water will tend to move downward (McClements, 2004). In an oil-in-water emulsion, oil droplets migrate to the top of the emulsion surface enhancing creaming and flocculation whereas in water-in-oil emulsions the difference in densities promotes water movement rapidly to the bottom causing sedimentation.

A spherical oil droplet is subject to gravitational forces acting on it due to the difference in density with its surroundings so that the droplet moves upward. As it moves there is also a frictional force acting opposite to the gravitational force affecting its mobility. This is expressed through Stokes' law equation as follows (McClements, 2004):

$$V_{Stokes} = -\frac{2gr^2\,(\rho_{oil}-\rho_c)}{9\eta_c} \qquad (7)$$

where V_{Stokes} is the creaming velocity, g is the gravitational acceleration, ρ_c the density of the continuous phase, ρ_{oil} the density of the dispersed phase, r represents the radius of the droplet and η_c the shear viscosity of the continuous phase. The sign of V_{Stokes} indicates whether the droplet moves to the top of the emulsion, in which case V_{Stokes} is positive and oppositely, when the droplet moves to the bottom, the sign is negative (McClements, 2004). Also it can be seen that the velocity of the droplets depends on the droplet radius so that larger droplets have larger velocities of creaming (Euston & Hirst, 1999; McClements, 2004). The physical principle denoted in equation 7 is suitable for explaining creaming and sedimentation behaviors.

2.2.3.2. Creaming and Sedimentation

According to Stokes' law (equation 7) droplet size has a square dependence on the creaming velocity so that larger droplets tend to move faster than smaller ones, until they cannot move anymore when they form a creaming layer (McClements, 2004). Over time this movement creates a droplet distribution throughout the emulsion with a transition state where three layers may be observed, a cream layer rich in large droplets, an intermediate layer where droplets with lower creaming velocities stayed, and a serum layer with small droplets. As more droplets are moving upward the boundary between the intermediate layer and the serum layer will disappear resulting in a two layer system: a cream layer at the top of the emulsion surface and a serum layer at the bottom (McClements, 2007). In polydisperse emulsions the serum layer usually is observed as a cloudy layer because small droplets may remain in this phase. On the other hand, the accumulation of droplets in the cream layer can initiate the formation of a neck plug which has been reported as a physical instability in emulsions containing alcohol (Banks & Muir, 1985; Banks et al., 1981; Dickinson & Golding, 1997; Dickinson et al., 1989). The thickness of the cream layer depends on the range of repulsive and attractive droplet-droplet interactions. When

attractive interactions between droplets are weak, their arrangement may easily change over time so that as more droplets arrive at the surface of the emulsion, they find enough space to stay on the top of the emulsion producing a thin cream layer. In contrast, strong attractive interactions lead to droplet attachment to each other resulting in a thicker cream layer. Since the attractive interactions are large as soon as droplets arrive at the surface, they remain together leaving less empty space for further droplets to reach the surface of the emulsion. As a result, as more droplets come close to the surface they cannot move further so that they pack together forming a relative thick cream layer (McClements, 2007). Environmental conditions may also induce or retard the movement of droplets and therefore creaming rates. Specifically for sodium caseinate, a concentration dependence in the development of a cream layer over a period of time has been reported where creaming rates are highly influenced by depletion flocculation and the presence of unadsorbed protein in the continuous phase (Dickinson et al.,1989; Euston & Hirst, 1999; Hemar et al., 2003; Ye, 2008). For example, Dickinson et al. (1997) evaluated creaming formation in oil-in-water emulsions (35-45 vol% oil) made with different sodium caseinate content, and concluded that there is a critical protein concentration at which creaming is enhanced. In the study of Dickinson et al. (1997), the most stable system against creaming was found at 2 %wt sodium caseinate content. Above this concentration creaming and sedimentation occurred. Nevertheless, it was also reported that at higher protein concentrations (6 %wt) a gel network developed and creaming velocity was reduced. These results point out the nonlinear relationship between protein content and gravitational separation. Therefore, parameters such as protein surface coverage and composition of the interfacial layer have been also related with unstable behaviors like creaming.

2.2.3.3. Depletion Flocculation

To Asakura & Oosawa (1954) is attributed the first observation of depletion flocculation in a colloidal system (Jenkins & Snowden, 1996; Radford & Dickinson, 2004; Tuinier & De Kruif, 1999). The system that serves as model for the study of the depletion mechanism consisted of unadsorbed species added to a colloidal solution (Mao et al., 1995; Jenkins & Snowden, 1996; Vincent, 1990). Since then, the depletion mechanism has been used to understand the stability of different systems including oil-in-water emulsions. Oil droplets of radius a, represent the spherical entities of a colloidal solution, and unadsorbed casein micelles with a radius of gyration, R_g, represent the unadsorbed species added to a colloidal solution (Figure 2.5).

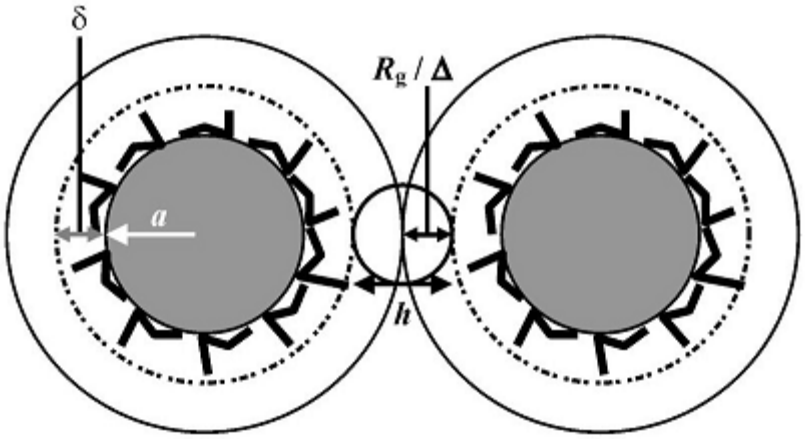

Figure 2.5 Schematic diagram of depletion flocculation mechanism, a represents the radius of spherical droplets, Δ the depletion layer thickness with magnitude equal of the radius of gyration of unadsorbed casein micelles, R_g, h represents the distance between the two adjacent droplets and δ the interfacial thickness (Adapted from Journal of Colloid and Interface Science, v. 274, Radford et al., Stability and rheology of emulsions containing sodium caseinate combined effects of ionic calcium and alcohol, p.684 Copyright (2004), with permission from Elsevier).

Droplets approach together until a point at which the gap, also called the interstitial space, between them is less than the diameter of the unadsorbed casein micelles. At this point, the unadsorbed casein micelles surrounding the droplets are excluded creating a depletion layer (Δ), where only solvent is present. Thus, the concentrations of unadsorbed casein micelles increase in the surrounding area and produce an osmotic pressure gradient (ΔP_{osm}). As a result, droplets are pushed into contact, and an overlap area with a characteristic overlap volume ($V_{overlap}$) is defined.

The unadsorbed casein micelles are postulated to be excluded from the interstitial space and generate an osmotic pressure gradient described by (Radford & Dickinson, 2004):

$$P_{osm} = \frac{NRT}{M} \qquad (8)$$

where N represents the number concentration of the unadsorbed casein micelles in the bulk phase, M the molecular weight of the unadsorbed casein micelles in the bulk phase, *R* is the molar gas constant and *T* is the temperature.

The depletion interaction energy (U_D), as a function of the droplet radius (a), the radius of the unadsorbed casein micelles (R_g) and the distance between the two adjacent droplets (h) is described by:

$$\begin{aligned} U_D &= -\frac{4\pi}{3}\left(a + R_g\right)^3 \left[1 - \frac{3h}{4\left(a+R_g\right)} + \frac{h^3}{16\left(a+R_g\right)^3}\right] P_{osm} && h < 2\left(a + R_g\right) \\ U_D &= 0 && h \geq 2\left(a + R_g\right) \end{aligned} \qquad (9)$$

It can be seen from equation 9 that the Asakura & Oosawa model predicts that the interaction energy is raised continuously with the concentration of unadsorbed casein micelles in the bulk phase. Therefore, the model is unable to predict changes in the depletion interaction potential at high concentration of unadsorbed casein micelle where

for a colloidal system stabilization towards depletion flocculation has been reported (Jenkins & Snowden, 1996; Vincent, 1990). Equation 9 also shows that the depletion energy is governed by the magnitude of the osmotic pressure gradient and the sizes of the droplets and unadsorbed casein micelles.

The size of the unadsorbed casein micelles plays an important role in the range of the depletion interaction. The value of R_g indicates the thickness of the depletion layer (Δ) as indicated in Figure 2.5 (Radford & Dickinson, 2004). Thus, it can be inferred that large values of R_g give large depletion interaction, although the concentration and shape of the unadsorbed casein micelles also affects the range of the interaction (Berli et al., 2002; Jenkins & Snowden, 1996; Radford et al., 2004).

The limitation of the Asakura & Oosawa model for describing the changes in depletion energy at high concentration of the unadsorbed species and the influence of the unadsorbed species and sizes of the spherical entities on the magnitude of the depletion energy have been considered in subsequent theoretical models developed to describe depletion flocculation. In this matter, two main lines have been followed: models which mainly consider the excluded volume effect that takes place at the interstitial space as the leading factor for depletion flocculation, and models which suggest a proportional reduction in the concentration of the unadsorbed species (density profile) in the interstitial space as the gap is reduced (Jenkins & Snowden, 1996; Radford & Dickinson, 2004 Vincent, 1990).

In particular for oil-in-water emulsions, the destabilization due to the generation of depletion forces is a driving force for flocculation because when the depletion interaction energy is enough to push two adjacent droplets together it induces floc formation (Dickinson & Golding, 1997; McClements, 2004). The maximum depletion interaction

energy can be estimated when the distance between two adjacent droplets is equal to zero, h=0, which corresponds to the maximum energy required to bring two originally non-interacting droplets together (McClements, 2004):

$$U_D = -2\pi R_g^2 P_{osm} \left(a + \frac{2R_g}{3}\right) \qquad h = 0 \qquad (10)$$

Equation 10 can be used to predict the interaction energy (in kT units) in order to have depletion flocculation between droplets for a given size and unadsorbed casein micelles of a specific molecular weight.

2.2.3.4. Theoretical Models of Depletion Interaction

Starting with the key premise of excluded volume effects: Vrij (1976), Sperry (1984), Walz & Sharma (1994) and Mao et al.(1995) presented interesting modifications to the Asakura & Oosawa model. The authors give special emphasis to resolving the limitation of the Asakura & Oosawa model at high bulk concentration of unadsorbed species where depletion stabilization can be reached (Jenkins & Snowden, 1996). Vrij (1976), and years later, Walz & Sharma (1994) redesigned the model incorporating a second virial coefficient (B_2) to express the changes in the magnitude of the osmotic pressure for a given volume fraction of unadsorbed species. According to the Vrij model the second virial coefficient has a negative sign and becomes more negative as the volume fraction of unadsorbed species increases; thus there is a decrease in the range of osmotic pressure gradient and as consequence a decrease in the depletion force (Jenkins & Snowden, 1996; Tuinier & De Kruif, 1999). The approach of Mao et al. (1995) is similar to Vrij (1976) and Walz & Sharma (1994), but they used a third order virial coefficient. This model forecast a kinetic stabilization at high concentrations of unadsorbed species under the assumption that as more unadsorbed species are added, there is a critical concentration of unadsorbed species to reach a depletion stabilization. The stabilization to depletion flocculation results

because at high concentrations, some unadsorbed species may remain in the interstitial space producing a “second” osmotic pressure gradient that compensates for the osmotic gradient generated for the unadsorbed species that stay in the bulk solution resulting in an overall reduction in the interaction depletion energy (Radford & Dickinson, 2004). Sperry (1984) introduced a critical volume fraction ($\Phi^{\dagger}$) of unadsorbed species to describe the changes in the depletion interaction energy as concentration increases. It changes with the radius of the unadsorbed species (R_g), that is, as radius (R_g) increases a lower critical volume fraction ($\Phi^{\dagger}$) is required to generate depletion flocculation.

The segment density profile models described by Vincent (1990) and Fleer et al. (1984) have calculations of the changes in the depletion interaction energy (U_D), as a function of the distance h, and the concentration of unadsorbed species, under the assumption that unadsorbed species close to two adjacent spherical entities may be not totally excluded from the interstitial space. Therefore the osmotic pressure gradient generated due to the unadsorbed species that reside in the bulk solution may cause a compression of the unadsorbed species closer to the interstitial space, so that the thickness of the depletion layer changes as the bulk concentration of unadsorbed species increases (Vincent, 1990; Jenkins & Snowden, 1996). The theoretical calculation of U_D at different critical volume fractions ($\Phi^{\dagger}$) of unadsorbed species as a function of the distance between the two adjacent spherical entities (h), predicted a primary minimum of depletion interaction energy at small values of h, and a maximum of depletion interaction energy as the distance, h, increases. The maximum of depletion interaction energy becomes larger as the concentration of unadsorbed species increases (Vincent, 1990).

2.2.3.5 Ostwald Ripening

Ostwald ripening occurs when large droplets grow in size due to mass transport from smaller droplets to larger ones, so that small droplets disappear as large droplets increase in size (Hemar & Horne, 1999; McClements, 2004). Higher solubility of the dispersed phase in the continuous phase increases the rate at which this phenomenon occurred. As a result the mass transportation of the dispersed phase from small droplets to larger droplets through the continuous phase is favoured (McClements, 2004). Therefore in oil-in-water emulsions, insoluble oils help to retard the ripening process. For example, oil-in-water emulsions containing triglycerides are more resistant to the ripening process than emulsions containing flavour oils (e.g., limonene) because triglycerides are less soluble in water than flavour oils (Dickinson, 2009). Furthermore, the Ostwald ripening process is highly related with unstable behaviors found in emulsions containing alcohol due to the effect of ethanol on the solubility of the dispersed phase (see section 2.2.5.2).

The LSW theory, proposed by Lifshitz & Slyozov and Wagner in 1961 described the development of Ostwald ripening as a shrinkage and growth process which causes the droplet distribution to rapidly increase over time at a rate proportional to the cube of the mean droplet radius ($\bar{r}^3$) (Hemar & Horne, 1999; McClements, 2007). The rate of droplet growth is described as:

$$\frac{d\bar{r}^3}{dt} = \frac{8\gamma D V_m}{9RT} \qquad (11)$$

where $\bar{r}$ represents the average droplet radius, D the diffusion coefficient of the dispersed phase through the continuous phase, γ the interfacial tension at the interfacial layer, V_m the molar volume of the dispersed phase, R the gas ideal constant and T the temperature. Equation 11 has been reported to give lower rates of droplet growth than experimentally obtained in oil-in-water emulsions (Dickinson et al, 1999; Hemar & Horne 1999;

McClements, 2004; Radford et al., 2004). However studies conducted to evaluate the ripening process in oil-in-water emulsion had reported a lineal growth in the cube of droplet radius over time as LSW theory predicted; therefore changes in droplet size over time can be used to monitor the development of Ostwald ripening (Dickinson et al., 1999; Radford et al., 2004).

2.2.4 Oil in Water Emulsions Stabilized by Casein

The casein structure described in section 2.1.1 gives casein good qualities as an emulsifier because its hydrophobic segments easily attach to the oil droplet surface creating the interfacial layer required to stabilize the oil in water system (Dauphas et al., 2008; Dickinson, 1999). The efficiency and performance of casein in oil-in-water emulsions is widely reported in the literature, and studies have been extended to evaluate the surface properties of specific casein fractions, such as α_{s1} and β-caseins, and the behavior of casein micelles obtained from fresh milk or after industrial processes, such as those applied to manufacture sodium caseinate (Dauphas et al., 2008; De Kruif, 1998; Dickinson, 1999; Dickinson, 2001; Horne, 1998; Horne & Davidson, 1986).

2.2.4.1 Interfacial Properties and Adsorption Behavior

The main fractions of casein, α_{s1}- and β-casein, exhibit differences in their adsorption behavior (Dickinson, 1999). Beginning with the adsorbed behavior of β-casein, its structure at the interfacial layer is represented in a train-loop-tail model. Trains and loops in contact with the surface of the droplets represent the predominantly hydrophobic segments of the casein fraction while tails represents the hydrophilic segments projecting into the aqueous phase (Figure 2.6) (Dickinson, 1999; Dickinson, 2001, McClements, 2004). The amino acid sequence of β-casein is highly responsible for its adsorptive behavior where the charged residues attached to the N terminal of the chain are protruding into the continuous

phase while the rest of the molecule is joined to the hydrophobic surface of the droplet (Dickinson, 1999; Dickinson, 2001; Husband et al., 1997). Dickinson (1999) described the adsorbed layer of β-casein as a random distribution of polar, non- polar and charged regions among the protein chain. For α_{s1}-casein, its hydrophobic and hydrophilic segments are more randomly organized than in β-casein and this gives to α_{s1}-casein a loop-like configuration where its hydrophilic residues are sufficiently exposed to the continuous phase and separate from its hydrophobic residues that are attached to the droplet surface (Figure 2.6 b) (Dickinson, 1999). This configuration causes the α_{s1}-casein to form a loop instead of a long tail. The adsorbed configuration described for β- and α_{s1}-casein illustrated that the distribution of the charged residues along the protein chain affects the conformational arrangement of the protein on the droplet surface.

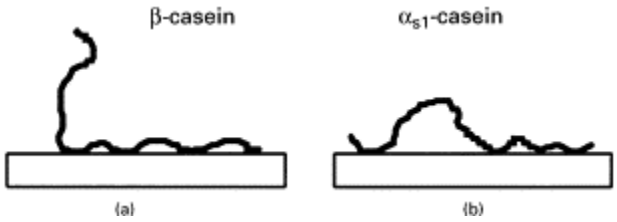

Figure 2.6 Adsorbed configuration of (a) β-casein and (b) α_{s1} casein on a hydrophobic surface (rectangular bars) (Adapted from International Dairy Journal, v. 9, Dickinson, E. Casein in emulsions: interfacial properties and interactions, p.308 Copyright (1999), with permission from Elsevier).

The configuration model described above for a monomeric adsorbed layer of α_{s1} and β, casein turns to a competitive behavior when mixtures of individual fractions are used as

emulsifier. In oil-in-water emulsions when mixtures of α_{s1} and β-casein are added with α_{s1} casein the major fraction, the surface coverage is reported to increase when α_{s1} casein is replaced by β-casein. For example at 98:2 α_{s1} casein/ β-casein ratio, a surface coverage of 4.9 mg m^{-2} is reported while at a 100:0 α_{s1} casein/ β-casein ratio, a surface coverage of 1.2 mg m^{-2} is reported for emulsions prepared with 45 %vol n-tetradecane and 5 wt% total protein. A mass balance would suggest that all the β-casein stays in the oil-in-water interface (Casanova & Dickinson, 1998). An explanation for the changes in surface coverage is that when a mixture of casein fractions (i.e., casein micelles) is used instead of individual casein fractions, it leads to a packed surface coverage where a multilayer arrangement around the surface of the oil droplet probably takes place (Casanova & Dickinson, 1998; Dickinson, 1997), or individual caseins adsorb randomly pack around the oil surface (Fang & Dalgleish, 1993; Srinivasan et al., 1999).

The interfacial properties of casein are therefore sensitive to the self-assembly and the composition of the adsorbed layer where environmental conditions may affect the state of aggregation at the interfacial layer (Casanova & Dickinson, 1998; Dickinson, 1999; Euston & Hirst,1999; Fang & Dalgleish, 1993; Robson & Dalgleish, 1987). The surface coverage reported in the literature increases as the total concentration of casein increases up to ~3-4 %wt casein concentration, but after that the increase in surface coverage is small. As can be seen in Table 2.1 the maximum surface coverage in sodium caseinate stabilized emulsion is 3 mg m^{-2} and after this concentration the adsorption of casein is restricted (Casanova & Dickinson, 1998; Fang & Dalgleish, 1993; Srinivasan et al., 1999). Fang & Dalgleish (1993) reported the minimum value of surface coverage required to have a stable emulsion is ~ 1 mg m^{-2}, and mentioned that the changes in the concentration of adsorbed protein are correlated with the difference in the emulsion layer thickness. At low concentration of adsorbed casein where the surface coverage was the order of 1 mg m^{-2} ,

the adsorbed layer was reported to be ~ 5 nm thick while at high concentrations of adsorbed casein, where the surface coverage was the order of 3 mg m^{-2}, the adsorbed layer was reported to be ~10 nm thick.

Table 2.1 Surface coverage (Γ) in caseinate stabilized emulsions with different emulsion compositions.

System	Surface Coverage mg m^{-2}	Reference
45%vol n-tetradecane 5%wt α_{s-1} Casein	1.2	Casanova & Dickinson (1998)
45%vol n-tetradecane 5%wt β Casein	1.1	Casanova & Dickinson (1998)
30%vol n-tetradecane 4%wt sodium caseinate	3.19	Radford, Dickinson & Golding (2004)
20%vol soya oil 0.3% Casein from skim milk	~1.0	Fang & Dalgleish (1992)
20%vol soya oil 2% Casein from skim milk	3.0	Fang & Dalgleish (1992)
30 % soya oil 4% sodium caseinate	~2.0	Srinivasan, Singh & Munro (1999)
35%vol n-tetradecane Sodium caseinate (% wt)		
1	1.4	
2	2.4	Dickinson & Golding (1997)
3	3.0	
4	3.1	
5	3.2	
6	3.3	

2.2.4.2 Influence of Environmental Conditions on Emulsion Stability

When the pH in the continuous phase is far away from the isoelectric point of casein, the charge density of the protein at the interfacial layer is high. Repulsive interactions between droplets are favoured and droplet collision is minimized so that the emulsion is less susceptible to flocculation and creaming (Dickinson, 2001).

Increasing the ionic strength, by adding salt, for example, causes a reduction in the electrostatic stabilization of the droplets because the charges at the interfacial layer are screened, reducing the repulsive interactions so that attractive interactions may be high enough (depending on salt concentration) to induce flocculation (Dickinson et al.,1997).

At low protein content, just enough for surface coverage and with an oil content of ~35-45 %vol, the adsorbed layer can be easily disrupted and the emulsion can be susceptible to flocculation and coalescence (two or more droplets come together forming a larger droplet). Emulsions made with low protein content and lower oil fractions (i.e., less than 35 %vol) will be unstable against bridging flocculation which refers to the formation of bridges between two or more droplets. Bridging is enhanced at low protein contents because oil is less covered by protein which allows attractive interaction between oil droplet surfaces. This condition may be accompanied by emulsion separation over time (Dickinson et al., 1997; McClements, 2004). As the protein content increases, such that there is an excess of protein in the continuous phase, depletion flocculation is the main unstable behavior. Nevertheless, the protein source used (e.g., skim milk power, sodium caseinate) has an impact on the concentration required to induce flocculation. Euston & Hirst (1999) reported that emulsions stabilized by skim milk powder were more stable towards depletion flocculation (in the range of 0.2 to 8 %wt of skim powder) because emulsions stabilized with skim milk powder tended to form larger protein aggregates which decreases the

magnitude of the osmotic pressure gradient and therefore the magnitude of the depletion interaction energy. In contrast, emulsions stabilized by sodium caseinate were reported to be more sensitive to depletion flocculation at high protein concentration.

The presence of calcium ions in the continuous phase has been reported to retard depletion flocculation at low concentrations (5-8 mM) (Dickinson & Golding, 1998; Dickinson et al., 2003). The implied mechanism is that calcium ions join to the phosphoserine residues of casein, changing its structural conformation and charge distribution; both factors may lead to unadsorbed casein moving into the interfacial layer. This reduces the number density of unadsorbed casein molecules, resulting in a decrease in the magnitude of the osmotic pressure gradient (equation 8), and as consequence the depletion forces are weak (Dickinson et al., 2003).

In summary, a change in environmental conditions and emulsion composition (i.e., protein and oil contents) that can minimize one unstable behavior may actually enhance other destabilization mechanisms (Dickinson, 1997; Ye, 2008).

2.2.5 Sodium Caseinate Stabilized Emulsion Containing Ethanol

Previous sections have focused on describing several variables that may be considered for understanding emulsion stability. In this section, special emphasis is given to the influence of ethanol on emulsion characteristics such as emulsion viscosity and its effect on protein configuration.

The studies evaluating the influence of ethanol on oil in water emulsions have been mainly conducted over a narrow range of casein/oil ratios. Dickinson and co-authors evaluated the influence of ethanol on emulsion prepared with 30-35 %vol oil (n-tetradecane) and 4%wt sodium caseinate, and ethanol contents of 0, 5, 10, 20 and 25 vol% (Dickinson &

Golding, 1998; Radford et al., 2004). Agboola & Dalgleish (1996) studied the system: 25% vol oil (soya oil), 5 %wt and 10%wt sodium caseinate and solutions of ethanol-water: 35: 65 v/v, 40:60 v/v, 45:55 v/v and 50:50 v/v. Although the methodologies for emulsion preparation used in these studies were similar (dissolution of sodium caseinate, mixing with oil and homogenization), the addition of ethanol into the emulsion in some studies was made before homogenization (as cream liqueurs are prepared) (Dickinson & Golding, 1998) or after homogenization (Radford et al., 2004) or by preparing an initial emulsion and diluting the system with ethanol water mixtures (Agboola & Dalgleish, 1996). Therefore comparison between different studies is difficult. However, all the authors agreed that there is a direct dependence on emulsion stability with the ethanol concentration in the continuous phase. This implies that unstable conditions such as protein aggregation, creaming and depletion flocculation due to the presence of ethanol can occur in either concentrated or diluted emulsions.

Dickinson & Golding (1998) reported that above 30-40 wt% ethanol content, the stability of the protein is affected because ethanol changes the polarity of the aqueous phase affecting the steric stabilization of the casein micelles and leading to protein aggregations. In contrast, at low concentrations, less than 20 wt%, ethanol enhances emulsion stability because ethanol reduces the interfacial tension between the oil and aqueous phase which allows reduction in the droplet size during homogenization, and lower droplet sizes retard creaming rates as indicated by Stokes' equation (Dickinson & Golding, 1998; McClements, 2004). The limit in ethanol concentration at which emulsions remain stable (< 20% v/v) corresponds to the stability range of casein solutions containing ethanol (from 0 to 20 %v/v ethanol) reported by Horne & Davidson (1986) (see Figure 2.4). Therefore the reduction in the hydrodynamic radius of casein micelles observed in casein solutions as ethanol increases may also occur in casein micelles present in the aqueous phase of an emulsion.

As presented in Table 2.2, the surface coverage of an emulsion containing alcohol increases versus the surface coverage of non-alcoholic emulsions reported in Table 2.1. This indicates that ethanol reduces the concentration of unadsorbed casein in the aqueous phase due to its effects on solvent quality and causes more casein to stay in the interfacial layer supporting the fact that ethanol highly influences the distribution of casein micelles between the oil-in-water interface and the aqueous phase (Radford et al., 2004).

Table 2.2 Surface coverage in sodium caseinate stabilized emulsions (30% vol n-tetradecane, 4%wt sodium caseinate) containing ethanol.

Ethanol (% wt)	Surface Coverage mg m^{-2}	Reference
0%	3.19	
10%	4.51	Radford et al., (2004)
25%	6.48	

2.2.5.1 Influence of Ethanol on Rheological Behavior and Stability

The oil volume fraction (ϕ) and the casein /oil ratio govern the dilute or concentrated regime into which emulsions can be classified and which leads to large changes in rheological behavior. At volume fractions < 0.05 emulsions behave as dilute systems and the droplets move mainly by Brownian forces and the rheological behavior is governed by the viscosity of the continuous phase (McClements, 2004). At volume fractions < 0.5 the emulsion is considered a concentrated system and the collision between droplets is high, but nevertheless, in this regime Newtonian behavior is still observed (Dickinson & Golding, 1997b; McClements, 2004). Volume fractions in the range: $0.5< \phi < 0.7$ are characteristic of a close packed system; as oil fraction increases the systems is close to the random close packing of ideal spheres (0.64) so that the rheological behavior turns to Non-Newtonian (McClements, 2004).

In terms of protein/oil ratios, low protein content, at levels where protein is not available for complete coverage of the droplet surface, lead to shear thinning behavior due to bridging flocculation (Dickinson & Golding, 1997b; Dickinson et al., 1997; McClements, 2004). If the protein content increases in such a way that all or almost all the protein stays in the interfacial layer (a very low fraction of casein micelles remains in the continuous phase) emulsions behave in Newtonian fashion. As protein content increases, depletion flocculation is favoured and the system turns to a shear thinning behavior (Berli et al, 2002; Dickinson & Golding, 1997b). The change in rheological behavior as concentration of unadsorbed protein increases suggested that emulsions with an excess of casein in the continuous phase developed floc networks that may hold in their structures a certain volume of the solvent causing an increase in emulsion viscosity (Berli et al., 2002; Dickinson & Golding, 1997b). Time dependent rheological studies in emulsion stabilized by sodium caseinate with an oil volume fraction of 35% vol and pH 6.8 showed that the decrease in the magnitude of viscosity as a function of time is less marked in emulsions prepared at 5 wt% casein compared to those made with 6 %wt casein. The studies indicated that there is a re-organization of flocs over time that at high protein concentrations results in a greater reduction in the emulsion viscosity and also indicated that at high protein concentrations, the emulsion flocculated more extensively than at low concentrations (Dickinson & Golding, 1997b).

Dickinson and co-workers conducted long term studies in emulsion containing alcohol (4%wt protein, 35% oil and ethanol in the range of 0 to 25%vol ethanol). Comparing ethanol-free emulsions with emulsions at low ethanol (5 %vol) contents, rheological behavior of emulsions moves from shear thinning fluids to Newtonian fluids as ethanol was added. Increasing the ethanol content up to 25% vol transformed the behavior compared to emulsions made with 5% ethanol from non-Newtonian to Newtonian. The authors

postulated that ethanol retards flocculation at high ethanol contents. The changes in polarity of the continuous phase as ethanol is added enhance protein aggregation at the surface of the droplet, but also they affect the protein-oil interaction in the interfacial layer. Repulsive interactions become greater than attractive interactions as ethanol content increases resulting in an overall reduction in droplet-droplet and droplet-submicelle interactions due to solvent polarity changes. These changes lead to a finite stability against flocculation and a change in the rheological behavior. The presence of ethanol was also reflected in the growth of droplet size over time. The droplet distribution of emulsions showed a unimodal distribution that at low ethanol contents (less than 10% vol) was unchanged over 12 days, whereas at high ethanol content (25 %vol) droplet size distribution shifted to higher diameters after 12 days. This trend in droplet size distribution is reported to be characteristic of Ostwald ripening (McClements, 2004). Therefore depletion flocculation and Ostwald ripening are the characteristic unstable behaviors that occur in emulsions containing ethanol.

2.2.5.2 Complication of Depletion Flocculation and Ostwald Ripening

Studies conducted to evaluate depletion flocculation as a factor in the developing instability of protein stabilized emulsions determined that unadsorbed protein is excluded from the interstitial space formed as two adjacent droplets approach together. Hence, the model for calculation of the depletion interaction potential described in equation 9 can be applied to casein stabilized emulsions assuming a critical casein submicelle size that will generate enough osmotic pressure to induce flocculation for a given casein-oil ratio (Berli, 2008; Berli et al., 2002; Dickinson & Golding,1997b; Radford & Dickinson, 2004).

The osmotic pressure of casein in the continuous phase of an emulsion as a function of the protein concentration is expressed as (Dickinson & Golding, 1997b; Radford &

Dickinson, 2004):

$$\mathrm{P_{osm}} = nK_bT(1 + 2\frac{C_b}{\rho_{sm}}) \qquad (12)$$

where C_b is the concentration of casein in the continuous phase, n is the number density of casein, K_b is the Boltzman constant, T is temperature and ρ_{sm} is the density of casein. The number density (n) of casein is expressed as:

$$n = \frac{C_b N_A}{M} \qquad (13)$$

where N_A is Avogadro's number and M is the molecular weight of the casein. The concentration of casein in the aqueous phase can be obtained from a balance between the total concentration (C) of protein and the protein adsorbed (C_{ad}):

$$\mathrm{C_b} = \frac{(\mathrm{C} - \mathrm{C_{ad}})}{(1 - \phi_{\mathrm{oil}})} \qquad (14)$$

where C_{ad} is calculated from:

$$\mathrm{C_{ad}} = \frac{6\Gamma\phi_{\mathrm{oil}}}{\mathrm{d_{32}}} \qquad (15)$$

where Γ is the surface coverage of the droplet

Based on equations 12-15 the osmotic pressure can be used to estimate the minimum size of unadsorbed casein required to generate a substantial depletion interaction energy (U_D) (equation 9) that will cause depletion flocculation. Radford & Dickinson (2004) predicted that for a sodium caseinate emulsion (4 wt% sodium caseinate, 30% vol oil, pH 6.8) with a droplet mean diameter (d_{32}) = 0.4 μm unadsorbed casein with a minimum radius of ~20 nm is required to generate the largest depletion interaction energy. This minimum radius was set after theoretically calculating the depletion interaction energy as a

function of unadsorbed casein radius in the range of 1-50 nm. The prediction of casein on micelles with a radius of ~20nm is close to the range of radius of gyration (R_g) reported by Lucey et al. (2000) for commercial sodium caseinate. Using a static light scattering technique, Lucey et al. (2000) determined R_g in the range from 22 to 49 nm.

The other factor to take into consideration due to the presence of ethanol in the continuous phase is the solubility of oil in ethanol which will enhance Ostwald ripening. Radford et al. (2004) reported that the cube of the droplet diameter of emulsions containing alcohol in the range of 0 to 25 %wt followed a time dependent changes which evidences the development of Ostwald ripening as predicted by the LSW theory (section 2.2.3.5). The rate at which the droplet diameter increases over time was reported higher for emulsions containing 25 %wt ethanol than for emulsion containing 5 or 10 %wt ethanol. It indicated that the changes on droplet sizes over time were dependent on the concentration of ethanol added.

As was mentioned in the previous section, rheological measurements conducted in oil-in-water emulsions containing ethanol, supported the statement that addition of ethanol retards depletion flocculation at ethanol content of 25 %wt. Nevertheless, the trend in droplet size observed over time indicated that Ostwald ripening proceeded rapidly at high ethanol contents (Dickinson & Golding, 1998; Radford et al., 2004). Therefore Ostwald ripening may be the leading mechanism affecting the stability of emulsions made with high ethanol content.

2.3 Lipid Oxidation in Emulsions

Oils are susceptible to oxidation due to their content of unsaturated fatty acids that are sensitive to reacting with oxygen. Oxidation stability of emulsions refers to chemical stability towards oxidative reaction that can occur between oil and oxygen and which can be accelerated by the presence of water soluble species such as transition metals (Chaiyasit et al., 2007). Lipid oxidation affects the shelf life of emulsions because it alters the flavour (e.g., rancidity) and physical properties (e.g., texture).

Important factors of emulsion composition and emulsion formation that influence the oxidation rate are:

(i) Droplet size, considering that the surface area of the droplet in contact with the aqueous phase of the emulsion increases as droplet size decreases, small droplet sizes enhance the possibility of interaction between oil and oxygen present in the aqueous phase (Chaiyasit et al., 2007; McClements, 2004).

(ii) Charge of emulsion droplets, positive charge at the surface of oil droplets generates electrostatic repulsion against transition metals such as iron, decreasing lipid oxidation. On the other hand, negative charge at the surface of the oil droplet means they are accessible to react with iron and so accelerating lipid oxidation (Chaiyasit et al., 2007; Hu et al., 2003; McClements, 2004).

(iii) Thickness of the interfacial layer, a thicker barrier protects oil against oxidation, hence emulsifier type and its concentration affects lipid oxidation rates. With respect to milk proteins, studies have shown that casein more efficiently protects oil droplets than whey protein (Hu et al., 2003; Ries et al., 2010). Casein in emulsions forms an interfacial layer with a thickness of ~ 10 nm whereas for whey protein the

thickness is ~ 1-2 nm, thus casein creates a good barrier to protect oil droplets (Dalgleish et al., 1995).

2.3.1 Canola and Coconut Oils and their Oxidative Stability

Oil processing includes refining, bleaching and deodorizing (RDB) processes to attempt to remove polar lipids such as phospholipids, mono and diacylglycerols and free fatty acids and improve the oxidative stability. Thus refined oils contained >99% triacylglycerols, less than 0.05% free fatty acids, and less than 0.1% phospholipids (Chaiyasit et al., 2007). Therefore the main components of refined oil susceptible to oxidation are unsatured fatty acids because the double bonds can easily react with oxygen species (Chaiyasit et al., 2007; Min & Boff, 2002). During the oxidation process lipid hydroperoxides are generated. As the reaction continues, secondary products such as aldehydes, ketones, hydrocarbons, and alcohols are formed. These products are responsible for the rancid flavour in foods (McClements, 2004; Chaiyasit et al., 2007). The concentration of lipid hydroperoxides is a parameter used to distinguish the oxidative stability of several food oils.

The major fatty acid fractions of coconut oil are lauric and myristic, representing almost 66% of the total fatty acid profile. The complete fatty acid profile is listed in Table 2.3. Coconut oil is considered a saturated oil because of the high concentration of low chain saturated fatty acids, plus it has a high solid fat content (SFC) of 35.6 % at 20°C (Pantzaris & Basiron, 2000). Due to its composition and its saturation characteristics, coconut oil shows good oxidation stability. On the other hand, canola oil is mainly composed of unsaturated fatty acids, oleic acid representing 61% and linoleic 21% of the total fatty acids; its unsatured character ensures that canola oil is susceptible to oxidation (Przybylski & Mag, 2002). In complex mixtures of saturated and unsaturated fatty acids such as anhydrous milk fat (see Table 2.3), the lineal relationship between unsaturated fatty acids

and the increase of oxidation rates is not completely suitable because the interactions between fatty acids and their esters affect the oxidation kinetics (Thurgood et al., 2007).

Table 2.3 Fatty acid profile of anhydrous milk fat, coconut and canola oils and melting points of pure fatty acids.

Fatty Acid Profile Common Name [1]	Carbon atoms [1]	Melting Point (°C) [1]	Anhydrous Milk Fat [2] %w/w	Coconut oil [3] %w/w	Canola Oil [4] %w/w
Saturated					
Butyric	4	-5.3	4.51		
Caproic	6	-3.2	3.12	0.4	
Caprylic	8	16.5	1.64	7.3	
Capric	10	31.6	3.86	6.6	
Lauric	12	44.8	4.07	47.8	
Myristic	14	54.4	10.99	18.1	0.1
Palmitic	16	62.9	28.73	8.9	3.6
Stearic	18	70.1	10.45	2.7	1.5
Arachidic	20	-49	0.6	0.1	0.6
Monounsaturated					
Palmitoleic	16 :1		3.12		0.2
Oleic	18 :1	16.2	20.92	6.4	61.6
Polyunsaturated					
Linoleic	18 :2	-5	1.86	1.6	21.7
Alpha Linoleic	18 :3	-11	1.65		9.6

Sources
1 Adapted from Gustone, F. (2008).
2 Adapted from Marangoni & Lencki (1998).
3 Pantzaris, T.P., Basiron, Y. (2000).
4 Przybylski, R., Mag, T. (2000).

Minor components of oils such as trace metals and water that remain in the bulk oil after refining can also affect the oxidative stability. However, the oil industry includes a polishing step at the end of the process to remove residual traces of undesirable components like iron such that iron concentration is less than 0.1ppm (Chaiyasit et al., 2007).

2.3.2 Oxidation Mechanism

The mechanism of lipid oxidation consists in a sequence of three steps: initiation, propagation and termination. It takes place between unsaturated fatty acids and oxygen compounds also called prooxidants (Chaiyasit et al., 2007; Min & Boff, 2002; McClements, 2004). The initiation involves the formation of a free alkyl radical by loss of a hydrogen from a fatty acid (i) when it reacts with prooxidants (i.e., trace metals, UV light) known as initiators. When oxidation occurs in unsaturated fatty acid chains in the triacylglycerols the formation of an alkyl radical is favoured. After that, oxygen and the free fatty acid radical create a peroxyl radical (ii) which is a reactive intermediate product so that it takes hydrogen from another unsaturated fatty acid (iii) producing a lipid hydroperoxide (LOOH) and a new free fatty acid radical (propagation step). The new free fatty acid radical behaves as initiator for the generation of more free radicals so that the propagation step interacts continually until non-radical species are formed which marks the end of the termination step (iv-vi). A schematic representation of the mechanism is as follows (Chaiyasit et al., 2007):

Initiation: $In^* + LH \rightarrow InH + L^*$ (i)

Propagation: $L^* + O_2 \rightarrow LOO^*$ (ii)

$LOO^* + LH \rightarrow LOOH + L^*$ (iii)

Termination: $LOO^* + LOO^* \rightarrow LOOL + O_2$ (iv)

$L^* + LOO^* \rightarrow LOOL$ (v)

$L^* + L^* \rightarrow LL$ (vi)

A secondary reaction can occur between the hydroperoxides (LOOH) and oxygen which produces volatile compounds causing rancidity (Chaiyasit et al., 2007; Kellerby et al., 2006).

2.3.3 Lipid Oxidation in Emulsions Stabilized by Casein

The efficient adsorption of protein at the interfacial layer with the accompanying surface coverage formed around the oil droplet promotes protein activity as an antioxidant. It is reported that sodium caseinate adsorbed preferably at the oil droplet and creates a thicker layer than whey protein, thus emulsions stabilized by sodium caseinate showed stronger stability against oxidation than emulsions stabilized by whey proteins (Hu et al., 2003; Ries et al., 2010). The amino acid profile of milk proteins also influences its efficiency as antioxidant, since it has been reported that tyrosine, phenylalanine, tryptophan, proline, methionine, lysine, and histidine have antioxidative qualities (Hu et al., 2003). Casein contains higher concentrations of tyrosine, methionine and proline than whey protein which is another factor marking the antioxidative property of casein (Hu et al., 2003).

Studies of the determination of lipid hydroperoxides in protein stabilized emulsions showed that lipid hydroperoxides decrease with rises in protein concentration as shown in Figure 2.7 (Hu et al., 2003; Ries et al., 2010). Low droplet sizes in combination with high protein contents gave the lowest concentration of lipid hydroperoxides in emulsions stabilized by sodium caseinate (10.6 % linoleic acid, protein 0 to 9%) (Ries et al., 2010). Nevertheless, as the time of aging increases (after 4-6 hours), emulsions with small droplet sizes are less capable of retarding the generation of lipid hydroperoxides because other factors such as availability of oxygen in the aqueous phase and generation of secondary reactions became more influential (Ries et al., 2010).

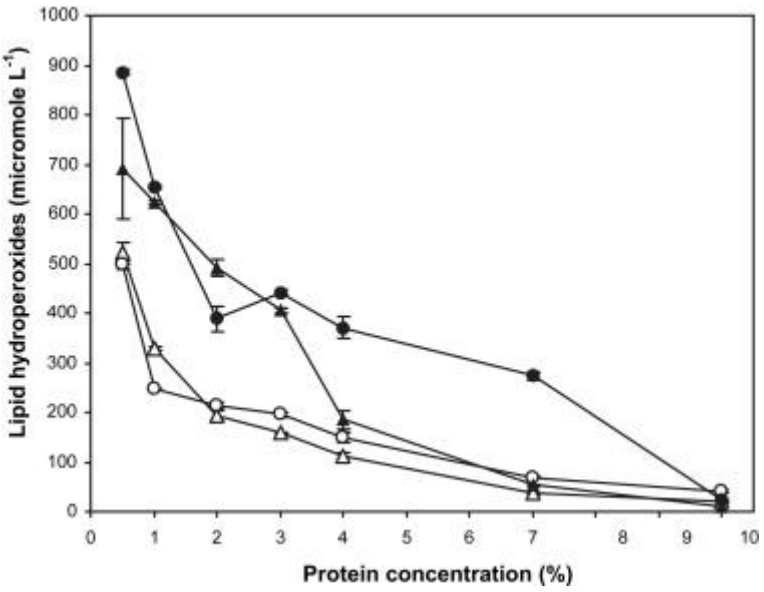

Figure 2.7 Lipid hydroperoxide concentration after 4h of storage at 50°C in whey protein isolate (WPI) emulsions (10.6% linoleic fatty acid) with an average droplet size of 0.65μm (●) and 0.31μm (○), and sodium caseinate emulsions with an average droplet size of 0.65μm (▲) and 0.31μm (△) (Adapted from International Dairy Journal, v. 20, Ries et al., Antioxidant properties of caseins and whey proteins in model oil-in-water emulsions, p.74 Copyright (2010), with permission from Elsevier).

The rate of oxidation in emulsions may increase due to the presence of iron in the continuous phase because iron will interact with lipid hydroperoxide promoting peroxyl radical (LOO*) and alkoxyl radical (LO*) formation (Chaiyasit et al., 2007; Kellerby et al., 2006). The interaction of iron with lipid hydroperoxides causes iron to go from a reduced state (Fe^{2+}) to an oxidized state (Fe^{3+}). The concentration of trace metals and their chemical state (reduced or oxidized) affected the rate of oxidation. As well, the presence of minor components in the oil, like free fatty acids, may accelerate the iron-lipid interactions because their presence increases the negative charge of the droplets

enhancing metal-lipid interactions in the interfacial layer (Chaiyasit et al., 2007; Sugiarto et al., 2010; Waraho et al., 2011).

Recently, It has been suggested that excess of protein in the continuous phase and the addition of chelating agents may reduce the rate of concentration of lipid hydroperoxides because prooxidative species that can be present in the oil phase, such as iron, may attach to protein in the interfacial layer, and this may be favoured by the presence of chelating agents (Sugiarto et al., 2010). Thus, iron can bind to casein forming complex structures. In this case, casein behaves as an antioxidant because it will inhibit the interaction of iron with the oil droplet surface. The binding is enhanced at neutral pH because protein is negatively charged acting as an anion while iron is positively charged acting as a cation (Sugiarto et al., 2010; Waraho et al., 2011). Due to the excess of protein, a potential exchange of protein from the interfacial layer to the continuous phase may remove prooxidative species from the oil surface which minimizes the efficacy of prooxidants in the formation of lipid radicals (Cho et al., 2003; Ries et al., 2010; Waraho et al., 2011).

2.3.4. Influence of Antioxidants on Lipid Oxidation

Antioxidants retard the rate at which lipid oxidation proceeds. Antioxidants donate a hydrogen atom to the peroxyl radical (LOO*), alkoxyl radical (LO*) or alkly radical (L*) forming lipid hydroperoxydes and an antioxidant radical (i-ii). The antioxidant radical has lower energy to continue reacting with unsaturated fat than free fatty acid radicals and therefore antioxidant radicals do not induce propagation steps as free fatty acid radicals do (Lampi et al., 1999; Chaiyasit et al., 2007).

$$LOO^* + AH \rightarrow LOOH + A^* \quad \text{(i)}$$

$$\mathrm{LO^* + AH \rightarrow LOH + A^*} \quad \text{(ii)}$$

$$\mathrm{L^* + AH \rightarrow LH + A^*} \quad \text{(iii)}$$

The non-polar antioxidant components such as tocopherols (α-,β-,γ-,δ- tocopherol) present in oil efficiently retard the oxidation rate in emulsions because they preferably stay at the interfacial layer protecting oil droplets and also because non-polar antioxidants form stable free radicals (Lampi et al., 1999; Schwartz et al., 2008; Waraho et al., 2011). Synthetic antioxidants such as BHA (butylated hydroxyanisole), BHT (tertiary butylated hydroxytoluene) can be incorporated into commercial oils to preserve their stability. Nevertheless, there is a trend to minimize the use of synthetic antioxidants in food products. The levels of synthetic antioxidants in commercial oils are not frequently reported on product labels. The FDA (Food and Drug Administration in the United States) establishes a maximum of 0.02% of fat or oil content for BHT and BHA (List of Food Additive Status Part I) while tocopherols are classified as GRAS (generally recognized as safe).

Lampi et al. (1999) reported that addition of α-tocopherol at levels < 50μg g^{-1} to rapeseed oil tryacylglycerols (main component of canola oil) retards the oxidation of oil and minimizes the formation of secondary products such as aldehydes and ketones. The same study reported that γ-tocopherol is more effective as an antioxidant when it is present at concentration above 100 μg g^{-1}. Also, the lower amount of tocopherols evaluated was 5μg g^{-1}; at this concentration the oxidation rate of oil remained in a low range up to 12 days and then rapidly increased. In commercial oils the level of total tocopherols for canola oil (rapeseed oil refined) is about 63 mg 100 g^{-1} while for coconut oil (refined) it is 0.32 mg 100 g^{-1} (Schwartz et al., 2008).

3. Materials and Methods

3.1. Materials

The materials used in emulsion preparation were: spray dried sodium caseinate (>87% protein,<6% moisture, < 4.5 % ash, < 0.2 % lactose) supplied by Canada Compound Corporation, ethanol food grade (95%AlcVol) supplied by Commercial Alcohols Inc, distilled water, 0.01%wt sodium azide (Sigma-Aldrich, analytical grade), canola and coconut oils that were commercial grade obtained from a local store. For lipid oxidation measurements, the analytical reagents were: methanol (99.8%), butan-1-ol (99.8%), isooctane (99%), 2-propanol (99%), ammonium thiocyanate (minimum 97.5%), barium chloride dihydrate (minimum 99%), ferrous sulphate heptahydrate (minimum 99%), and cumene hydroperoxide (technical grade,80%). All the reagents were supplied by Sigma-Aldrich.

3.2. Methods

The methods and procedures described in the following sections were carried out for the two systems subject to study: sodium caseinate-canola oil-ethanol and sodium caseinate-coconut oil-ethanol.

3.2.1. Construction of Phase Diagrams

The system studied was a mixture of sodium caseinate, ethanol, and oil as an oil in water emulsion. To evaluate its phase behavior, the ratio of sodium caseinate and water was fixed. Hence, the three components represented in the phase triangle are: sodium caseinate, oil, and ethanol (Figure 3.1).

The sodium caseinate-water ratio was based on the amount of water needed to achieve a complete hydration of the casein powder. The ratio was established under the following considerations:

(i) Casein dispersions are considered as a colloidal system that can be described by an adhesive hard sphere model. This model defines a casein micelle as a hard sphere where the attraction force between two micelles is short versus the radius of the micelles so that they cannot overlap in space (De Kruif, 1998).

(ii) The amount of casein micelles in the sodium caseinate solutions was chosen to cover the same range as the amount of casein micelles from fresh milk. The casein-water ratio was estimated using an effective hydrodynamic volume of casein micelles of 4.4 $cm^3 \cdot g^{-1}$ (De Kruif, 1998), and a specific volume of dried casein of 0.618 $cm^3\ g^{-1}$ (Berlin & Pallansch, 1968). Thus, 4.4 $cm^3 \cdot g^{-1}$ - 0.618 $cm^3 \cdot g^{-1}$ = 3.78 $cm^3 \cdot g^{-1}$ gives the water volume per gram of casein. Considering that hydrated casein micelles are random packing with a volume fraction of 0.64, then 5.91$cm^3 \cdot g^{-1}$ represents the amount of water required for minimal hydration of the dried casein. For this study the moisture content of the sodium caseinate powder was less than 6% (product specification), and as a consequence the ratio of water per gram of sodium casein was chosen as 5.5 cm^3 of water per gram of wet protein. Thus 100% of sodium caseinate in Figure 3.1 represents a solution of 153.85 g of wet sodium caseinate in 846.15 g of water.

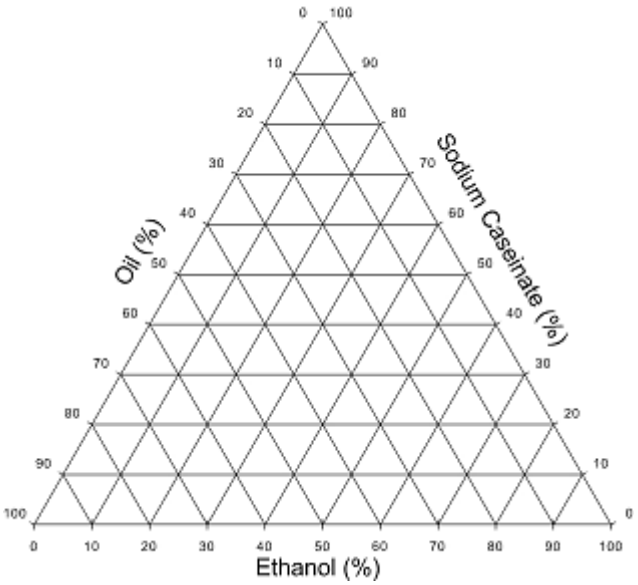

Figure 3.1 Pseudo-ternary phase diagram for the system sodium caseinate-oil-ethanol.

3.2.2. Emulsion Preparation

Appropriate amounts of sodium caseinate, water, oil, and ethanol were weighed such that the weights of the sodium caseinate solution, oil and ethanol add up to 100% in every point of the phase diagram.

The emulsion was prepared based on the procedure proposed by Lynch & Mulvihill (1997). Sodium caseinate was dissolved in hot water (55°C) with continuous mixing using an OMNI MIXER TYPE OM for at least 20 minutes. At this point, sodium azide was added as an antimicrobial agent. Then the appropriate amount of oil was added and the emulsion was stirred for another 20 minutes. Oils had been preheated to 55°C prior to addition. After that, the required amount of ethanol at 95%v/v was slowly incorporated into the emulsion. Temperature and mechanical agitation remained constant during emulsion preparation.

The final product was homogenized in a two stage homogenizer (APV Model 15MR-8TA) by a single pass at a feed temperature of 55°C under a pressure of 17.5MPa (first stage) and 4MPa (second stage). After homogenization the emulsion was cooled to 20°C (Muir & Banks, 1986; Medina-Torres et al., 2009). To do this, the emulsion was placed in a water bath at < 4°C, with the sample under constant agitation until it reached 20°C-22°C, and at that time it was transferred into 100 ml glass cylinders. To evaluate phase stability, two glass cylinders per preparation were used; they were stored in a water bath at 26°C.Two emulsions per each composition were made.

3.2.3. Determination of the Region of Emulsions Stability

The analysis was conducted based on adaption of a procedure described by Elysée-Collen & Lencki (1996). Emulsions at different concentration of sodium caseinate solution, ethanol and oil were prepared followed the procedure indicated in section 3.2.2. A first series of emulsions, with weight increments of 20% from 0 to 100% for each ingredient

were made to determine the general phase regions of emulsion stability. In order to delimit the phase regions, based on those results a second series of emulsions were prepared with 5-2% of weight increments within the range of the general regions established in the first series and the phase behavior was recorded. For moving from one point to another, the respective increments in sodium caseinate, oil, and ethanol concentrations were calculated moving horizontally on the phase diagram, that is, the sodium caseinate concentration was fixed, and the ethanol and oil concentrations changed. When a change in emulsion stability was observed (e.g., formation of creaming, flocculation, sedimentation) from one preparation to the next preparation in the range, the samples were selected as boundary points and the regions of emulsion stability were delimited on the phase diagram. To determine the boundary lines within the stable regions a third series of emulsions was prepared, with the points selected in the second trial being the start points to establish the boundary lines. Samples in the third trial were prepared followed the same procedure of increments in concentrations described for the second trial. For each series, the order of emulsion preparation was randomly arranged.

After preparation, all emulsions were kept in a water bath at 26°C and the phase behavior was recorded 72 hours later by visual observation. The time was set on the basis of preliminary experiments where the stability of emulsions at different concentrations was evaluated at 1, 24, and 72 hours after preparation. The results showed that at 72 hours, unstable behavior, such as serum separation and creaming, was easier to observe by eye.

The software Grapher Gold, Version 8, was used to generate the phase diagrams.

3.2.4. Emulsion Characterization

In order to cover the entire region of emulsion stability obtained in section 3.2.3 for the sodium caseinate-canola-oil-ethanol system and for the sodium caseinate-coconut oil-ethanol system, ten points which represented a specific composition of emulsion within the stable region were selected. Nine extreme points, close to the boundary lines, and one central point for each system were established. Two separate emulsions were prepared for each point following the procedure described in section 3.2.1. Emulsion phase behavior was evaluated using the following methodologies: determination of droplet size distribution, evaluation of rheological behavior and measurement of lipid oxidation. The experimental design followed for emulsion characterization is shown in Figure. 3.2. The first two tests were selected based on previous time stability studies for cream liqueur and sodium caseinate stabilized emulsions, which show that changes in emulsion characteristics are highly related to variations in droplet size distribution, and viscosity due to the development of unstable mechanisms such as flocculation, coalescence and Ostwald ripening (Banks & Muir 1985; Dickinson & Golding, 1998; Radford et al., 2004). It is reported that casein protein in emulsions behaves as an antioxidant, and that the rate of oxidation in an emulsion is affected by protein content, emulsion characteristics (i.e., droplet size) and bulk conditions (i.e. presence of pro-oxidative species, solvent quality) (Chaiyasit et al., 2007; Ries et al., 2010). Therefore, measurement of lipid oxidation was selected in order to evaluate the oxidation stability in emulsions when their composition (i.e., casein/oil ratio, ethanol content) and oil type changed.

The characterization of the system was made 72 hours after emulsion preparation and 30 days after. The preparation of the ten selected points and their respective duplicate were randomly ordered. No more than four emulsions were prepared per day so that the three tests for each emulsion were performed the same day. Samples were kept during the

length of the experiment in a water bath at 26°C. The temperature and length of the experiment represent approximately an accelerated shelf life of six months for cream liqueurs that are stored at 4°C.

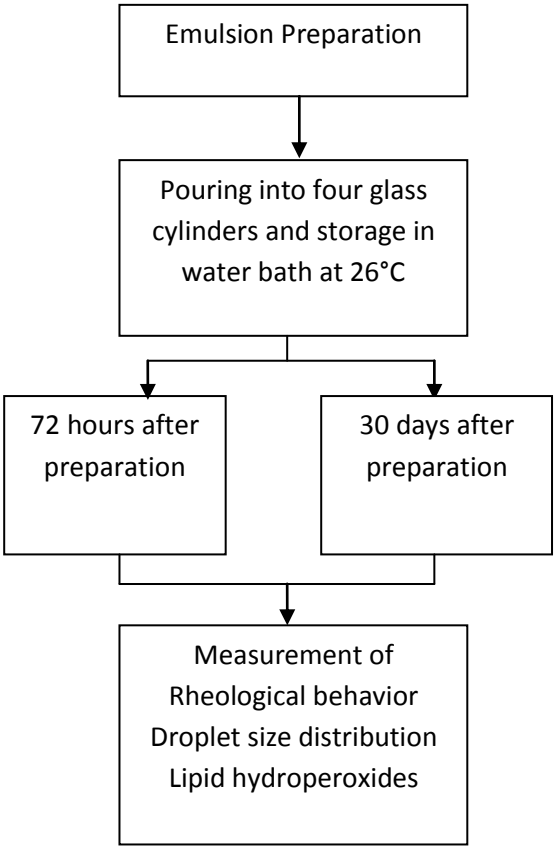

Figure 3.2 Experimental design for emulsion characterization.

3.2.4.1. Droplet Size Determination

Droplet size distributions of the samples were measured using a light scattering analyzer (Malvern MasterSizer 2000). It captures the scattering pattern that droplets create when light passes through the emulsion and then calculates the size of droplets assuming a spherical shape and considering the refractive index of the sample. The refractive index of emulsions containing casein micelles reported in the literature goes from 1.56 to 1.36 (Griffin & Griffin, 1985; Mimouni et al., 2009). For example, to determine the droplet size

distribution of an emulsion containing milk proteins, Parkinson & Dickinson (2004) used a refractive index ratio of 1.074 (refractive index of oil / refractive index of aqueous phase), while for oil in water emulsion Chantrapornchai et al. (2001) used a ratio of 1.08, considering the refractive index of water equal to 1.333. Since this study involves the use of two types of oils, the refractive index set for samples containing canola was 1.465 (Przybylski & Mag, 2000), a value of 1.448 for samples prepared with coconut oil (Pantzaris & Basiron, 2000), and 1.333 for water as continuous medium. Droplet size determination was based on the procedure described by Kim et al. (2004) except that samples were kept in a water bath at 26°C prior to measurement.

Once the samples were ready to evaluate, the emulsion was taken out of the water bath and agitated for 3 s by vortexing, inverted, and agitated for 3 s again to guarantee a homogeneous sample. Then samples were diluted (~1:1000) with distilled water (Kim et al., 2004). The dilution prevents multiple scattering effects from distorting droplet size determinations. The effect occurs when droplets are close enough that the scattered light could consider two or more droplets as one unit, and so the result will not be reliable. Emulsions were continuously stirred during the measurement process (instrument stirring set at 50%). The results were displayed in a histogram which represented the droplet size distribution. The surface-average mean diameters (d_{32}) (calculated by the Malvern Mastersizer software) were reported as the average of two measurements made on two subsamples for each emulsion.

3.2.4.2. Rheological Measurements

The viscosity of sodium caseinate stabilized emulsion is reported as a function of shear stress (Dickinson & Golding, 1997; Casanova & Dickinson, 1998; Radford et al., 2004) or as a function of shear rate (Bouchoux et al., 2009; Dahbi et al., 2010; Lynch & Mulvihill,

1997). In order to quantify the differences in the rheological behavior, viscosity was measured as a function of the shear rate ($\dot{\gamma}$).

The shear flow curve was carried out using a controlled shear rheometer (AR 2000 rheometer; TA Instruments) with the temperature maintained at 26°C. Twenty-five milliliters of sample were transferred to a concentric cylinder (cup radius of 15 mm and DIN conical rotor radius of 14 mm and height of 42 mm), then the sample was presheared for 2 minutes at 1000 s^{-1} to ensure uniform shear (Dahbi et al., 2010). For measurement of emulsion viscosity, the shear rate was increased from 10^{-4} to 1000 s^{-1}. Viscosity measurements were reported in mPa·s, and two measurements per emulsion were performed.

3.2.4.3. Determination of Lipid Hydroperoxides

Oxidation stability of emulsions formulated with coconut and canola oil was analyzed using a procedure adapted from Hu et al. (2003) and Ries et al. (2010). The method is based on the determination of the oxidation of ferrous ions to ferric ions by the presence of peroxides (Shantha & Decker, 1994). The level of oxidation is proportional to the concentration of lipid hydroperoxides. The reaction of ferrous ions with hydroperoxides gives a red pigment, thus the concentration of hydroperoxides can be quantified by a spectrophotometric technique.

The procedure followed for the measurement of lipid oxidation is shown in Figure 3.3. An aliquot of the emulsion (0.3 mL) was mixed with 1.5 mL of isooctane/2-propanol (3:1, v/v) by vortexing for 10 s for a total of 3 times. The mixture was separated by centrifugation at 1000g for 2 minutes. The supernatant (200 µL) was collected, added to a test tube containing 2.8 mL of methanol/1-butanol (2:1,v/v) and vortexed. Immediately, 15 µL of ammonium thiocyanate and 15 µL of ferrous iron solution were added followed by

vortexing for 10 s. After that, the test tube was kept in the dark for 20 minutes, at which point, 1 μL of the resulting solution was taken and poured into a rectangular transparent cuvette and the absorbance was determined at 510nm using a spectrophotometer (Ultrospec 2000). A blank that contained all the reagents except the emulsion was also prepared and evaluated as control. Two subsamples from each emulsion were tested. Lipid hydroperoxide concentration was expressed in μmol L^{-1} and calculated from a standard curve made with cumene hydroperoxide.

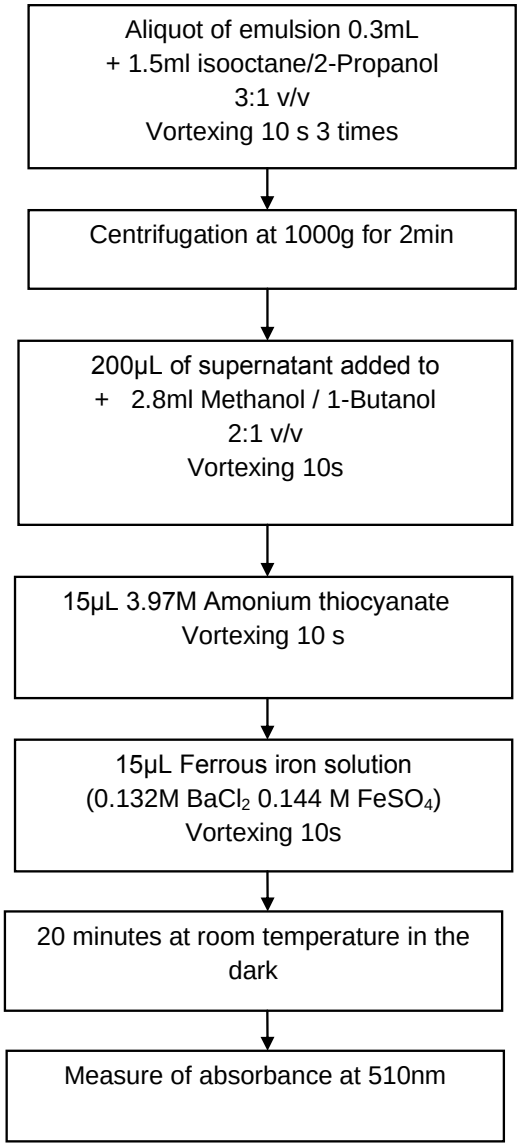

Figure 3.3 Procedure followed for the measurement of lipid oxidation.

For the construction of the calibration curve, cumene hydroperoxide, 44 mg, was dissolved with the organic solvent, methanol/1-butanol (2:1,v/v), to 1000mL. Appropriate amounts of this solution were diluted with the solvent (methanol/1-butanol (2:1,v/v) in a volumetric flask as shown in Table 3.1. Aliquots of 0.3 mL of each dilution were taken and treated as emulsion sample (as was described above). At least two subsamples from each dilution were tested. The results were plotted in a graph where the x axis represented the concentration of cumene hydroperoxide (in μmol L^{-1}) and the y axis the absorbance at 510 nm.

Table 3.1 Cumene hydroperoxide concentrations used to generate the calibration curve.

Aliquot Volume	Dilution Volume	Cumene Hydroperoxide
mL	mL	μmol L^{-1}
90	100	211.473
70	100	164.479
60	100	140.982
120	250	112.785
90	250	84.589
60	250	56.393
20	250	18.798
10	250	9.399
5	500	2.350
2	500	0.940

The ferrous iron (0.132 M $BaCl_2$, 0.144 M $FeSO_4$) and ammonium thiocyanate (3.97 M) were made just before the test was conducted to ensure their stability. To prepare the ferrous iron solution, 1.612 g of barium chloride was dissolved in 50 ml distilled water. Separately, 2.002 g of iron sulfate was dissolved in 50 ml distilled water. Then the barium chloride solution was added to the iron solution and mixed. 1 ml of 0.4 M HCl was added

to the resulting solution. After mixing, barium sulfate and iron (II) were formed, the salt (barium sulfate) precipitate was separated from the iron (II) solution using a 0.5 μm membrane filter. The clear solution was stored in a brown bottle. The ammonium thiocyanate solution was prepared dissolving 7.555 g of ammonium thiocyanate in 25 mL of distilled water and was stored in a brown bottle too.

4. Results and Discussion

4.1. Pseudo-Ternary Phase Diagrams

After preparing and examining more than sixty emulsions for the two systems: sodium caseinate-canola oil-ethanol and sodium caseinate-coconut oil-ethanol, three phase regions were defined based on the visual behavior observed. Points plotted in Figure 4.1 represent all the emulsions that were prepared for both systems to establish the phase regions. As was described in section 3.2.3 when a change in emulsion stability was observed from one preparation to the next in range, the emulsion was taken as the boundary point and the regions of emulsion stability were delimited.

Region 1

The system is unstable with phase separation occurring in all cases, although details of the phase separation depend on composition. Phase separation is observed among all possible ratios of ethanol in samples containing less than 28 %wt of sodium caseinate. All samples prepared under this range formed insoluble aggregates that remain at the bottom of the glass cylinder, and with a cloudy layer at the top. Clearly, the addition of ethanol enhances protein precipitation and droplet aggregation causing phase separation. As the oil/protein ratio decreases, the aggregates slowly move up and down upon manual agitation, in others words, they tend to resuspend, being in a “fluffy state”. When the oil/protein ratio tends to a minimum, that is, low oil content, foam formation and serum separation were noticed. In contrast, as ethanol concentration approaches 100%, and the sodium caseinate approaches its minimum, the sedimentation rate increases and the cloudy layer at the top of the glass cylinder became clearer.

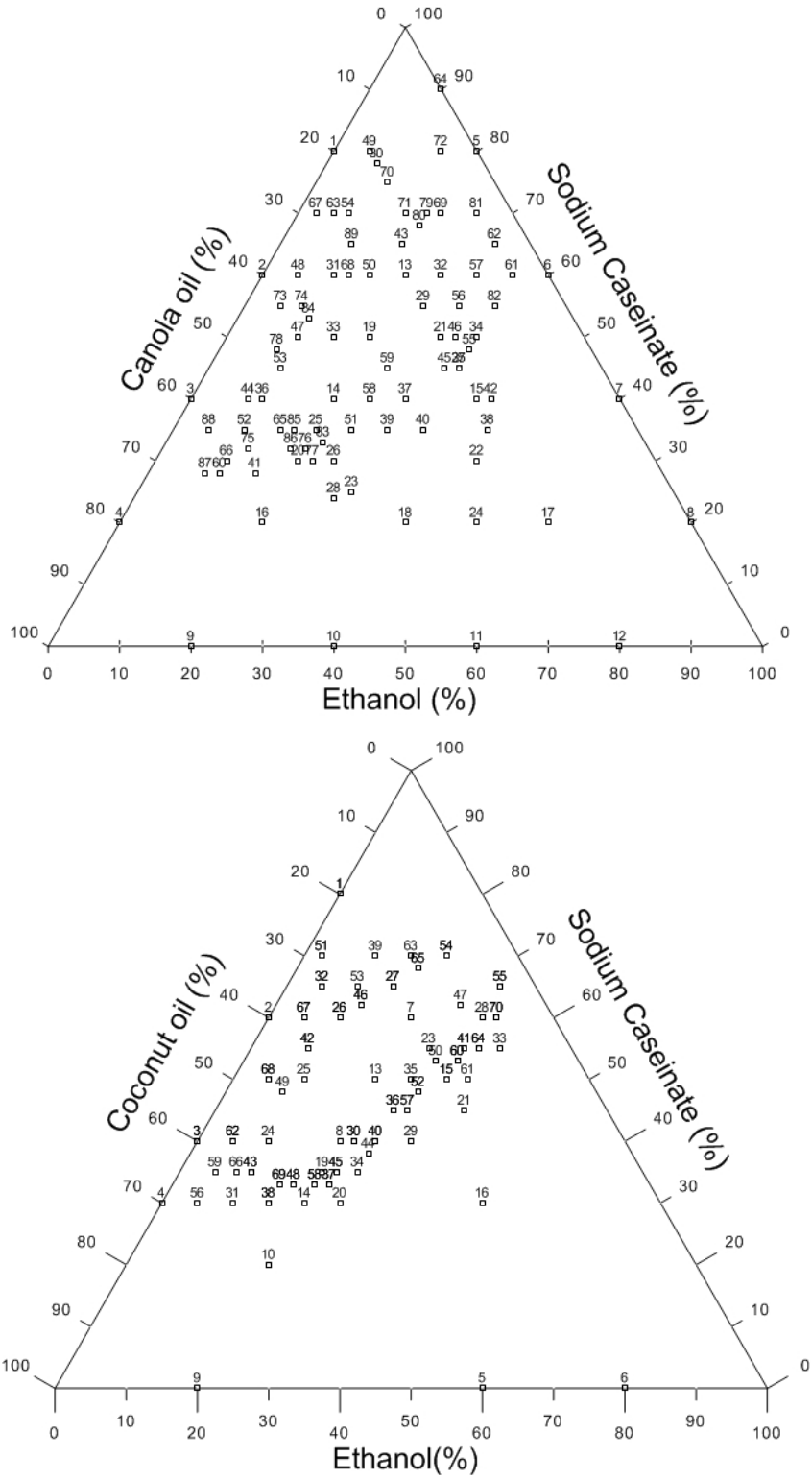

Figure 4.1 Determination of phase regions for the systems: (a) sodium caseinate-canola oil-ethanol, (b) sodium caseinate-coconut oil-ethanol. The points plotted on the phase diagram indicate emulsions that were prepared and their visual behavior examined after 72 hours of storage at 26°C.

Region 2

All ingredients coexist in one phase. Emulsions that lay in this region remained stable, but slight changes in color were observed as the oil content increased. Emulsions go from a white color at ethanol and oil levels close to 35 %wt and 10 %wt respectively, to a light yellow color when the proportions are the opposite. In the same way, emulsions were visually thick at high oil contents and became thin as oil content decreased. The emulsion behavior when the system is close to the boundary line that divided region 2 and 3 can be described as a saturated system (high concentration of oil and protein); at this point, the addition of ethanol causes a reduction in the interfacial tension which disrupts the gel structure that the protein and oil are tending to form. The phase behavior in emulsions on the boundary lines between region 2 and 1 is governed by gravitational separation (i.e., creaming and sedimentation) and droplet aggregation.

Region 3

The system remains in one phase. Emulsions are white in color and highly viscous; as alcohol is reduced, the systems behave as an alcohol-free emulsion, so that the droplets became closer to each other enhancing flocculation until they attain a state where the emulsion has a solid like behavior (soft gel).

4.1.1. Sodium Caseinate-Canola Oil-Ethanol System

Figure 4.2 shows the phase diagram with the corresponding three regions established for the system sodium caseinate-canola oil-ethanol. Square marks on the phase diagram indicate emulsions that were prepared to establish the boundary lines as was described in section 3.2.3. The region of emulsion stability (region 2) is delimited for concentrations of sodium caseinate in solution in the range of 32 %wt - 68 %wt, oil contents from 8 to 56

%wt and ethanol contents from 10 to 35 %wt. Thus, on the phase diagram region 2 is going from right to left, from a dilute emulsion where the ethanol and sodium caseinate concentration are the major fractions to a concentrated emulsion where the ethanol content decreases and oil fraction increases.

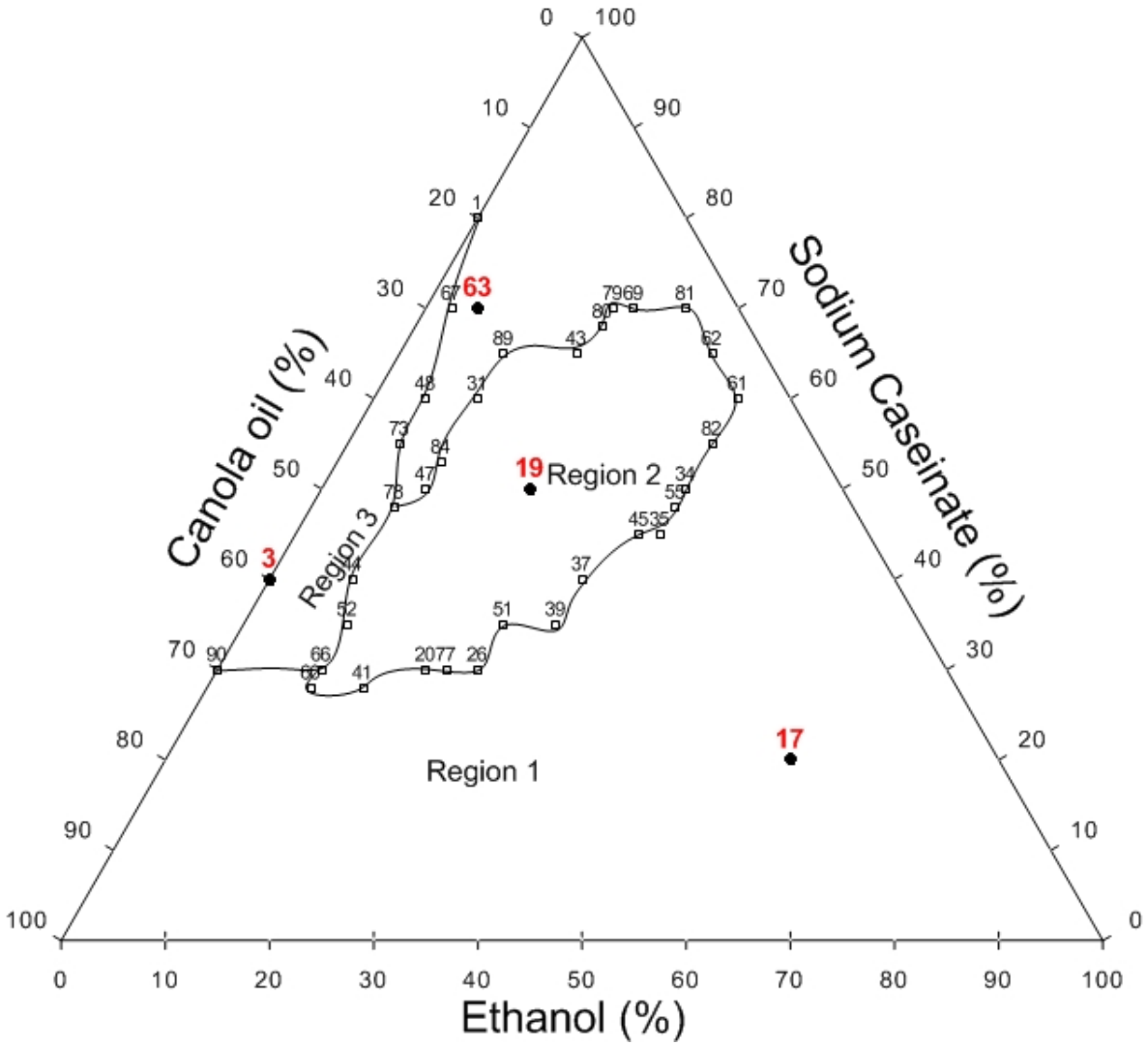

Figure 4.2 Pseudo-ternary phase diagram for the system: sodium caseinate-canola oil-ethanol (see section 4.1 for region descriptions). The points plotted on the phase diagram indicate emulsions prepared to establish the boundary lines. The points highlighted in each region (3, 17, 19 and 63) correspond to the emulsion pictures in Figure 4.3.

As described in the previous section, there are 3 regions representing the phase behavior of the sodium caseinate-canola oil-ethanol system. In Figure 4.2, four samples: 3,17,19 and 63 are highlighted; they are presented as examples of the emulsion composition in each region with the characteristic behavior observed for each of these samples. Sample 17 (Figure 4.3 a) located in region 1 denoted an unstable emulsion, where the large amount of ethanol induces protein precipitation and phase separation. In the same region, emulsion 63 (Figure 4.3 b) showed foam formation at the top of the glass cylinder. Emulsion 19 (Figure 4.3 c) is in the region of emulsion stability (region 2), and by visual observation this emulsion can be described as a white stable emulsion. The solid like behavior observed in Region 3 is well illustrated for emulsion 3 (Figure 4.3 d), which behaves as a concentrated emulsion that is low in alcohol content.

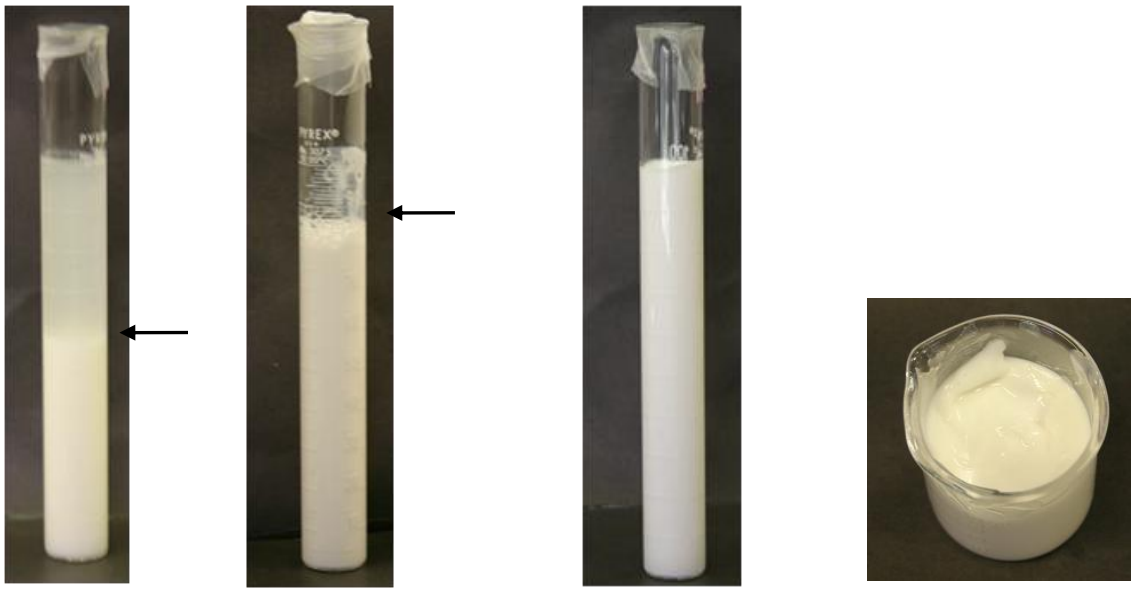

(a) (b) (c) (d)

Figure 4.3 Emulsions after 72 hours of preparation representing the 3 regions established in the phase diagram. Emulsion compositions are: (a) emulsion 17, 20 %wt sodium caseinate in solution, 20 %wt canola oil and 60 %wt ethanol (region 1); (b) emulsion 63, 70 %wt sodium caseinate in solution, 25 %wt canola oil and 5 %wt ethanol (region 1); (c) emulsion 19, 50 %wt sodium caseinate in solution, 30 %wt canola oil and 20 %wt ethanol (region 2); (d) emulsion 3, 40 %wt sodium caseinate in solution, 60 %wt canola oil and 0 %wt ethanol (region 3). In figure 4.3 (a), the arrow denotes phase separation and protein precipitation. In figure 4.3 (b), the arrow denotes foam formation. Figure 4.3 (c), illustrates a stable emulsion. Figure 4.3 (d) illustrates the solid like behavior observed in region 3.

4.1.2. Sodium Caseinate-Coconut Oil-Ethanol System

The phase diagram for emulsion prepared with coconut oil is shown in Figure 4.4. Like in emulsions prepared with canola oil, square marks on the phase diagram represents emulsions that were prepared in order to limit the phase regions.

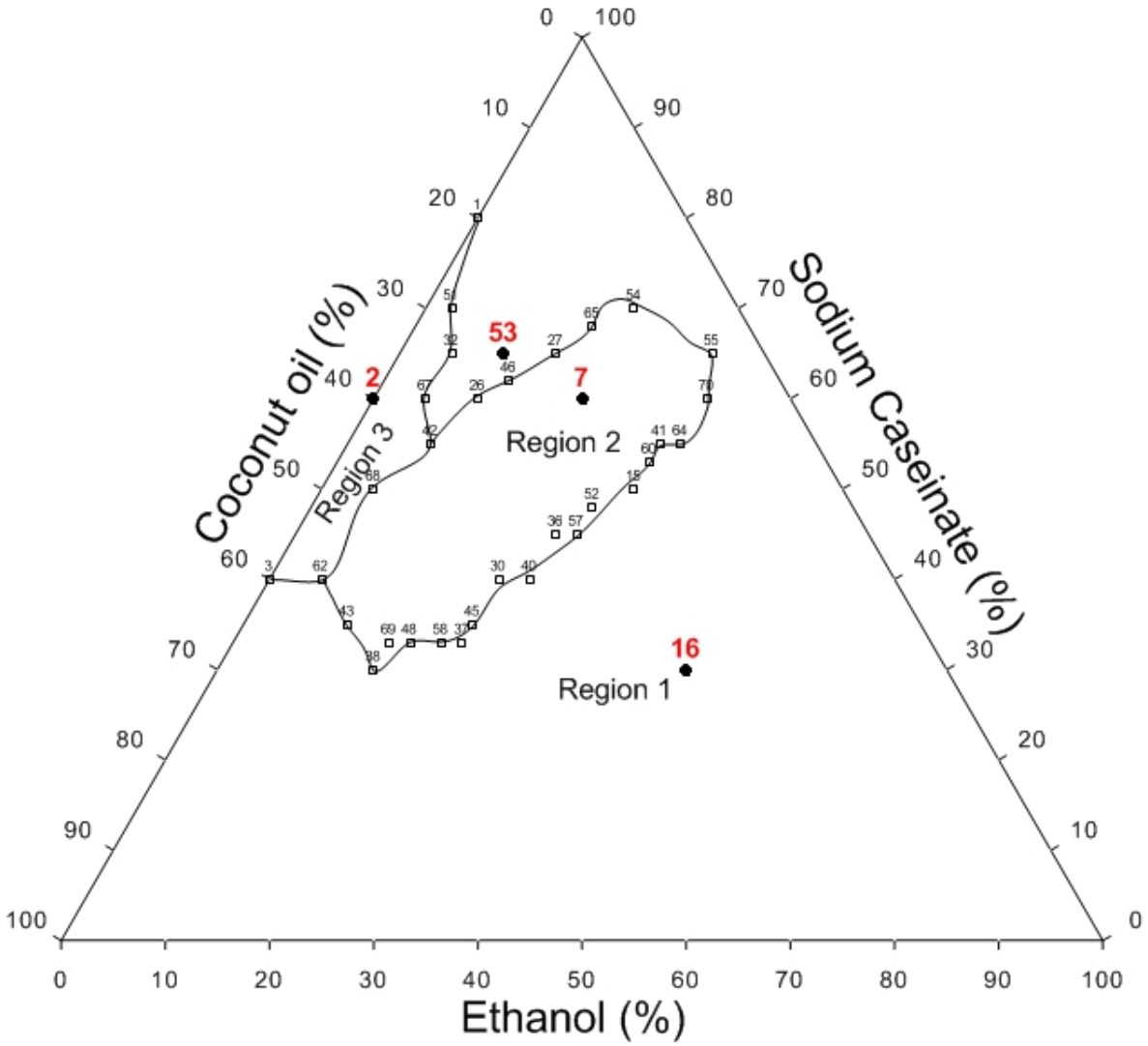

Figure 4.4 Pseudo-ternary phase diagram for the system: sodium caseinate-coconut oil-ethanol (see section 4.1 for region descriptions). The points plotted on the phase diagram indicate emulsions prepared to establish the boundary lines. The points highlighted in each region (2, 7, 16 and 53) correspond to the emulsion pictures in Figure 4.5.

The range of emulsion compositions for the stable region is limited for sodium caseinate concentrations between 32 and 70 %wt, coconut oil concentrations from 10 to 53 %wt and ethanol contents from 8 to 30 %wt. As can be seen in Figure 4.5, emulsions in region 1 are represented by emulsions 16 and 53. Emulsion 16 (Figure 4.5 a) was unstable, since its protein precipitated and a clear layer at the top of the glass cylinder was observed. In the same region, emulsion 53 (Figure 4.5 b) that contained low level of ethanol and oil, a foam layer that easily collapsed was the unstable behavior that was recorded. Emulsion 7 (Figure 4.5 c) which corresponds to the region of emulsion stability (region 2) represents a white stable emulsion. Emulsion 2 (Figure 4.5 d) corresponds to an emulsion that is highly viscous and solid-like.

The sodium caseinate-coconut oil-ethanol system gave a smaller region of emulsion stability, region 2, than the sodium caseinate-canola oil-ethanol-system. Visual observations of the samples that lay on the phase boundaries between region 1 and 2 are dominated by the formation of an oil layer at the top of the glass cylinder which tends to be in a solid state, due likely to the high solid fat content of coconut oil, which is 35.6 % at 20°C (Pantazaris & Basiron, 2000). As the ethanol content increases, the height of the oil upper layer decreases until a point where a thin creaming layer appears instead. Region 3 is also smaller than the region defined for the system containing canola oil. The main differences in the emulsion behavior of the two systems were observed in preparations containing low concentrations of ethanol and protein in combination with high concentration of oil. These preparations lay close to the boundary line between region 3 and 1, which corresponds to sodium caseinate contents ~40 %wt, ethanol concentration < 8%wt and oil contents close to 60 %wt. The sodium caseinate-coconut oil-ethanol system emulsions prepared in this range showed a light yellow oil layer at the top of the glass cylinder and a white layer at the bottom in which protein aggregates were clearly

observed. The height of the upper layer increased as sodium caseinate was reduced. The concentration of ethanol (8-32 %wt) within the range of the region of emulsion stability for both systems is in agreement with that reported in the literature for emulsions containing ethanol; concentration of ethanol between 30-40 %wt is reported as the maximum level of ethanol before protein precipitation is observed due to changes in the polarity of the continuous phase (Dickinson & Golding, 1998; Radford et al., 2004).

In the following sections the points plotted in Figures 4.2 and 4.4 as boundary points are presented as square marks (□) without numbers. The purpose is to avoid confusion with the sample order presented later for emulsion characterization within the stable (2) region.

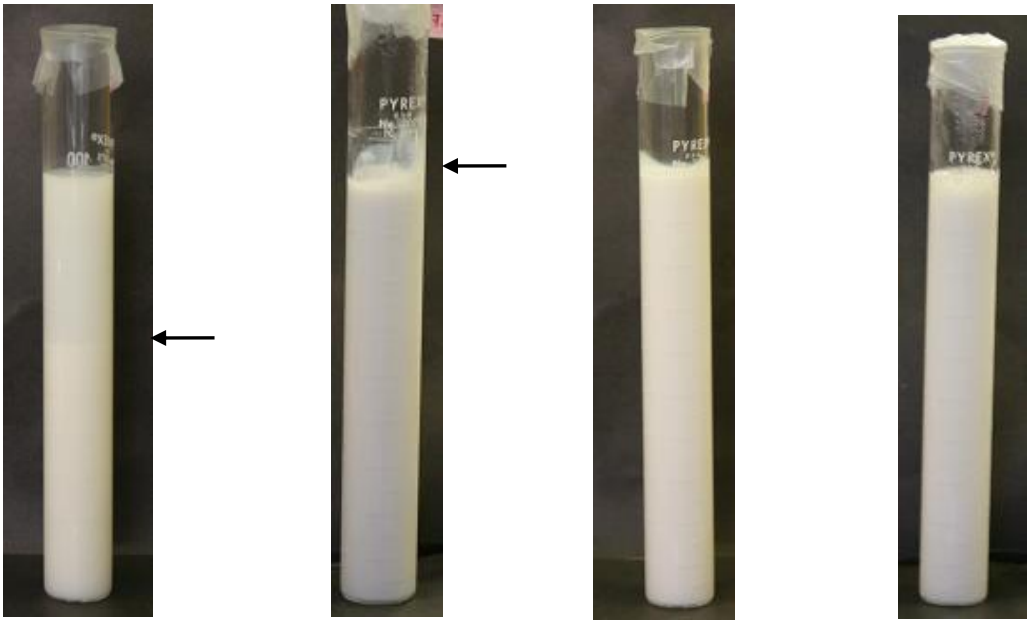

(a) (b) (c) (d)

Figure 4.5 Emulsion samples after 72 hours of preparation representing the 3 regions established in the phase diagram. Emulsion compositions are: (a) emulsion 16, 30 %wt sodium caseinate in solution, 25 %wt coconut oil and 45 %wt ethanol (region 1); (b) emulsion 53, 65 %wt sodium caseinate in solution, 25 %wt coconut oil and 10 %wt ethanol (region 1); (c) emulsion 7, 60 %wt sodium caseinate in solution, 20 %wt coconut oil and 20 %wt ethanol (region 2); (d) emulsion 2, 60 %wt sodium caseinate in solution, 40 %wt coconut oil and 0% wt ethanol. In Figure 4.5 (a), the arrow denotes phase separation and protein precipitation. In Figure 4.5 (b), the arrow denotes foam formation. Figure 4.5 (c) represents an stable emulsion. Figure 4.5 (d) illustrates a creamy and viscous emulsion.

4.2. Emulsion Characterization

4.2.1 Stability observations

The composition of the 10 emulsions selected for emulsion characterization for both systems are presented in Tables 4.1 and 4.2. As was described in section 3.2.4, emulsions were evaluated at 72 hours and 30 days after preparation. At 72 hours the ten samples prepared for both systems remained stable. Emulsions prepared at high oil fractions (> 30 %wt), low ethanol concentrations (between 8 and 15 %wt), and sodium caseinate solution below ~40 %wt showed visually a very thick behavior. This was expected because emulsions lay in the area close to the boundary line that separated the liquid stable region (region 2) from the solid like region (region 3). When emulsions where prepared with high ethanol concentrations (> 15 %wt), emulsions showed visually a less thick behavior.

Table 4.1 Emulsion compositions for emulsion characterization of the system sodium caseinate-canola oil-ethanol.

Sample #	Sodium caseinate in solution %wt	Canola oil %wt	Ethanol %wt
1	32	56	12
2	32	46	22
3	40	50	10
4	40	35	25
5	50	38	12
6	50	28	22
7	50	18	32
8	60	28	12
9	60	8	32
10	68	10	22

Table 4.2 Emulsion compositions for emulsion characterization of the system sodium caseinate-coconut oil-ethanol.

Sample #	Sodium caseinate in solution %wt	Coconut oil %wt	Ethanol %wt
1	32	53	15
2	35	47	18
3	40	52	8
4	40	40	20
5	50	42	8
6	50	32	18
7	50	22	28
8	60	25	15
9	60	10	30
10	70	12	18

At 30 days, the unstable behaviors observed in some emulsions for both systems were phase separation, creaming and neck-plug formation. Emulsions 2, 4 and 10 prepared with canola oil broke down during storage during 30 days. A cloudy serum layer at the bottom, and a thick oil layer at the top of the glass cylinder were observed for samples 2 and 4, whereas for sample 10, a large cream layer and a serum layer that was easily redispersed by soft agitation was recorded. Regarding samples containing coconut oil, two samples became unstable to phase separation at 30 days: samples 8 and 10. A cream layer that corresponded to about 20% of the volume of the glass cylinder and a serum layer were recorded. The serum layer was cloudy which indicated that oil and some protein aggregates remained in the serum layer (Dickinson & Golding, 1998). The locations of the 10 emulsions used for emulsion characterization are plotted on the phase diagram as shown in Figures 4.6 and 4.7. The unstable samples are highlighted indicating that these samples were not evaluated at 30 days.

Emulsion 7 showed a good stability against neck plug formation in both systems, but the rest of the nine samples were prone with respect to neck plug formation during storage for 30 days. For the samples that remained stable throughout the storage period by visual observation there was no evidence of a sharp separation at the bottom or at the top of the test tube that could be regarded as a cream or serum layer; thus neck plug formation is distinct from creamy destabilization (Dickinson et al., 1989). These emulsions were considered to be essentially stable and homogenous.

The thickness of the plug formed at the top of the glass cylinder by visual assessment was less than ~5mm. Although nine emulsions showed a neck plug at the top of the glass cylinder, it was slightly thicker in emulsions with high oil concentrations, which corresponded to emulsions 1, 2, 3, 4 and 5. The neck plug observed matched the description given by Dickinson et al. (1989) in a study conducted to evaluate neck plug formation in cream liqueurs. The authors described the neck plug as a semi-solid thick layer where the solid region looked like yellow fat lumps. As well, it was pointed out that neck plug formation occurs as a result of the conjunction of three main factors: (i) formation of a cream layer due to a creaming mechanism, but at this point the cream layer may be redispersible (ii) formation of a cream layer due to partial coalescence of oil droplets, and this layer is not redispersible (iii) formation of solid fats as a result of fat aggregation on the surface of the emulsion.

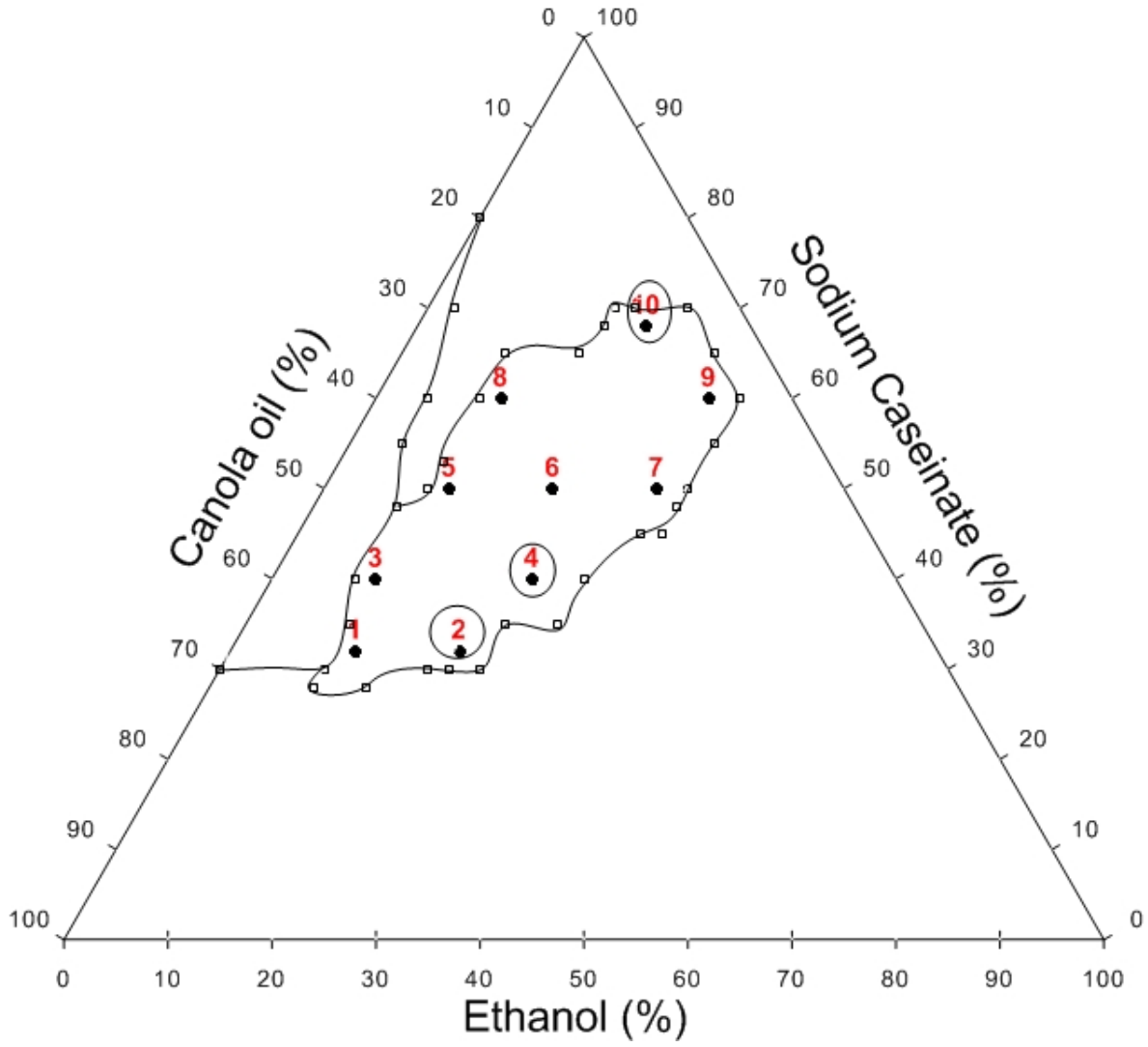

Figure 4.6 Pseudo-ternary phase diagram for the system: sodium caseinate-canola oil-ethanol. 1-10 represents the emulsion samples selected for emulsion characterization; ○ represents samples that were unstable during storage for 30 days; □ represents the boundary points.

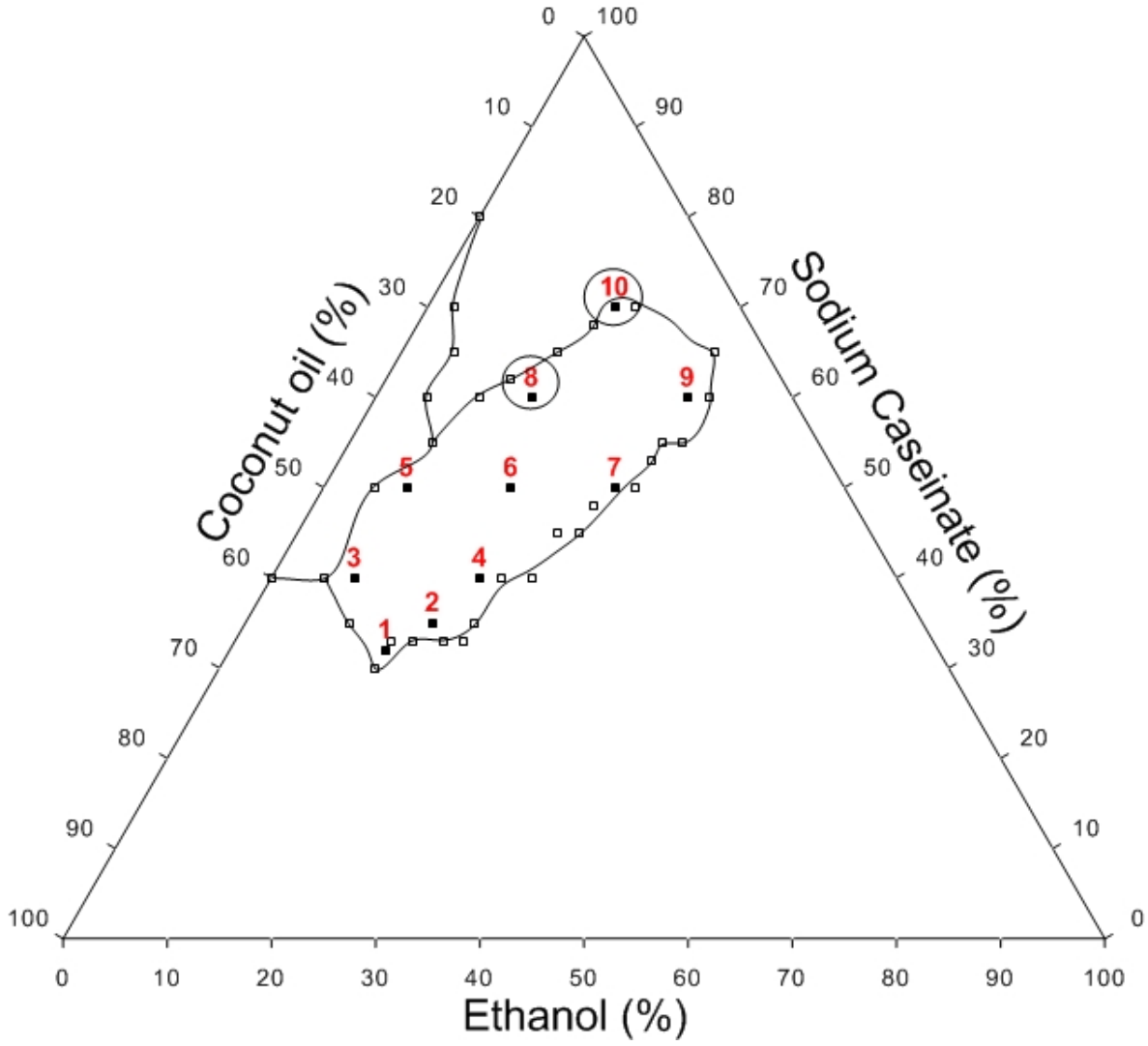

Figure 4.7 Pseudo-ternary phase diagram for the system: sodium caseinate-coconut oil-ethanol. 1-10 represents the emulsion samples selected for emulsion characterization; ⬯ represents samples that were unstable during storage time for 30 days; ☐ represents the boundary points.

4.2.2 Rheological Behavior

4.2.2.1 Sodium Caseinate-Canola Oil-Ethanol System

Rheological behavior of emulsions is affected by emulsion composition; based on the concentrations of the dispersed and continuous phase, emulsions can behave as Newtonian or non-Newtonian fluids (McClements, 2004). For example, when protein is at a level enough to cover oil droplets in such a way that a very low fraction of the protein stays in the continuous phase, the emulsion behaves as a Newtonian fluid. If the protein content in the emulsion increases to a level that there is an excess to beyond coverage of the oil droplets, so that more protein remains in the continuous phase, the rheological behavior of the emulsion turns into a shear thinning behavior due to droplet flocculation (Dickinson & Golding, 1997b; Berli et al., 2002). Therefore, in this project differences in rheological behavior were expected due to the large range of emulsion compositions studied. The results indicated that emulsion viscosities were highly dependent on ethanol content, that is, the viscosity decreased as ethanol content increased. In order to show the differences in the magnitude of the shear stress in emulsions with high and low ethanol content, the flow curves at 72 hours and 30 days are displayed in two graphs. Figure 4.8 shows the shear flow curves for emulsions with ethanol content above 22 wt% where the viscosities were in the range of 30 mPa·s -70 mPa·s while Figure 4.9 shows the shear flow curves for emulsions with ethanol content below 22 wt% where the viscosities were in the range of 100 mPa·s – 300 mPa·s. It can be seen from both figures that the shear stress increases gradually as shear rate increases following a good linear relationship, thus emulsions can be considered as Newtonian fluids in the tested range. The rheological behavior of the ten emulsions is in agreement with the rheological behavior reported in the literature for emulsions containing ethanol at concentrations > 10% where Newtonian behaviour was exhibited (Dickinson & Golding, 1998; Radford et al., 2004).

The significance of the coefficient of determination (r^2) was used to judge the adequacy of the model fit. Since the flow curves fit a lineal model well they are considered as Newtonian fluids. The lineal equation was the best fit to the shear flow curves obtained from the experimental data, so that the slope of the equation represented the viscosity of each emulsion. The slopes values presented in Table 4.3 are reported as the average of the slopes obtained from the lineal model of two independent samples, and there are two subsamples in the slope value of each sample. The standard deviation was calculated for the corresponding slope values.

Table 4.3 Viscosity values at 72 hours and 30 days after emulsion preparation (system: sodium caseinate-canola oil-ethanol).

Sample #	72 hours		30 days	
	Viscosity [1] mPa·s	Coefficient of determination (r^2)	Viscosity [1] mPa·s	Coefficient of determination (r^2)
1	329.5 ± 30.9	0.998	316.4 ± 9.2	0.998
2	102.4 ± 3.2	0.997	NA	NA
3	251.4 ± 9.4	0.990	212.3 ± 27.6	0.991
4	69.3 ± 0.9	1.000	NA	NA
5	128.6 ± 1.8	0.991	125.4 ± 1.1	0.992
6	70.0 ± 3.7	0.999	106.8 ± 22.8	0.999
7	32.0 ± 0.6	0.999	38.9 ± 4.2	1.000
8	132.2 ± 8.2	0.993	115.7 ± 3.3	0.993
9	28.1 ± 1.4	0.999	28.9 ± 2.5	0.999
10	40.8 ± 1.9	1.000	NA	NA

1 Determined from mean ± standard deviation (obtained for two independent samples) slopes of plots of shear stress vs shear rate.
NA: Data not available, unstable emulsion.

(a)

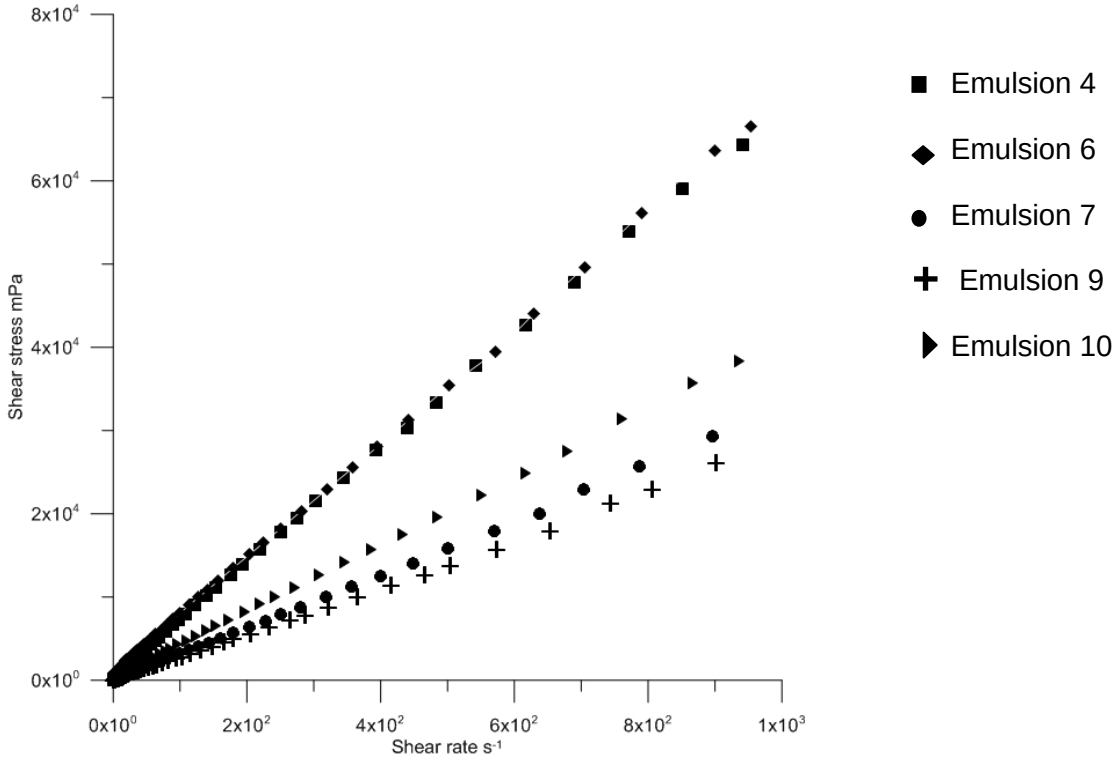

(b)

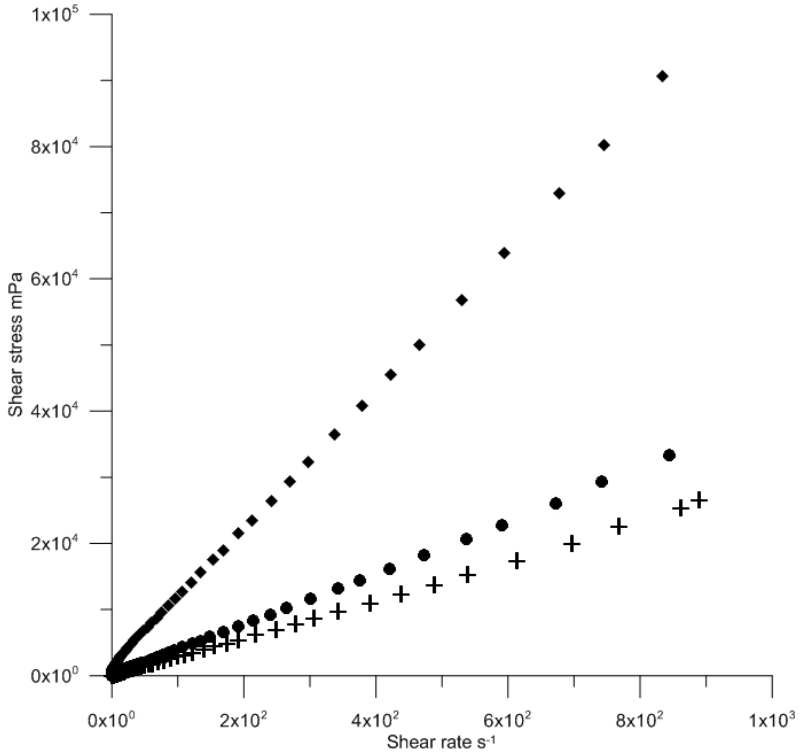

Figure 4.8 Shear flow curves for emulsions at 26°C (sodium caseinate-canola oil-ethanol system) in the region of emulsion stability at high ethanol content (> 22 wt %) at (a) 72 hours, (b) 30 days.

(a)

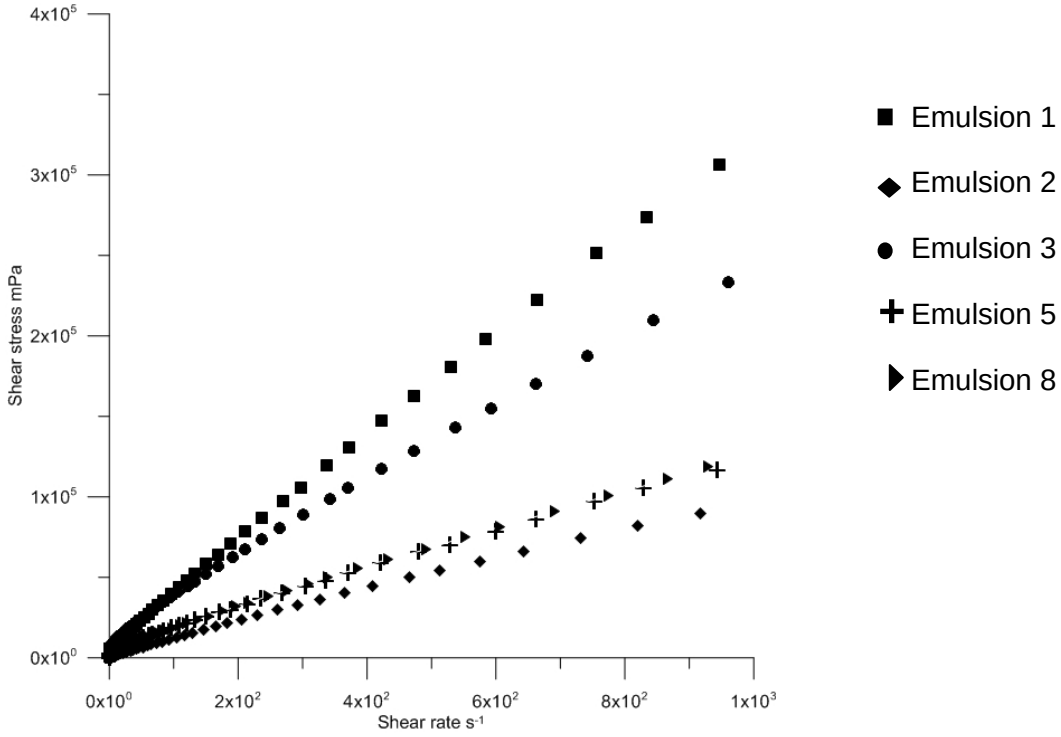

(b)

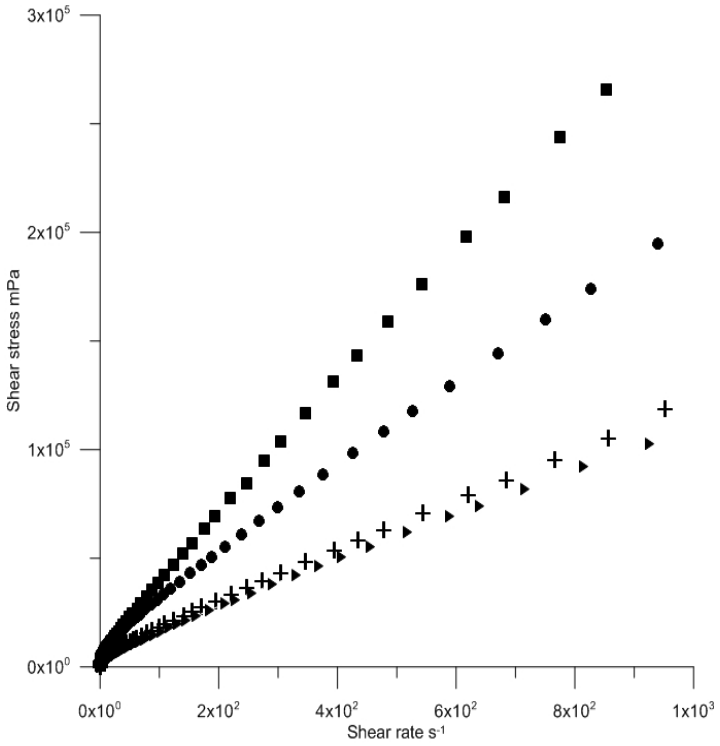

Figure 4.9 Shear flow curves for emulsions at 26°C (sodium caseinate-canola oil-ethanol system) in the region of emulsion stability at low ethanol content (< 22 wt %) at (a) 72 hours, (b) 30 days.

The rheological behavior of the emulsions was classified on the phase diagram (Figure 4.10) as rheological lines that represented the range of viscosity at 72 hour of storage. This representation gives a general overview of the change in viscosity in the region of emulsion stability, moving from right to left on the ethanol axis, the viscosity increases as ethanol decreases. The lines through samples 4, 6, 7, 9 and 10 represent a zone where, at high ethanol content, as ethanol increases viscosity decreases, whereas lines through samples 1, 2, 3, 5 and 8 represent a zone where, at low ethanol content, as oil content increases viscosity increases.

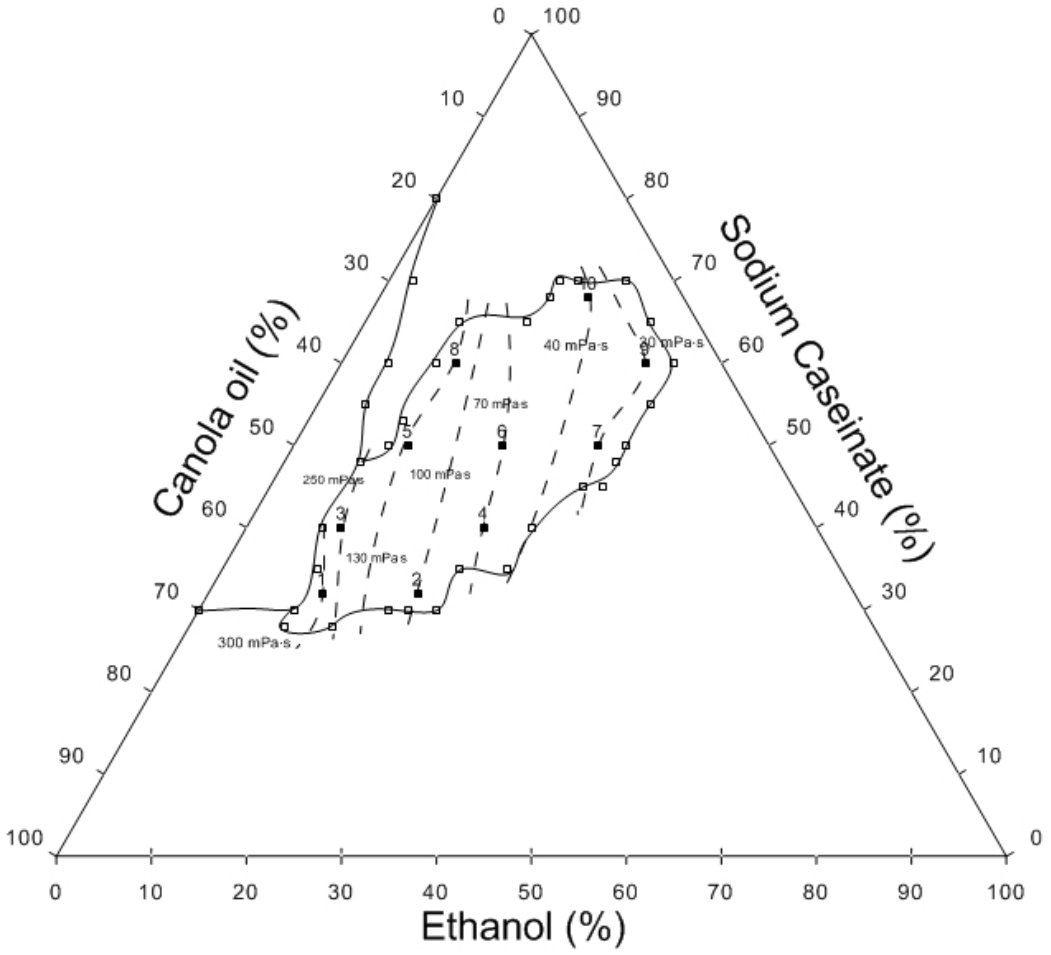

Figure 4.10 Dashed lines represent the range of viscosity observed in the region of emulsion stability at 72 hours for the system sodium caseinate-canola oil-ethanol.

4.2.2.2 Sodium Caseinate-Coconut Oil-Ethanol System

The rheological results for the sodium caseinate-coconut oil-ethanol system follow the same trend described for the sodium caseinate-canola oil-ethanol system, that is, emulsions behave as Newtonian fluids for all the range of ethanol content evaluated. As was described for the sodium caseinate-canola oil-ethanol system, the shear flow curves are displayed in two graphs (Figures 4.11 and 4.12) indicating emulsions with low and high ethanol content, respectively. Comparing the flow curves of emulsions 6 and 8 (emulsions with high ethanol content) versus emulsions 1 and 3 (emulsions with low ethanol content) at 72 hours, it can be seen that the linearity of the flow curves is improved denoting a clear Newtonian behavior. Some shear thinning characteristics are evident in the low ethanol systems, a result also observed by Dickinson & Golding (1998) when ethanol (5 and 10 %vol) was added to sodium caseinate stabilized emulsions. The shear flow curves of emulsions 7 and 9, corresponding to the higher ethanol concentration (28-30 %wt), leads to a substantial reduction in the shear stress which in turn represents a low viscosity emulsion.

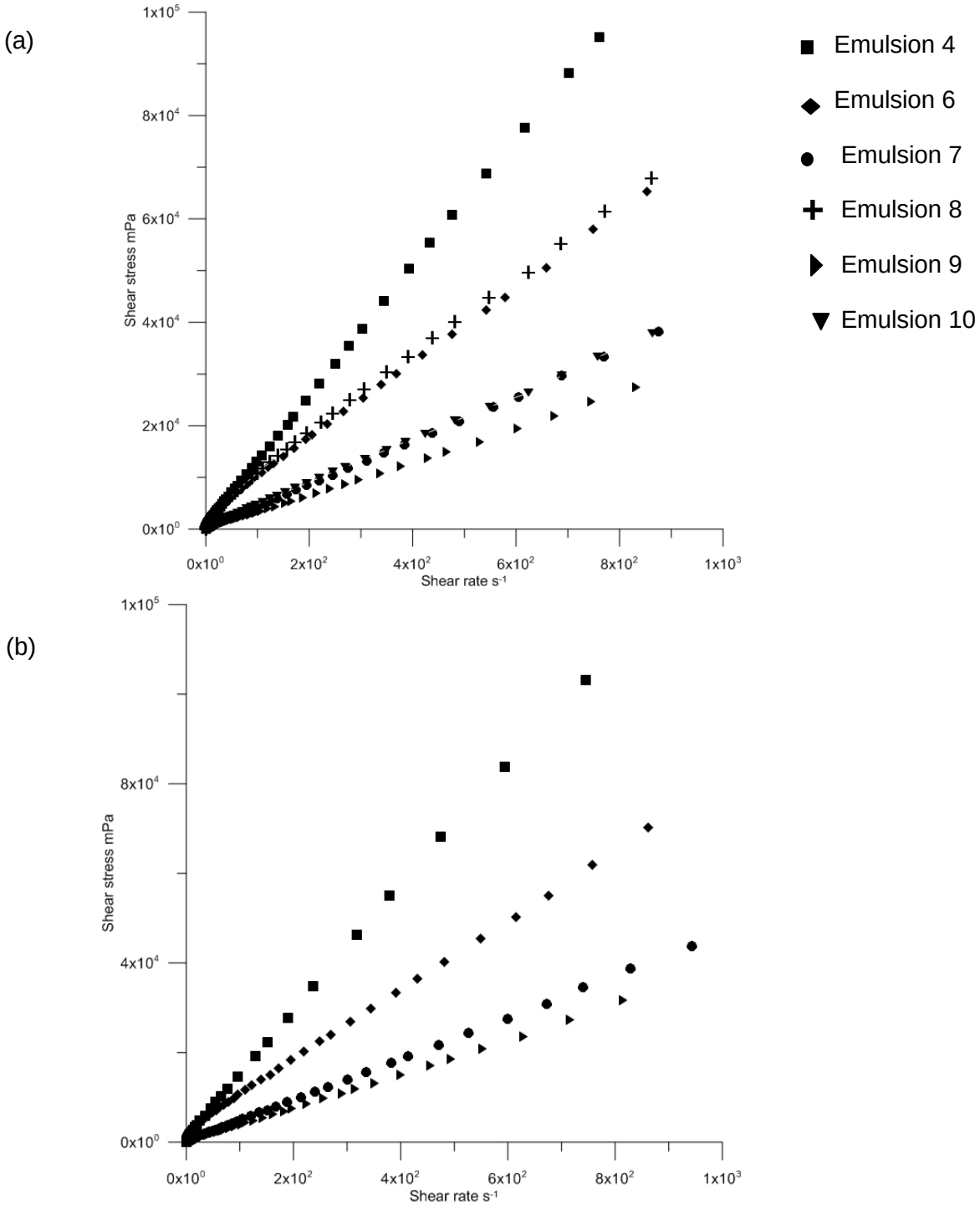

Figure 4.11 Shear flow curves for emulsions at 26°C (sodium caseinate-coconut oil-ethanol system) in the region of emulsion stability at high ethanol content (>20 wt%) at (a) 72 hours, (b) 30 days.

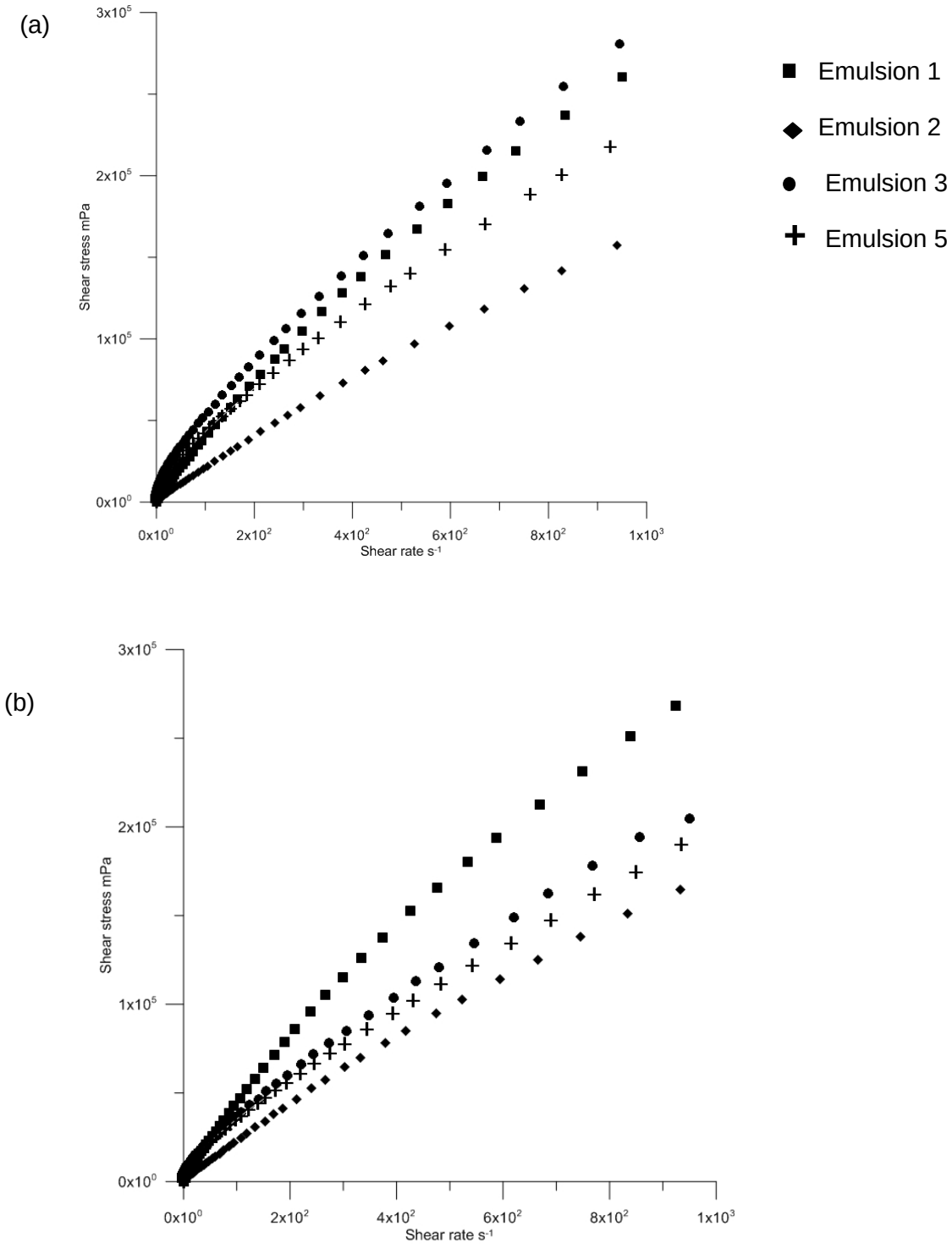

Figure 4.12 Shear flow curves for emulsions at 26°C (sodium caseinate-coconut oil-ethanol system) in the region of emulsion stability at low ethanol content (< 20 %wt) at (a) 72 hours, (b) 30 days.

The shear flow curve for the ten samples evaluated fit a lineal model well (coefficient of determination r^2 >0.95), thus emulsions are considered a Newtonian fluid throughout the length of the experiment. The results are summarized in Table 4.4. The slopes values are reported as the average of the slopes obtained from the lineal model of two independent samples, and there are two subsamples in the slope value of each sample. The standard deviation was calculated for the corresponding slope values.

Table 4.4 Viscosity values at 72 hours and 30 days after preparation for the system: sodium caseinate-coconut oil-ethanol.

Sample #	72 hours		30 days	
	Viscosity [1] mPa·s	Coefficient of determination (r^2)	Viscosity mPa·s	Coefficient of determination (r^2)
1	297.8 ± 8.2	0.991	296.4 ± 6.3	0.987
2	176.5 ± 18.2	0.996	187.7 ± 24.9	0.995
3	315.3 ± 28.3	0.981	229.7 ± 93.4	0.986
4	125.6 ± 7.6	1.000	137.8 ± 0.9	0.999
5	252.4 ± 18.9	0.977	212.5 ± 8.6	0.983
6	76.8 ± 3.0	0.994	80.9 ± 0.6	0.995
7	42.9 ± 1.7	1.000	46.4 ± 0.6	1.000
8	80.9 ± 0.6	0.994	NA	NA
9	32.3 ± 3.5	0.997	38.0 ± 4.0	1.000
10	43.5 ± 1.0	0.999	NA	NA

1 Determined from mean ± standard deviation (obtained for two independent samples) slopes of plots of shear stress vs shear rate.
NA: Data not available, unstable emulsion

As can been seen in Figure 4.11 and 4.12, the rheological behavior of emulsions prepared with coconut oil followed essentially the same behavior as emulsions prepared with canola oil, curves for all samples being very lineal. The representation of the rheological results on the phase diagram as rheological lines also show an increase in viscosity as ethanol content is reduced (Figure 4.13). The lines through emulsions 4, 6, 7, 8, 9 and 10 denoted

a zone of low viscosity. In contrast, the lines through emulsions 1, 2, 3 and 5 represented a zone of high viscosity.

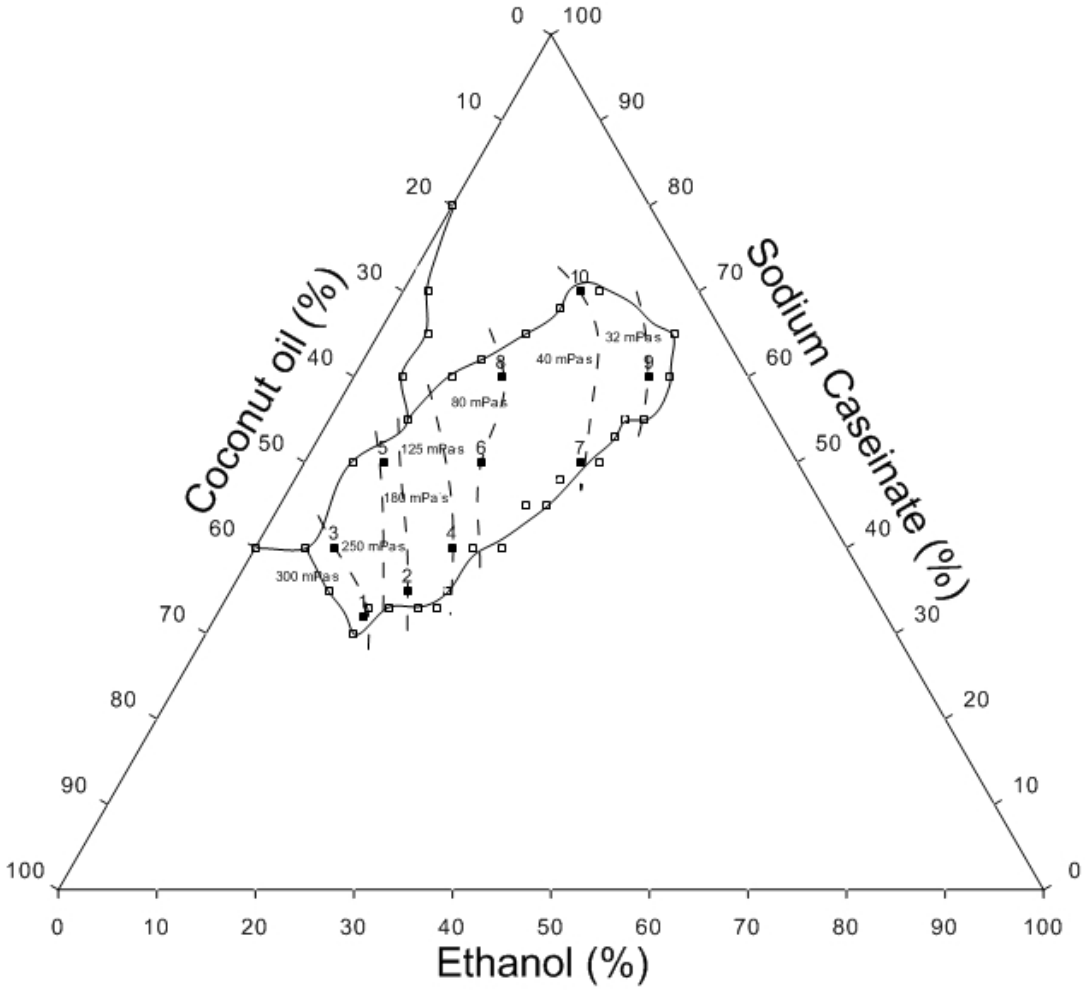

Figure 4.13 Dashed lines represent the range of viscosity observed in the region of emulsion stability at 72 hours for the system sodium caseinate-coconut oil-ethanol.

The rheological result for both systems are consistent with the Newtonian behavior described by Dickinson & Golding (1998) in emulsions prepared with a constant sodium casein concentration (4 %wt) and ethanol contents of 5, 10, 20 and 25 %vol. The relatively small change in the magnitude of the slope of the flow curve over 30 days can be attributed to a restructuring of the conformation of the droplets. Considering that the rheological behavior of alcohol-free emulsions is protein content-dependent, at low protein

content the emulsions behave as Newtonian fluids while as protein increases emulsions behave as non-Newtonian fluids which is attributed to flocculation (Dickinson & Golding, 1997b; Berli et al., 2002). The Newtonian behavior obtained in emulsions with high protein content due to the addition of ethanol suggests that a high concentration of ethanol retards the development of flocculation (Dickinson & Golding, 1998).

The driving mechanism for the reduction in viscosity as ethanol increases seems to be the result of the large influence of ethanol on the steric stabilization of casein (i.e., collapse of the k-casein hair layer) (Horne, 1985, Horne & Davidson, 1986), in combination with the changes in the oil-protein and protein-protein interactions in the interfacial layer due to the change in the polarity of the aqueous phase as ethanol is added (Dickinson & Golding, 1998). These changes alter the properties of the casein micelles in the continuous phase, and hence alter the rheology of the emulsions. Two potential changes are that casein micelles in the continuous phase can aggregate or they will diffuse to the interface layer. At the interface, the aggregates may create a secondary layer that interacts with the primary layer (created during emulsion formation) likely via hydrophobic interactions increasing the overall thickness of the interfacial layer (Dickinson & Woskett, 1988). Thus less protein remains in the continuous phase and the strength of the depletion flocculation process is reduced. Consequently, higher ethanol emulsions exhibit an enhanced stability against flocculation (Dickinson & Golding, 1998), with these emulsions exhibiting Newtonian behavior because the floc formation that is responsible for the non-Newtonian behavior is retarded.

Interestingly, at the highest ethanol content, the emulsions prepared either with canola oil or coconut oil (emulsions 7 and 9) exhibited similar results in viscosity (~40 mPa·s), that supports the statement that the rheological behavior of emulsions are highly dependent on the ethanol content regardless of the type of oil. Moreover, the differences in viscosity

between emulsions made with the same amount of sodium caseinate, for example, emulsions 5, 6 and 7, suggested that the reduction in viscosity due to ethanol content seems more affected by oil content than by protein content.

4.2.3 Droplet Size Distribution

The droplet size distribution were evaluated at 72 hours and 30 days after emulsion preparation, the mean droplet diameter (d_{32}) is reported as the average of two independent samples and there are two subsamples making the mean value of each sample. The standard deviation and the coefficient of variation of the corresponding mean value were also calculated.

4.2.3.1 Sodium Caseinate-Canola Oil-Ethanol System

The mean droplet diameter for the sodium caseinate-canola oil-ethanol system at 72 hours and 30 days is presented in Table 4.5.

Emulsion prepared with the lowest protein content, emulsion 1, showed a jump in the mean droplet size after 30 days of storage from d_{32} of 0.4 to 0.7 μm, while emulsions 3, 5, 8 and 9 showed a minor increase in the mean droplet diameter from 0.3 to 0.4 μm over the course of the experiments.

Apart from the emulsions with a large droplet size (2, 4 and 7), the droplet size distribution at 72 hours (Figures 4.14-4.17) showed a non-unimodal distribution, with a small peak at ~0.2 μm and a large peak at ~0.4-0.5 μm. After 30 days the droplet size distribution shifts to higher sizes and the smaller peak tends to disappear. The peak at 0.2 μm observed in the droplet size distribution of emulsions 8 and 9 (Figure 4.16) at 72 hours was very small and disappeared after 30 days.

Table 4.5 Mean droplet diameters (d_{32}) of the ten samples prepared for emulsion characterization of the system: sodium caseinate-canola oil-ethanol.

	72 hours after preparation		30 days after preparation	
Sample #	d_{32} μm [1]	Coefficient of variation	d_{32} μm	Coefficient of variation
1	0.450 ± 0.015	3.4	0.757 ± 0.042	5.6
2	3.428 ± 0.078	2.3	NA	NA
3	0.385 ± 0.008	2.0	0.480 ± 0.006	1.2
4	2.296 ± 0.019	0.8	NA	NA
5	0.316 ± 0.004	1.3	0.482 ± 0.028	5.8
6	0.299 ± 0.001	0.5	0.299 ± 0.004	1.3
7	1.774 ± 0.109	6.1	2.113 ± 0.042	2.0
8	0.317 ± 0.011	3.5	0.424 ± 0.034	7.9
9	0.263 ± 0.021	8.1	0.366 ± 0.080	21.7
10	0.234 ± 0.004	1.5	NA	NA

[1] Mean ± standard deviation (obtained for two independent samples)
NA: Data not available, unstable emulsion

The droplet size distribution of emulsion 1 (Figure 4.14) showed the least unimodal distribution with the presence of 3 peaks at 72 hours, but the distribution shifts to a wide bimodal distribution after 30 days. Considering that the mean diameter of casein micelles reported in the literature is 0.2 μm, it can be assumed that this small peak is not only represented small oil droplets, it can represent casein micelles too. Since the small peak tends to disappear at 30 days and the higher peak shifted to higher sizes, it would suggest that casein micelles in the continuous phase are aggregated or that casein micelles move to the interfacial layer which will increase the protein surface coverage (Dickinson & Woskett, 1988). These changes will reduce the strength of depletion interaction.

In particular, for emulsion 2 and 4 from the results of mean diameter (d_{32}) at 72 hours, an unstable behavior was expected because large droplet sizes affects colloidal interactions

and enhances unstable behaviors such us creaming and flocculation (McClements, 2004). For emulsion 2 the droplet size distribution at 72 hours (Figure 4.14) showed a large peak at ~5 μm and a very small peak at ~1 μm while for emulsions 4 and 7 the droplet distribution (Figure 4.15) was monomodal with a center value ~ 2 μm. It is evident that large droplets are formed at 72 hours. Studies have reported that Ostwald ripening leads to monomodal distributions and that the rate at which droplets grow is proportional to the solubility of the oil in the continuous phase (Hemar & Horne, 1999; McClements, 2007). Considering that emulsions 2 and 4 contain 22 and 25 %wt ethanol, respectively, the solubility of oil in the continuous phase may be favored and therefore Ostwald ripening is enhanced. During storage for 30 days, large droplets may tend to cream faster as predicted by Stokes equation and then phase separation may occur as a consequence.

The fact that emulsion 7 also contained a large amount of ethanol and had a monomodal distribution but was stable during 30 days appears contradict the explanation given for the physical separation of emulsions 2 and 4. In the previous section, it was pointed out that the presence of a large amount of ethanol in the continuous phase promotes migration of unadsorbed casein to the interfacial layer and casein aggregation. Since emulsion 7 has a higher ethanol content than emulsions 2 and 4, more unadsorbed casein would migrate to the interfacial layer, and consequently the development of depletion flocculation is retarded. The changes in the polarity of the continuous phase due to the presence of ethanol will increase repulsive interactions between droplets and droplets-casein over a range sufficient to maintain a finite stability even with the formation of large droplets and casein aggregates.

(a)

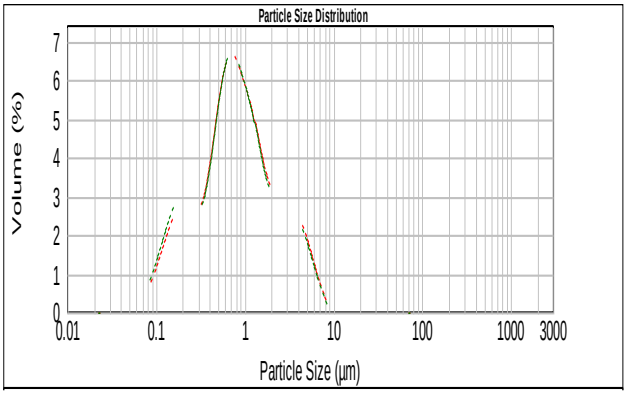

(b)

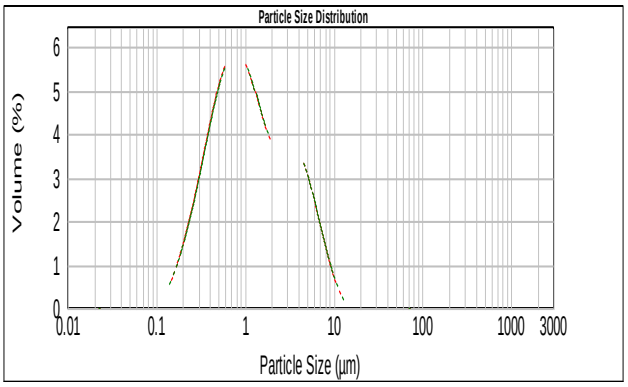

(c)

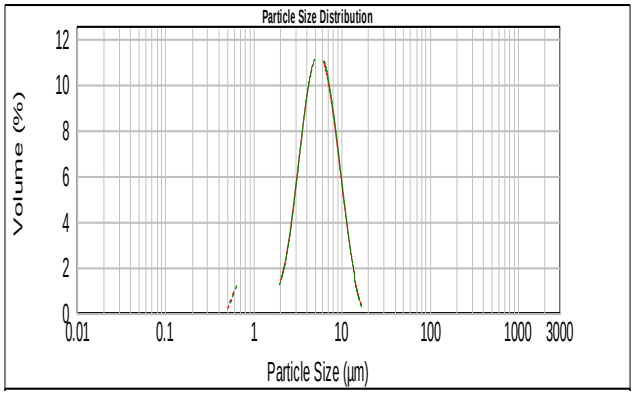

(d)

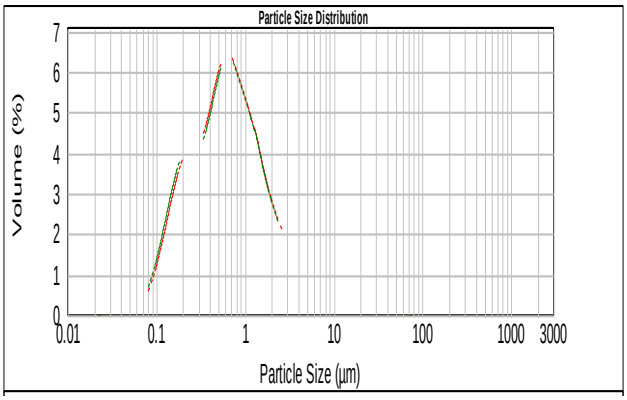

(e)

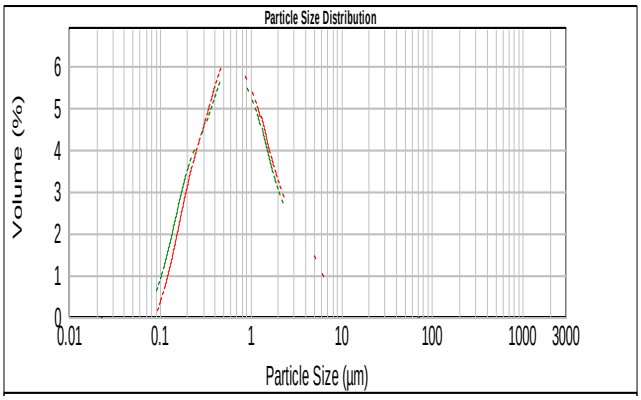

Figure 4.14 Droplet size distribution of emulsions (sodium caseinate-canola oil-ethanol system) (a) emulsion 1 at 72h; (b) emulsion 1 at 30 days; (c) emulsion 2 at 72h; (d) emulsion 3 at 72h; (e) emulsion 3 at 30 days. Each graph shows the droplet size distribution of two independent samples.

(f)

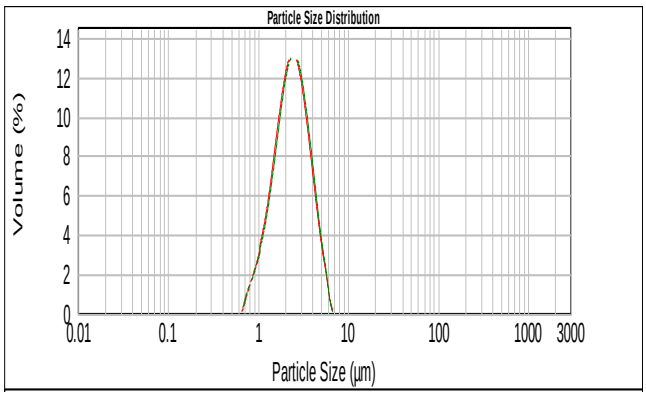

(g)

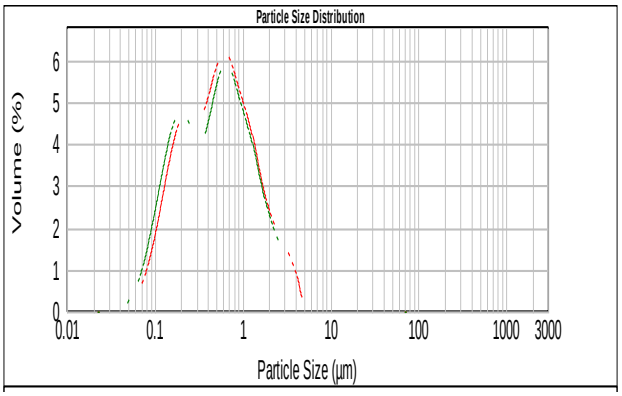

(h)

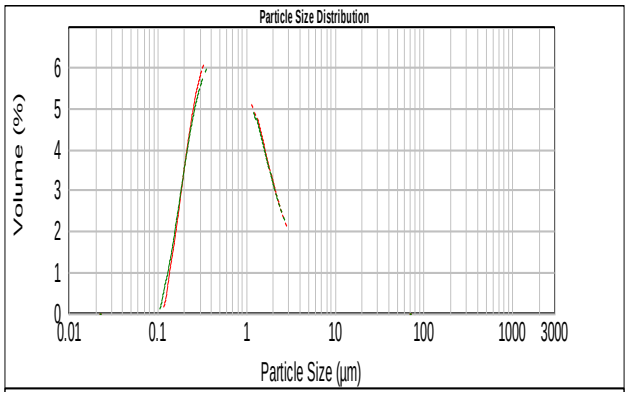

(i)

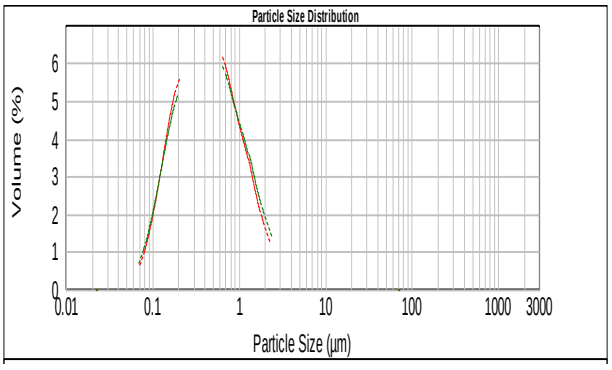

(j)

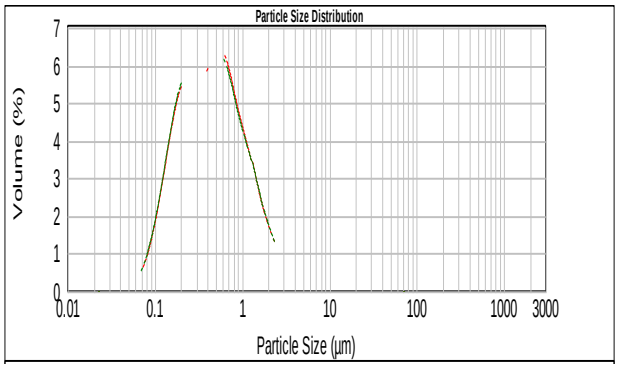

Figure 4.15 Droplet size distribution of emulsions (sodium caseinate-canola oil-ethanol system) (f) emulsion 4 at 72h; (g) emulsion 5 at 72h; (h) emulsion 5 at 30 days; (i) emulsion 6 at 72h; (j) emulsion 6 at 30 days. Each graph shows the droplet size distribution of two independent samples.

(k)

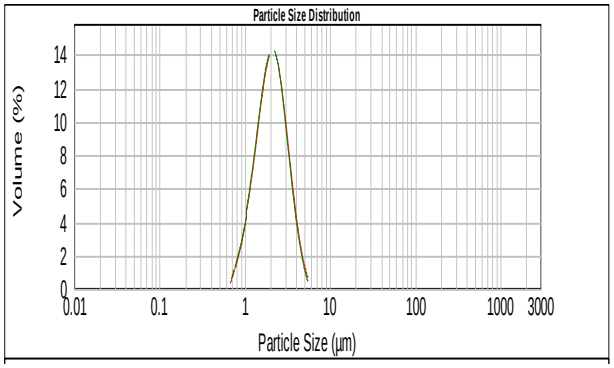

(l)

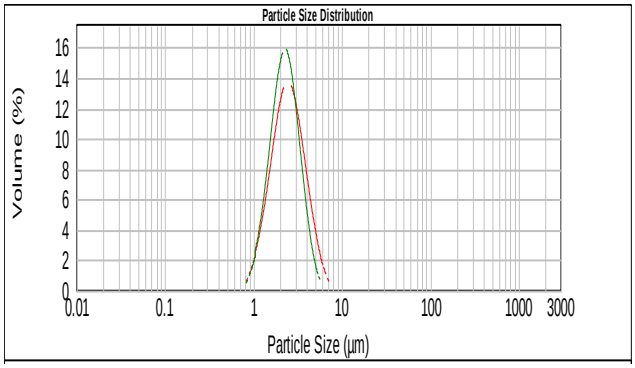

(m)

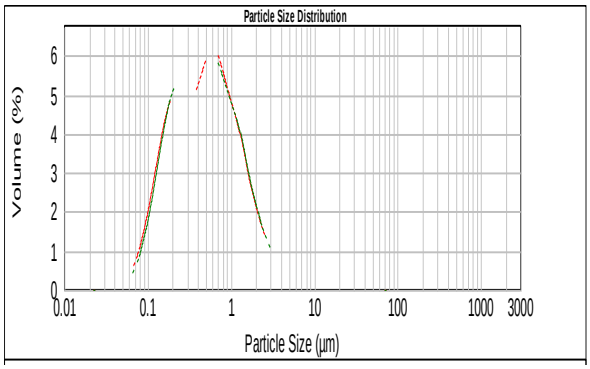

(n)

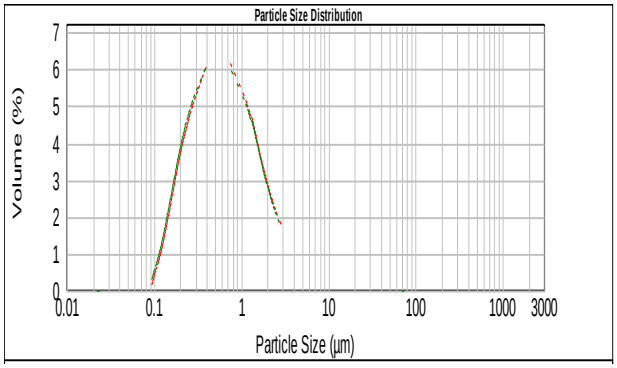

(o)

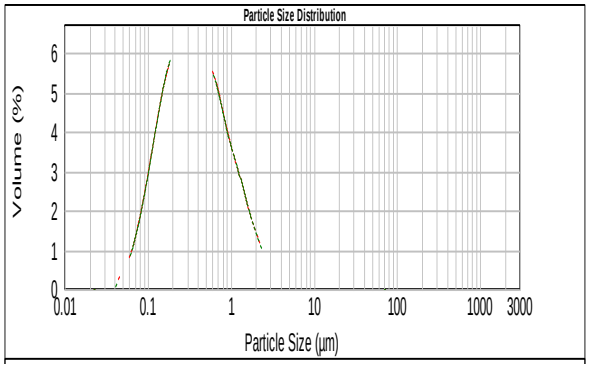

(p)

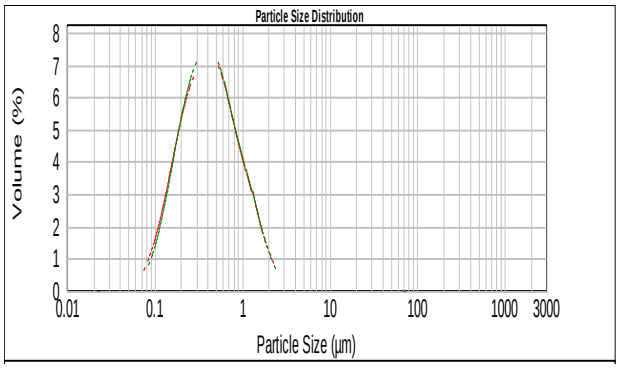

Figure 4.16 Droplet size distribution of emulsions (sodium caseinate-canola oil-ethanol system) (k) emulsion 7 at 72h; (l) emulsion 7 at 30 days, (m) emulsion 8 at 72h; (n) emulsion 8 at 30 days; (o) emulsion 9 at 72h; (p) emulsion 9 at 30 days. Each graph shows the droplet size distribution of two independent samples.

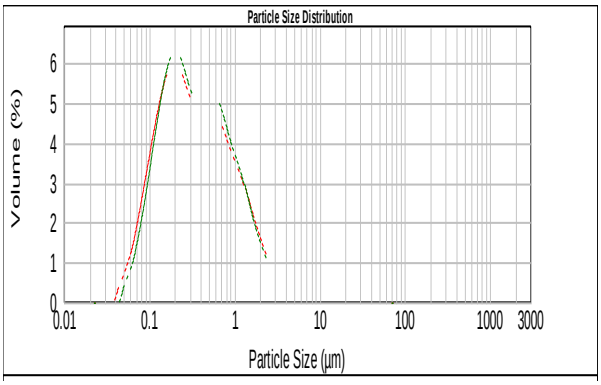

Figure 4.17 Droplet size distribution of emulsion 10 at 72h (sodium caseinate-canola oil-ethanol system). Graph shows the droplet size distribution of two independent samples.

4.2.3.2. Sodium Caseinate-Coconut Oil-Ethanol System

The mean droplet diameter (d_{32}) for the ten emulsions evaluated for the characterization of the sodium caseinate-coconut oil-ethanol system at 72 hours and 30 days is presented in Table 4.6.

Table 4.6 Mean droplet diameters (d_{32}) of the ten samples prepared for emulsion characterization of the system: sodium caseinate-coconut oil-ethanol.

Sample #	d_{32} µm [1]	Coefficient of variation	d_{32} µm	Coefficient of variation
1	1.339 ± 0.126	9.4	1.436 ± 0.023	1.6
2	1.501 ± 0.113	7.5	1.570 ± 0.160	10.2
3	0.500 ± 0.037	7.5	0.551 ± 0.025	4.6
4	1.004 ± 0.044	4.4	1.069 ± 0.027	2.5
5	0.434 ± 0.001	0.2	0.387 ± 0.019	4.8
6	0.291 ± 0.014	4.7	0.312 ± 0.030	9.8
7	0.737 ± 0.025	3.4	1.326 ± 0.018	1.4
8	0.290 ± 0.012	4.3	NA	NA
9	0.367 ± 0.006	1.7	0.380 ± 0.046	12.2
10	0.224 ± 0.022	9.6	NA	NA

[1] Mean ± standard deviation (obtained for two independent samples)
NA: Data not available, unstable emulsion

Emulsions 3 and 5 made with low ethanol content (8 %wt) and high oil fraction (> 42 %wt) showed a small droplet mean diameter and a wide droplet distribution (Figures 4.19- 4.20). The droplet distribution of emulsion 3 showed a small peak on the right side of the droplet distribution that became less distinct over 30 days. It indicated that there is a growth in droplet size even thought the mean droplet diameters at 72 hours and 30 days are very close in value. The droplet size distributions shown in Figure 4.19-4.21 for emulsions 5, 6 and 10 at 72 hours exhibited a wide distribution with a center value between 0.3-0.4 μm. Like in emulsions made with canola oil, emulsion 9, with the lowest oil content and the highest ethanol content, showed a small mean droplet diameter and a wide droplet size distribution (Figure 4.21). In sample 7 (Figure 4.20), a small peak at ~0.2 μm can be observed at 72 hours that disappeared after 30 days. For emulsions 8 and 10 the peak at ~0.2 μm was smaller than the peak observed in emulsions made with canola oil. As was mentioned in the previous section, this small peak at 72 hours can represent casein micelles. The shift in droplet size distribution from bimodal to monomodal for emulsion 7 and a corresponding increase in the mean droplet diameter indicated a growth in droplet size which is characteristic of Ostwald ripening (McClements, 2004). Nevertheless, the assumption that the small peak at ~0.2 μm represented unadsorbed casein micelles and the fact that it disappeared at 30 days, can also be attributed to the migration of casein micelles from the continuous phase to the droplet surface.

With the exception of emulsions 8 and 10 that were unstable, emulsions showed no discernible change in the average droplet size at 30 days. To support this conclusion, the differences in mean droplet diameters were also evaluated by a t-test analysis considering each sample with its corresponding subsample as separate data. Thus, the two samples with their corresponding subsamples give four data to be used to evaluate the significance of the difference in the mean droplet diameter after 72 hours and 30 days. The statistical

analysis supported the conclusion that only sample 7 had a significant change in mean droplet diameter over 30 days storage, increasing from 0.7 to 1.3 μm.

(a)

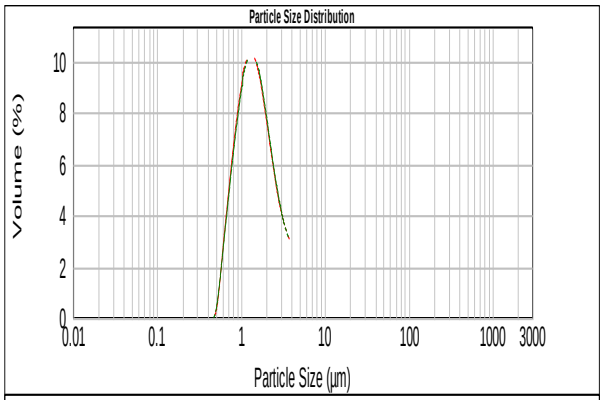

(b)

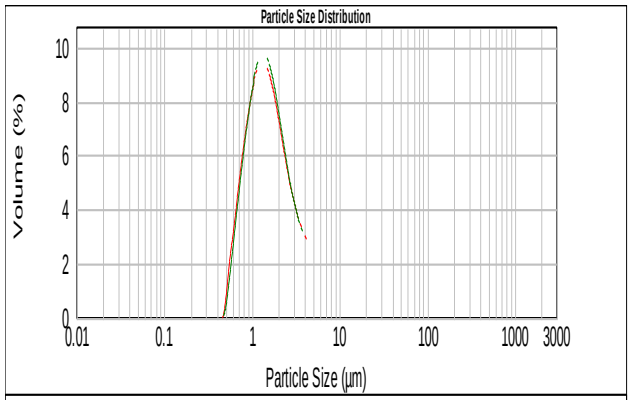

(c)

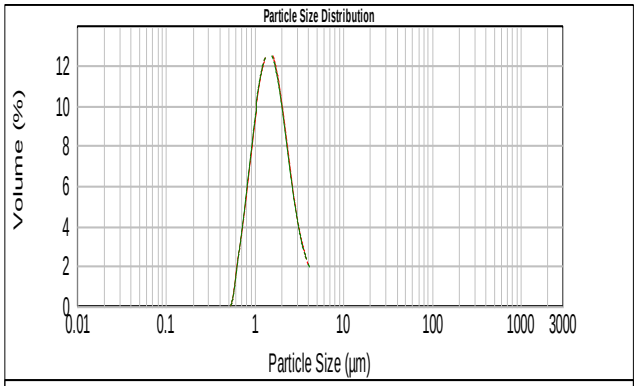

(d)

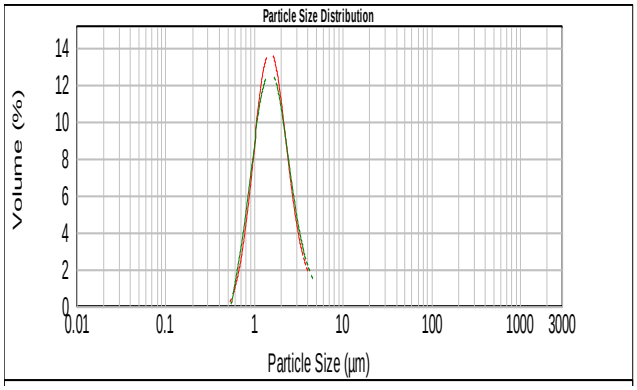

Figure 4.18 Droplet size distribution of emulsions (sodium caseinate-coconut oil-ethanol system) (a) emulsion 1 at 72h; (b) emulsion 1 at 30 days; (c) emulsion 2 at 72h; (d) emulsion 2 at 30 days. Each graph shows the droplet size distribution of two independent samples.

(e)

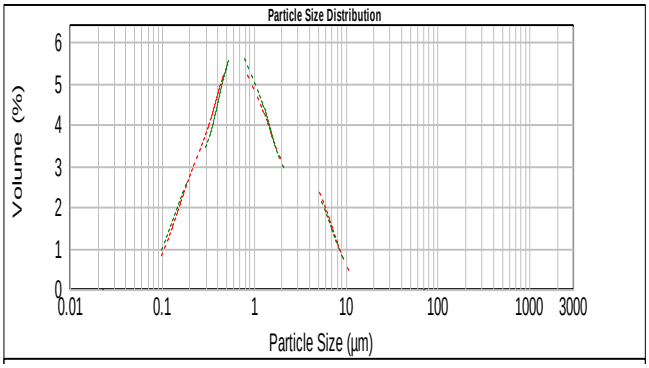

(f)

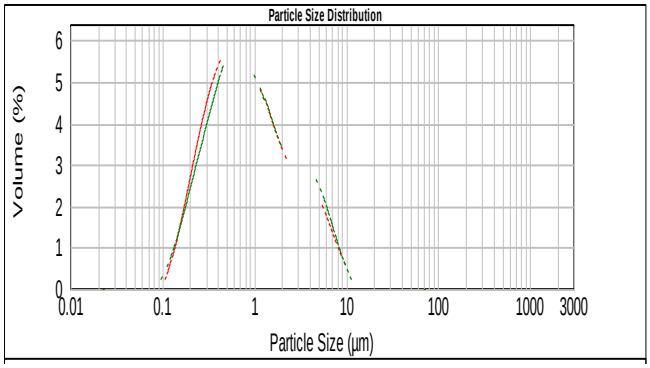

(g)

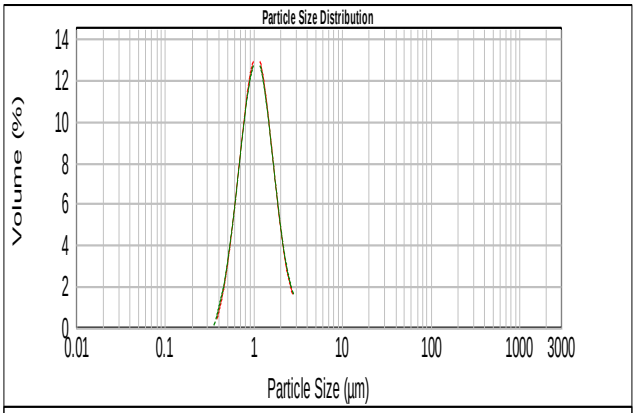

(h)

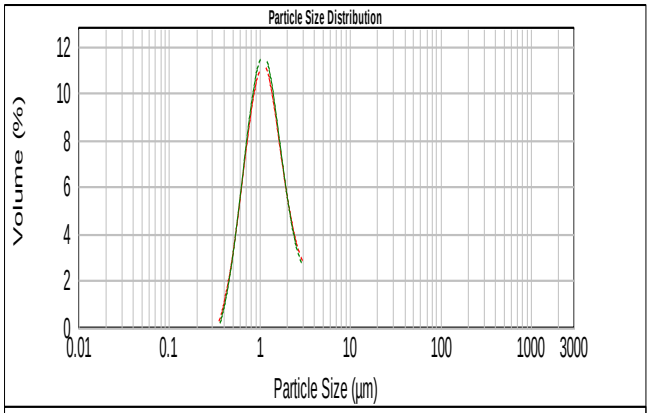

(i)

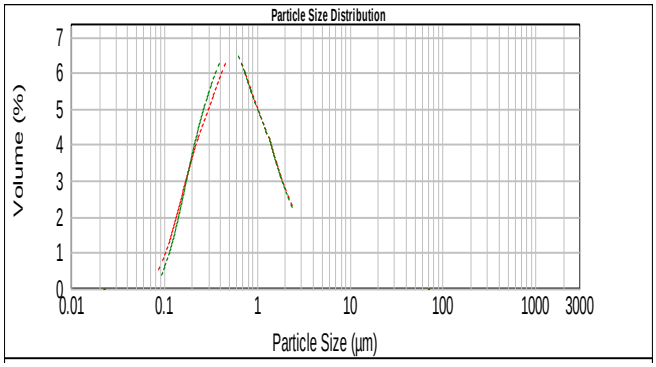

(j)

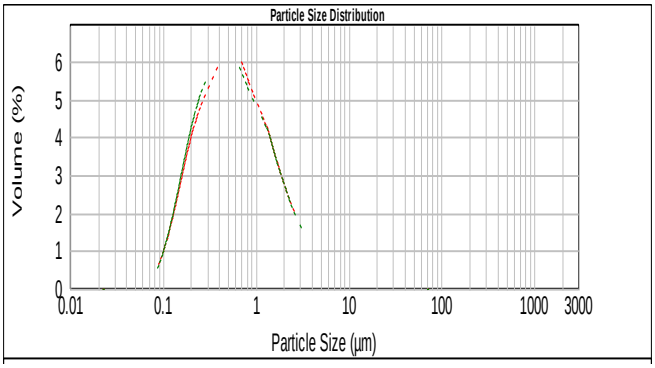

Figure 4.19 Droplet size distribution of emulsions (sodium caseinate-coconut oil-ethanol system) (e) emulsion 3 at 72h; (f) emulsion 3 at 30 days; (g) emulsion 4 at 72h; (h) emulsion 4 at 30 days; (i) emulsion 5 at 72h; (j) emulsion 5 at 30 days. Each graph shows the droplet size distribution of two independent samples.

(k)

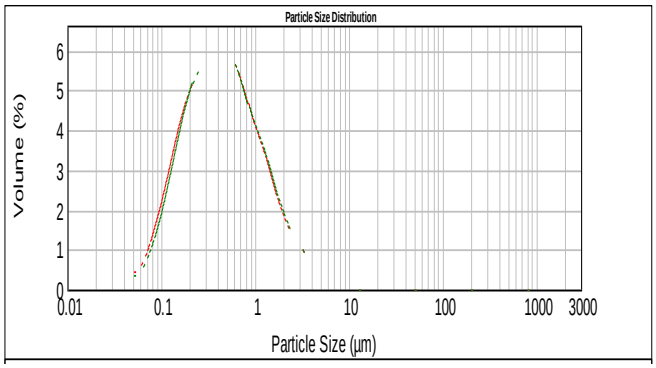

(l)

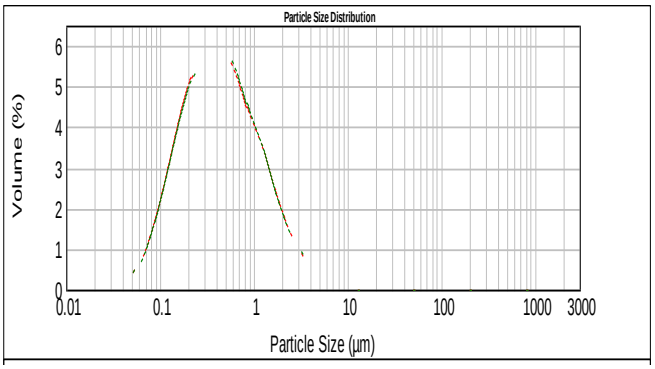

(m)

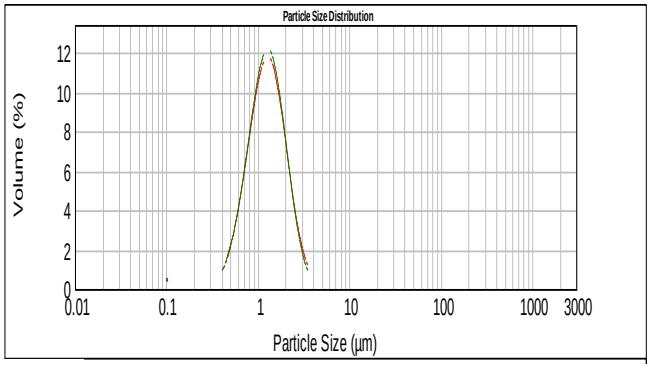

(n)

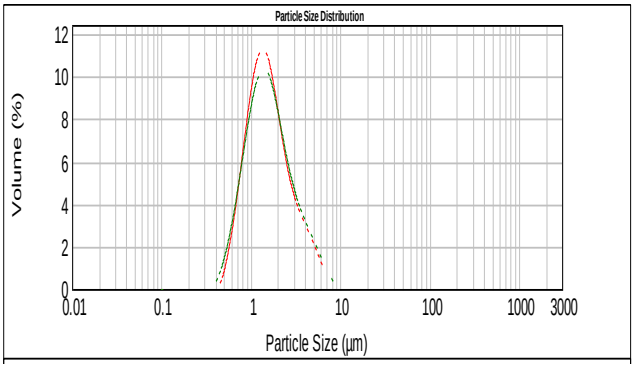

(o)

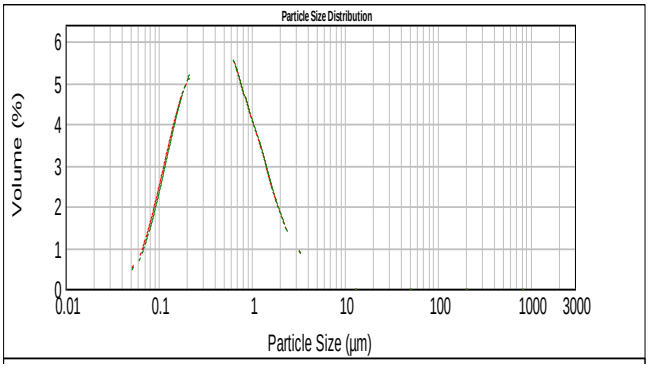

Figure 4.20 Droplet size distribution of emulsions (sodium caseinate-coconut oil-ethanol system) (k) emulsion 6 at 72h; (l) emulsion 6 at 30 days; (m) emulsion 7 at 72h; (n) emulsion 7 at 30 days; (o) emulsion 8 at 72h. Each graph shows the droplet size distribution of two independent samples.

(p)

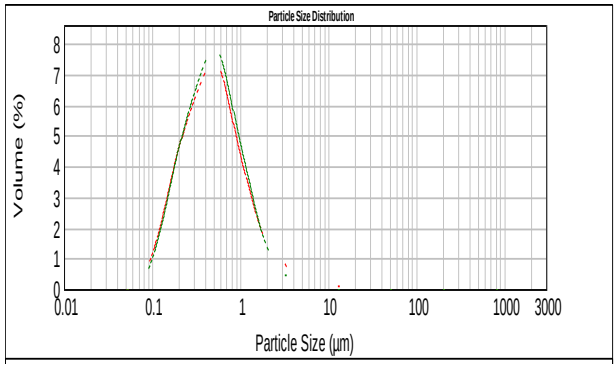

(q)

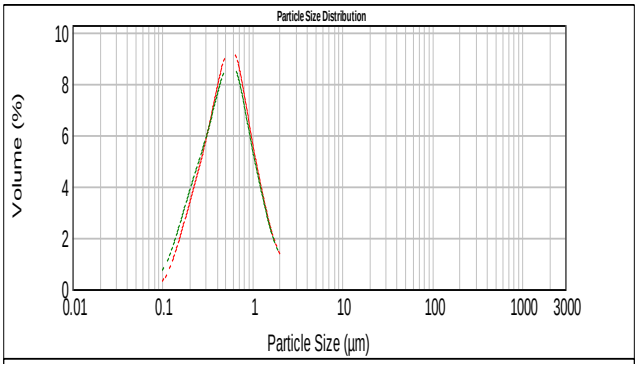

(r)

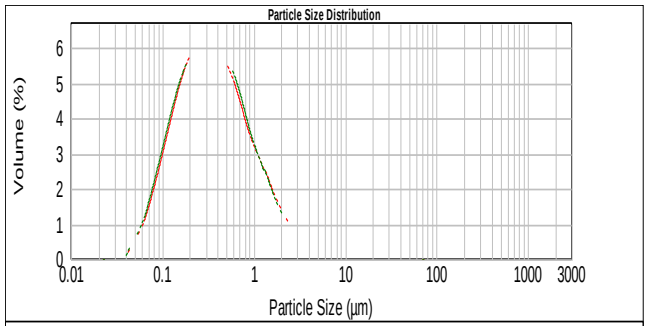

Figure 4.21 Droplet size distribution of emulsion (sodium caseinate-coconut oil-ethanol system) (p) emulsion 9 at 72h; (q) emulsion 9 at 30 days; (r) emulsion 10 at 72h. Each graph shows the droplet size distribution of two independent samples.

It is reported that changes in droplet size distribution in sodium caseinate stabilized emulsions are affected by protein concentration, its adsorption at the interfacial layer and its structural changes during storage time (Dickinson, 1999). Casein adopted an α-helix structure when it was exposed to a large amount of ethanol in order to reduce the contact between the amino acids groups of casein and the solvent (Dickinson & Woskett, 1988; Radford et al., 2004). Studies carried out to evaluate the changes in the protein adsorbed layer during storage time led to the conclusion that in sodium caseinate stabilized

emulsions a protein crosslinking is favored over time and is enhanced at high temperatures (e.g., 30 and 40°C) (Euston & Mayhill, 2001). The implication is therefore that the adsorption of protein at the interface may proceed at different rates in each system mainly influenced by the changes in the polarity of the continuous phase due to ethanol addition. This condition implies that ethanol also induces changes in droplet size of emulsions due to its effect on the location of casein. To illustrate the effect of ethanol on the droplet size of the emulsions, the mean droplet sizes for both systems were plotted on the phase diagram. The dashed lines on the phase diagrams show a zone of large droplet size, at the right hand side of the x axis, which corresponds to emulsions with high contents of ethanol and sodium caseinate but low contents of oil. Moving to the left hand side on the x axis, it corresponds to a zone of small droplet size characterized for emulsions that contain a low concentration of ethanol in combination with high concentrations of oil and sodium caseinate.

(a)

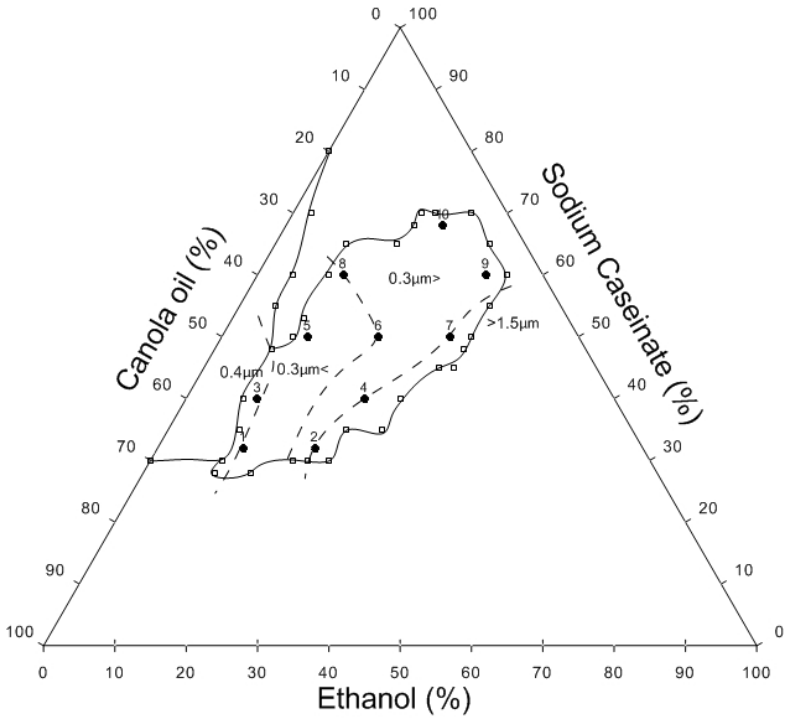

(b)

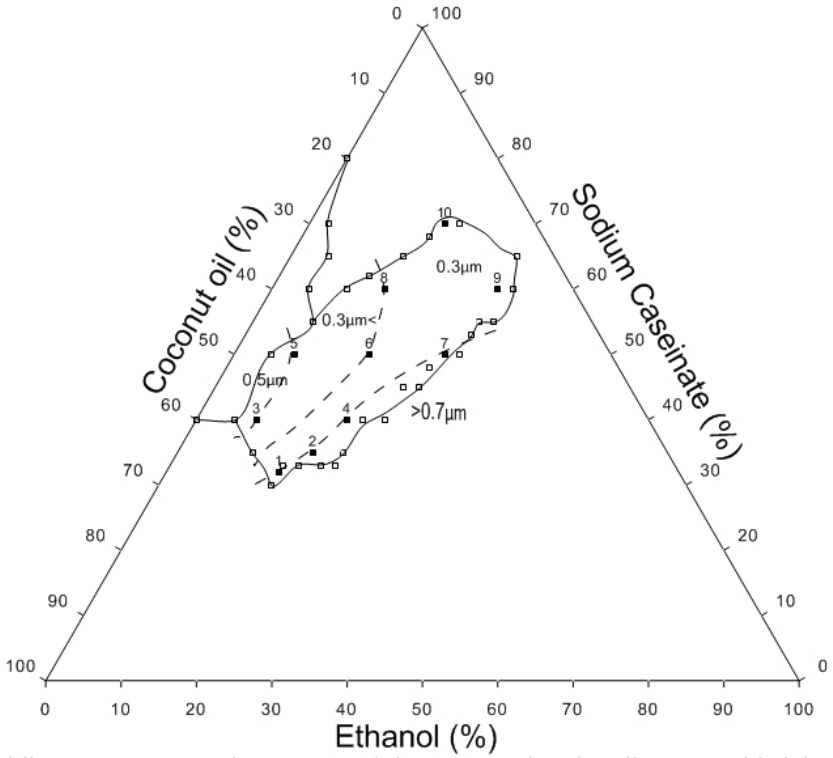

Figure 4.22 Dashed lines represent the range of the mean droplet diameter (d_{32}) in the region of emulsion stability at 72 hours for (a) sodium caseinate-canola oil-ethanol system (b) sodium caseinate-coconut oil-ethanol system.

4.2.4 Discussion on Emulsion Characterization

From the rheological behavior and the droplet size distribution reported in previous sections, it can be seen that emulsion properties were highly affected by ethanol content. In particular, a window of finite emulsion stability was observed at ethanol concentrations of ~ 28 %wt characterized by a low viscosity and a wide monomodal droplet size distribution. Depletion flocculation is reported as the predominant source of unstable behavior in oil-in-water emulsions containing unadsorbed protein (Dickinson & Golding, 1997b; Kim et al., 2004). As was described in section 2.2.3.3 the strength of the depletion interaction energy (U_D) depends on the size of the unadsorbed casein micelles, the oil droplet radius and the magnitude of the osmotic pressure gradient generated due to the exclusion of casein submicelles from the gap created between two adjacent oil droplets. In section 2.2.5.2 a theoretical model was presented to calculate the concentration of protein in the interface layer (C_{ad}), the protein concentration in the continuous phase (C_b), and the osmotic pressure gradient (P_{osm}) for a given emulsion composition (equations 12-15). These equations can be therefore used to analyse the depletion interactions at work in the region of emulsion stability.

The parameters cited above were calculated for a large range of emulsion compositions, under the premise that: sodium caseinate in the continuous phase exists as casein submicelles (equal in size and shape), and that it represents the unadsorbed casein available in the system that will generate an osmotic pressure gradient which is proportional to the magnitude of the depletion interaction energy (U_D) (equation 9). It should be noticed that all calculations are made only for the sodium caseinate-canola oil-ethanol system however the conclusions are valid for both systems because the selection of one system over the other implies only a very small difference in the oil density used to calculate the oil volume fraction.

In order to estimate the oil volume fraction, $\phi = \frac{\phi\rho_C}{\phi\rho_c + \rho_{oil}(1-\phi)}$ (equation 3), required to calculate the concentration of adsorbed casein, $C_{ad} = \frac{6\Gamma\phi_{oil}}{d_{32}}$ (equation 15), the density of the oil phase, ρ_{oil} , was set to 0.914 g cm^{-3} which corresponds to the density of canola oil (Przybylski & Mag, 2000). The density of the continuous phase, ρ_c , was calculated considering the changes in its density when significant amounts of ethanol are added. Thus, the density of the continuous phase is calculated as $\rho_c = \phi_{casein}\,\rho_{casein} + (1 - \phi_{casein})\rho_{w-e}$, where ϕ_{casein} represent the fraction of sodium caseinate, ρ_{casein} represents the density of sodium caseinate in solution and ρ_{w-e} the density of the ethanol-water mixtures.

The density of sodium caseinate in solution, ρ_{casein} , was set under the following considerations: (i) a hydrodynamic volume of casein micelles of 4.4 $cm^3 \cdot g^{-1}$ (De Kruif, 1998), (ii) a specific volume of dried casein of 0.618 $cm^3\ g^{-1}$ (Berlin & Pallansch, 1968), so that 3.78 $cm^3 \cdot g^{-1}$ corresponds to the water volume per gram of casein, (iii) considering a random packing of hydrated casein micelles with a volume fraction of 0.64, thus 3.78 $cm^3 \cdot g^{-1}$ divided by 0.64 gives the water required for minimal hydration of 1gram of dried casein, 5.91 $cm^3 \cdot g^{-1}$. The density of water is considering 0.997 g cm^{-3} at 26°C, so that 5.91 cm^3 of water equal to 5.96 g of water. Therefore, the average density of sodium caseinate in solution can be established as 1.055 $g \cdot cm^{-3}$. The density of the ethanol-water mixtures, ρ_{w-e} , was taking from Perry's Chemical Engineer Handbook (Table 2-110).

As can be seen from equation 15, the surface coverage (Γ) is also required to estimate the concentration of adsorbed casein. A first approach was made considering a constant surface coverage for all the emulsion compositions used in the analysis. So the surface coverage was set to 3 mg m^{-2} (Fang & Dalgleish, 1992; Dickinson & Golding, 1997b). With regards to the mean droplet diameter (d_{32}), it was selected on the basis of the

experimental data obtained from the droplet size distribution. In section 4.2.3, it was reported that essentially all emulsions had a droplet size distribution with a small peak at ~ 0.2 μm and a d_{32} at approx ~0.5 μm; thus these two values were used separately to calculate the concentration of adsorbed casein for each emulsion composition. The concentration of adsorbed casein obtained from equation 15, and the oil volume fraction obtained from equation 3 were used to calculate the concentration of sodium casein in the continuous phase, C_b, $C_b = \frac{(C - C_{ad})}{(1 - \phi_{oil})}$ (equation 14), that represents the unadsorbed casein. Finally, the results are plotted on the phase diagram (Figure 4.23) where + represented an emulsion composition with a specific mean droplet diameter (0.2 μm or 0.5 μm) with enough unadsorbed casein that will generate an osmotic pressure gradient and therefore potentially promote depletion flocculation. The line plotted on the phase diagram represents a boundary line that separates emulsion compositions that contain the minimum concentration of unadsorbed sodium caseinate needed to create an osmotic pressure gradient (the right side of the boundary line) versus emulsion compositions with not enough unadsorbed casein to remain in the continuous phase (the left side of the boundary line). The solid segment of this line represents the region where ethanol content is within the range of the region of emulsion stability (0-32 %wt ethanol) while the dashed line represents the region where ethanol is out of this range.

It can be seen in Figure 4.23 that with a mean droplet diameter of 0.2 μm, 38 %wt sodium caseinate in solution represents a lower limit to have a minimum concentration of unadsorbed casein at low ethanol concentrations. As ethanol increase the total amount of sodium caseinate required to have unadsorbed casein decreases gradually. In Figure 4.24 the minimum unadsorbed casein concentration was calculated based on a mean droplet diameter of 0.5 μm. Comparing Figure 4.23 versus Figure 4.24, it can be seen that the boundary line that limited the region of emulsions with enough unadsorbed casein moves

down, and the slope of the boundary line became lower. Under this condition the concentration of sodium caseinate required to have unadsorbed casein is ~18 %wt. The large difference in the boundary lines between the two figures demonstrates that larger mean droplet diameters promote more casein remaining in the continuous phase, enhancing depletion flocculation as predicted by equation 9.

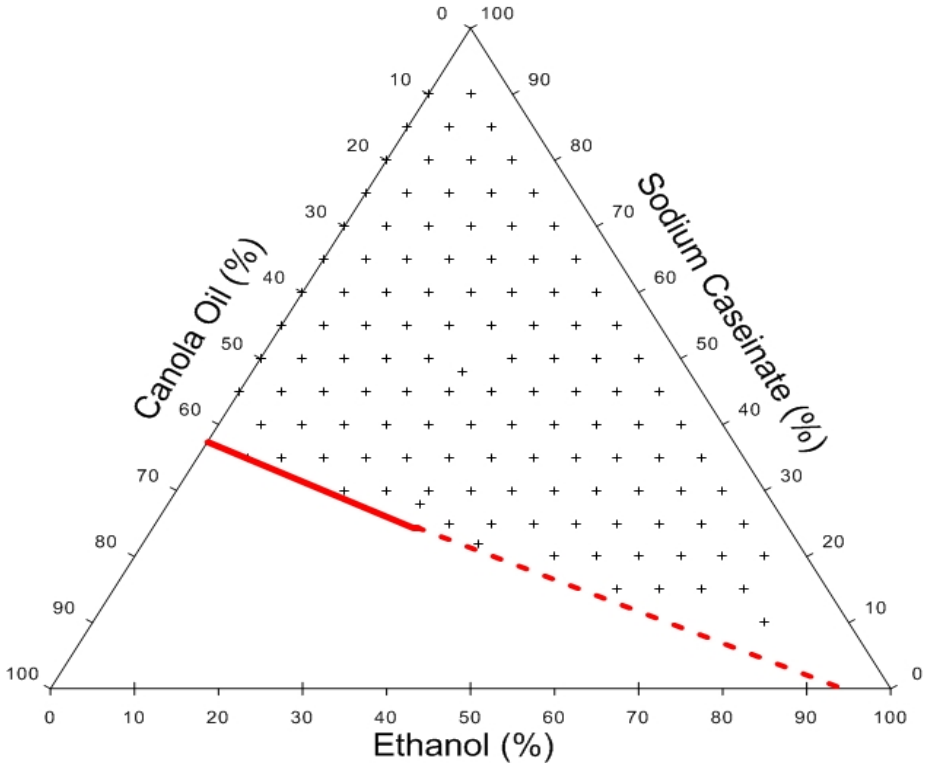

Figure 4.23 Concentrations where unadsorbed casein (+) is present calculated from equation 14 for different emulsion compositions. It is assumed that mean droplet diameter (d_{32}) is 0.2 μm, and a surface coverage of Γ = 3mg m^{-2} produces a stable emulsion (Fang & Dalgleish, 1993; Dickinson & Golding, 1997). The solid line represents the boundary line within the range of ethanol between 0-32 %wt where emulsions contain the minimum level of unadsorbed casein to generate an osmotic pressure gradient. The dashed line represents the boundary line for emulsions with an ethanol content higher than 32 %wt.

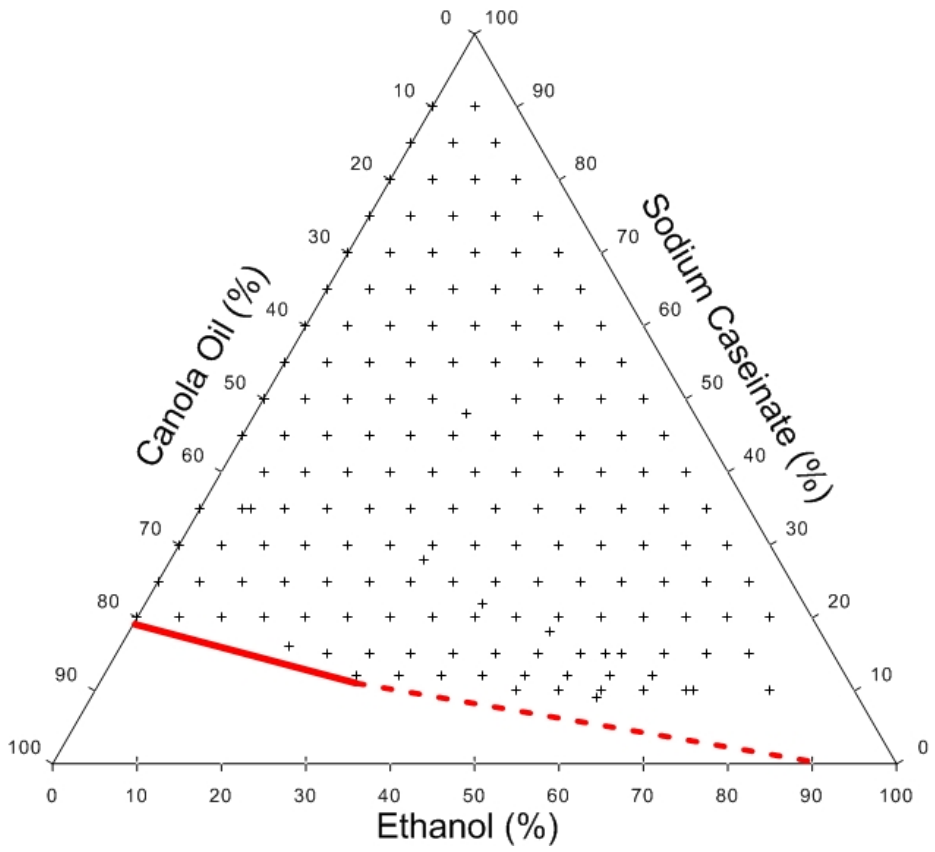

Figure 4.24 Concentrations where unadsorbed casein (+) is present calculated from equation 14 for different emulsion compositions. It is assumed that mean droplet diameter (d_{32}) is 0.5 μm, and a surface coverage of Γ = 3 mg m^{-2} produces a stable emulsion (Fang & Dalgleish, 1993; Dickinson & Golding,1997). The solid line represents the boundary line within the range of ethanol between 0-32 %wt where emulsions contain the minimum level of unadsorbed casein to generate an osmotic pressure gradient. The dashed line represents the boundary line for emulsions with an ethanol content higher than 32 %wt.

However it is not likely sensible to employ a constant value for casein surface coverage, given that casein conformation is affected by ethanol content (Horne, 1985; Horne & Davidson, 1986; Radford et al., 2004). Therefore, in a second approach I considered the

values reported by Radford et al. (2004) for surface coverage in an ideal emulsion (30 vol% oil and 4 wt% sodium caseinate) containing 0, 10 or 25 %wt of ethanol, as reported in Table 2.2. These values were used to calculate the minimum concentration of unadsorbed casein for the same emulsion compositions used in the first approach. The results became more interesting because the boundary line moved up on the phase diagram (Figure 4.25). In others words, the total sodium caseinate concentration which is expected to be the minimal concentration of unadsorbed casein to generate depletion interaction moves to 40 %wt of sodium caseinate solution and runs almost parallel to the x axis. The same trend was observed from the calculations made considering a mean droplet diameter of 0.5 μm (Figure 4.26). In this case, the lower total concentration of sodium caseinate moves from 18 wt% when a constant surface coverage was considered to 20 wt% when surface coverage changes as ethanol increased.

These results illustrate the strong influence of ethanol on the adsorption behavior of casein. As well, the results are consistent with the mechanism cited in section 4.2.2.2, that is, the presence of ethanol promotes protein movement to the oil surface, increasing the density of casein submicelles in the interfacial layer, which resulted in an increase in surface coverage which in turn reduces the concentration of unadsorbed casein and therefore reduces the range of depletion forces (Dickinson & Golding, 1998; Radford et al., 2004).

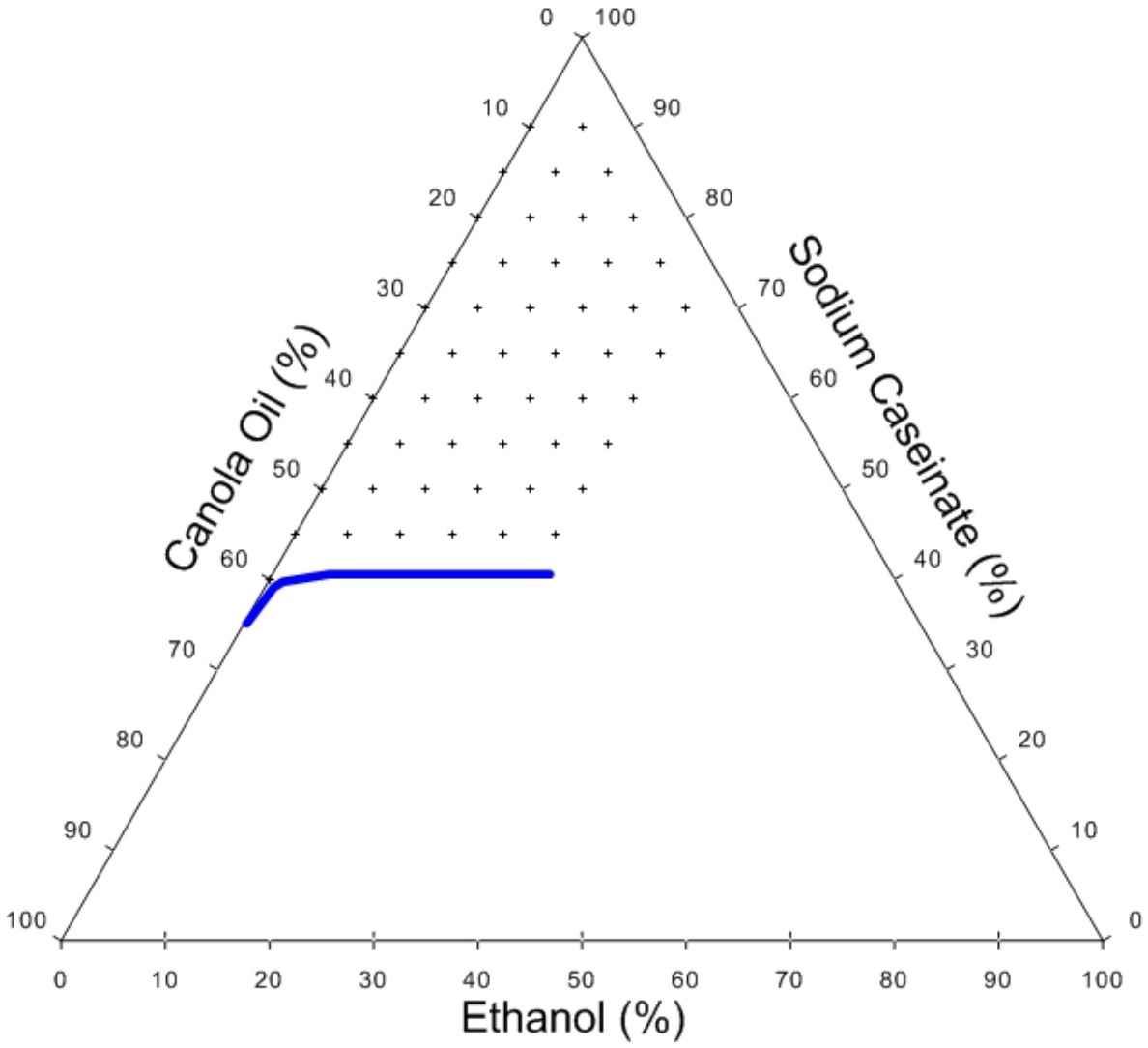

Figure 4.25 Concentrations where unadsorbed casein (+) is present calculated from equation 14 for different emulsion compositions. It is assumed that mean droplet diameter (d_{32}) is 0.2 μm. The surface coverage values reported by Radford et al. (2004) in emulsions containing ethanol are used to calculate the concentration of adsorbed casein. The solid line represents the boundary line within a range of ethanol between 0-25 %wt at which emulsions contain the minimum concentration of unadsorbed casein to generate an osmotic pressure gradient.

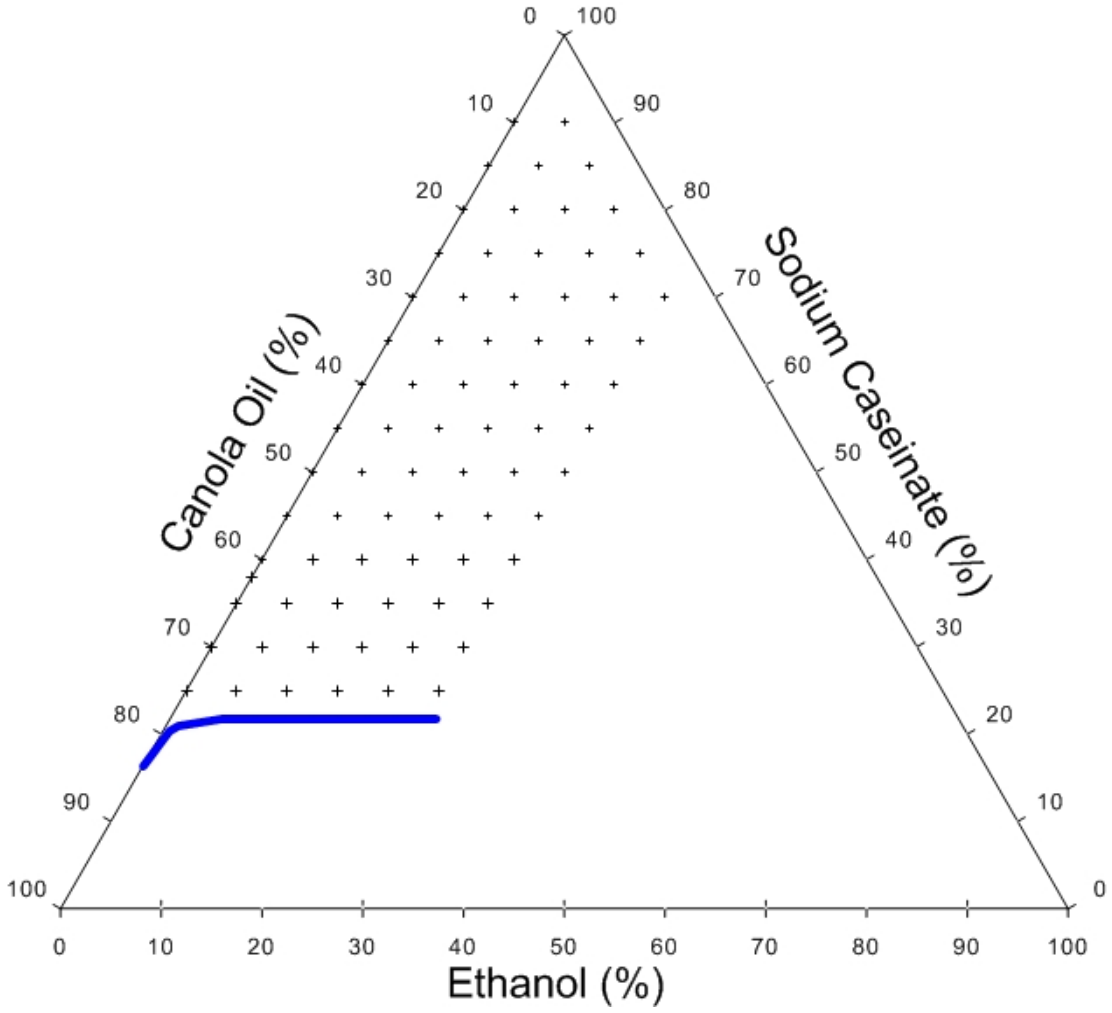

Figure 4.26 Concentrations where unadsorbed casein (+) is present calculated from equation 14 for different emulsion compositions. It is assumed that mean droplet diameter (d_{32}) is 0.5 μm. The surface coverage values reported by Radford et al. (2004) in emulsions containing ethanol are used to calculate the concentration of adsorbed casein. The solid line represents the boundary line within a range of ethanol between 0-25 %wt at which emulsions contain the minimum concentration of unadsorbed casein to generate an osmotic pressure gradient.

The boundary line plotted in Figure 4.25 lies on the bottom of the region of emulsion stability on the phase diagram; specifically, it runs through emulsions 3 and 4. Emulsions 1 and 2 are below this boundary line. This leads to the conclusion that for emulsion 1 and 3 since the alcohol level is low (less than 12 %wt for emulsion made with canola oil, and less than 15 %wt for emulsions made with coconut oil), it may be just enough casein to cover the surface of the oil droplets that in combination with the high oil volume fraction creates a close packed system which is consistent with the high viscosity observed for these emulsions. For emulsions 2 and 4, where the alcohol content is higher (>18 %wt), insufficient casein may be available for complete coverage of the oil droplets and this compromises their long term stability. Thus, the physical separation observed in emulsions 2 and 4 made with canola oil may arise due to a larger droplet-droplet depletion interaction that enhances flocculation and creaming behaviors (Dickinson & Golding, 1998; Dickinson et al., 1997; Radford et al., 2004). This argument seems inconsistent for the sodium caseinate-coconut oil-ethanol system, because for this system emulsions 2 and 4 were stable against phase separation. An explanation can be found by evaluating the droplet size results of these samples. Emulsions 2 and 4 made with canola had a larger droplet size at 72 hours (d_{32} = 3.4 μm for emulsion 2 and d_{32} = 2.3 μm for emulsion 4) than emulsions made with coconut oil (d_{32} = 1.5 μm for emulsion 2 and d_{32} = 1.0 μm for emulsion 4). Therefore, in addition to depletion flocculation, Ostwald ripening seems more prevalent in emulsions 2 and 4 made with canola oil. The presence of higher ethanol concentration (22-25 %wt) in emulsions made with canola oil will contribute to enhanced solubilization of oil in the continuous phase. It is also reported that the solubility of oils in oil-ethanol-water systems increases when the oil contains a greater number of double bonds (Silva et al., 2010); thus canola oil is expected to be more soluble in the aqueous phase than coconut oil.

Although the calculation of the unadsorbed casein is based on an idealized system of a monodisperse assembly of casein micelles, their graphical representation through the phase diagrams (Figures 4.25-4.26) provided a useful insight of the relation between emulsion composition (i.e., casein, oil and ethanol content), and the level of casein available in the continuous phase that will generate an osmotic pressure gradient.

These calculations also help to explain the finite stability observed in emulsions 7 and 9 compared with emulsions 2 and 4 though the former have a high ethanol content (> 28 wt%). There is a difference in protein content between these two set of emulsions that in combination with the high ethanol content (> 22 %wt) causes the number density of unadsorbed casein in emulsion 7 and 9 to be reduced at the same time that the density of casein in the interfacial layer is increased. Consequently, less protein remains in the continuous phase, limiting its effectiveness at inducing an osmotic pressure gradient (Radford et al., 2004). Therefore, the depletion forces in emulsions 7 and 9 are weak and the hydrophobic and electrostatic interactions suffice to maintain a finite stability against flocculation even at high ethanol contents. This explanation is also consistent with the fact that the reduction in the hydrodynamic radius of casein micelles is ethanol dependent (Horne & Davidson, 1986); thus, the range and magnitude of the depletion interaction may be reduced at high ethanol concentrations (~ 25-32 %wt ethanol content) because the unadsorbed casein will have a reduced size. The finite stability at high ethanol content is diminished as the casein-oil ratio became larger, as occurred in emulsion 10, because the excess of casein in the continuous phase in combination with high ethanol content will produce aggregation of casein micelles.

The theoretical calculation made in the second approach for the concentration of unadsorbed casein was used to calculate the osmotic pressure, $\mathrm{P_{osm}} = nK_bT(1 + 2\frac{C_b}{\rho_{sm}})$,

equation 12, where the number density of casein molecules, $n = \frac{C_b N_A}{M}$, equation 13, and considering a molecular weight for the casein micelle, M, of 2.5 x 10^8 Da (Dewan et al., 1974; Morr et al., 1973) where N_A corresponds to Avogadro's number, 6 x 10^{23} mol^{-1}. The maximum depletion interaction energy (U_D) when h = 0, was calculated from $U_D = -2\pi R_g^2 P_{osm} \left(a + \frac{2R_g}{3}\right)$, equation 10. The radius of unadsorbed protein (R_g) was selected based on the diameter of casein micelles reported in the literature of 0.2 μm (Dalgleish & Law, 1998; De Kruif, 1999), while the radius of the droplet was set from the droplet size results; essentially emulsions had a mean diameter of 0.5 μm. Therefore R_g was equal to 0.1 μm, a was equal to 0.25 μm. Figure 4.27 shows the attractive depletion energy as a function of ethanol content for sodium caseinate concentrations between 30-70 wt% which corresponds to the range of sodium caseinate content in the region of emulsion stability.

Figure 4.27 illustrates that the depletion interaction energy increased as ethanol was reduced. Also it shows that high concentrations of sodium caseinate in combination with low ethanol content generated larger depletion interaction potentials that lead to flocculated systems which are characterized by high viscosities (Dickinson & Golding, 1997b). Therefore a reduction in ethanol content and an increase in the attractive depletion interaction are reflected in a change in viscosity going from a low viscosity at high ethanol content to a high viscosity at low ethanol content. The calculations of the maximum attractive depletion interaction U_D appear to be consistent with the rheological behavior observed in the region of emulsion stability. But it does not provide a more deep explanation in terms of the effects of ethanol on droplet size distribution.

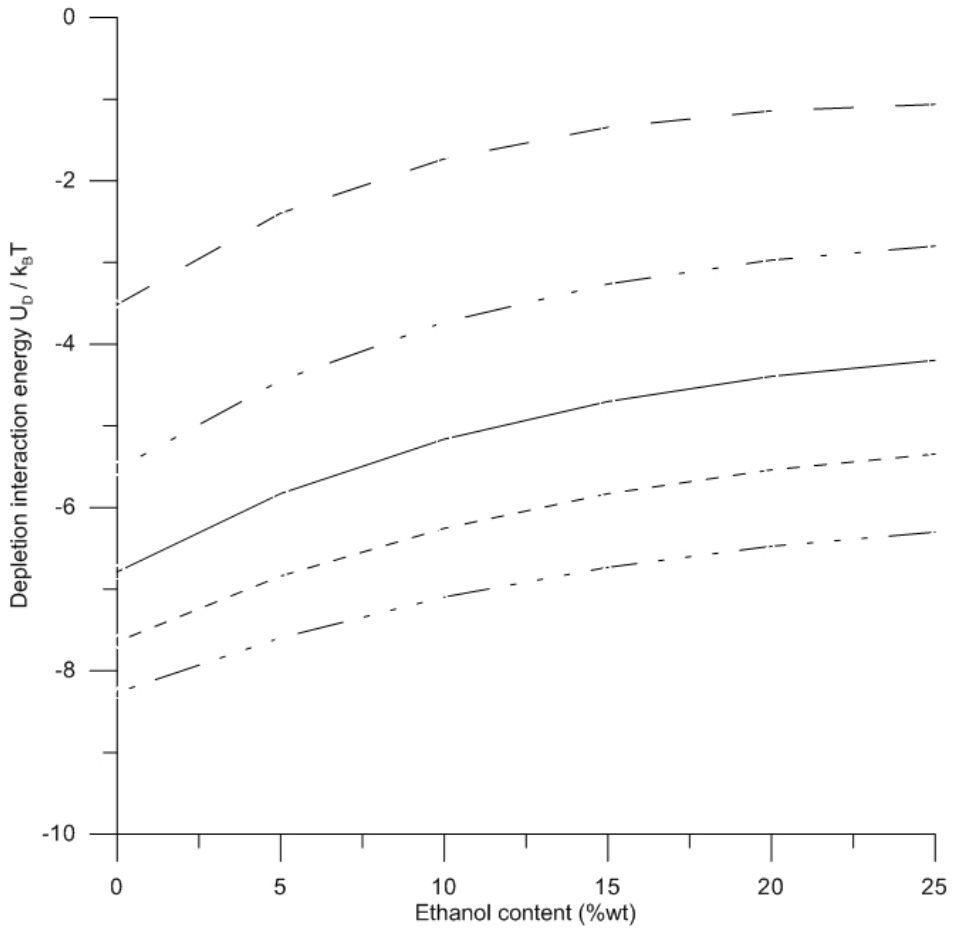

Figure 4.27 Depletion interaction energy (U_D) calculated from equation 10 as a function of ethanol content. Each data series represents calculations made for different emulsion compositions containing a fixed amount of sodium caseinate in solution. Sodium caseinate concentrations from top to bottom: 30 wt%, 40 wt%, 50 wt%, 60 wt% and 70 wt%. U_D is calculated assuming a droplet radius of 0.25 μm, and an unadsorbed casein radius of 0.1 μm. The concentration of unadsorbed casein is calculated considering the protein surface coverage values reported by Radford et al. (2004) for emulsions containing ethanol.

The values of depletion interaction energy obtained from equation 10, assuming unadsorbed casein micelles with a radius of 0.1 μm, were lower in comparison to values of U_D reported in literature. However a direct comparison is not possible because other studies assumed a radius of unadsorbed casein in the range of 5 to 30 nm, and a caseinate stabilized emulsion that contains 4 wt% protein and 30%vol oil (Dickinson & Golding, 1997b; Radford & Dickinson, 2004) which gives values of U_D in the range of -140 to 0 in kT units. A change in number density changes osmotic pressure and that impacts directly on the range of the depletion interaction energy. The reduction in the range of the depletion interaction energy as ethanol increases supports the argument that as ethanol increases the casein present in the continuous phase will tend to migrate to the oil-water interface so that less casein remains in the continuous phase, thus the lower the concentration of unadsorbed casein, C_b , the lower the number density and therefore the lower osmotic pressure and consequently the range of depletion interaction decreases.

The approaches made based on the calculation of the concentration of unadsorbed casein at several emulsion compositions seem to offer a useful interpretation of the influence of ethanol on the distribution of casein micelles between the continuous phase and the interfacial layer.

4.3 Lipid Oxidation Results

A calibration curve made with cumene hydroperoxide according to the procedure described in section 3.2.4.3 was used to calculate the concentration of lipid hydroperoxides in emulsions. Figure 4.28 shows the calibration curve made with 10 points. The lineal equation represented the change in value of absorbance (y axis) for a given concentration of cumene hydroperoxide (x axis). This equation is used to calculate the concentration of hydroperoxides presented in emulsions for a given value of absorbance obtained after running the lipid oxidation test. Thus, the values of lipid hydroperoxides are reported as μmol of hydroperoxides per liter of solvent (μmol L^{-1}). Each point on the graph represents the mean value of five replicates and error bars represent the standard deviation of the corresponding means.

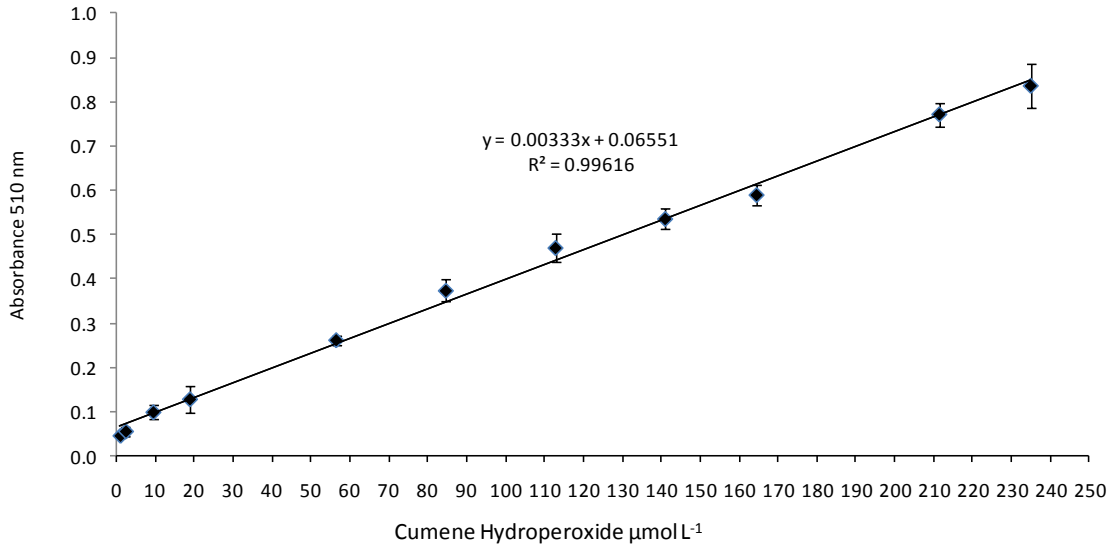

Figure 4.28 Calibration curve for the determination of hydroperoxide content in emulsions using a method proposed by Shantha & Decker (1994) that was slightly modified.

4.3.1. Sodium Caseinate-Canola Oil-Ethanol System

Table 4.7 shows the concentration of lipid hydroperoxides with the respective standard deviation obtained for the 10 emulsions evaluated 72 hours and 30 days after preparation. At 72 hours, emulsions 9 and 10 had the lowest concentration of hydroperoxides as was expected due to the low oil fraction and the high protein content. Samples 1-7 exhibited values in the range ~60 to 80 μmol L^{-1} (solvent). Emulsion 8 showed the highest concentration of lipid hydroperoxides at 72 hours.

Table 4.7 Lipid hydroperoxide concentrations of emulsions made with canola oil after 72 hours and 30 days of storage at 26°C.

	72 hours after preparation	30 days after preparation
Sample	Lipid Hydroperoxide [1] μmol L^{-1}	Lipid Hydroperoxide μmol L^{-1}
1	71.2 ± 6.2	26.4 ± 7.2
2	79.9 ± 0.8	NA
3	54.6 ± 0.3	5.2 ± 5.4
4	77.0 ± 1.3	NA
5	81.8 ± 5.8	15.2 ± 9.1
6	59.4 ± 2.9	11.3 ± 1.8
7	61.8 ± 13.1	54.1 ± 10.0
8	108.6 ± 5.9	6.2 ± 1.5
9	46.7 ± 2.3	20.4 ± 1.9
10	36.2 ± 3.8	NA

1 Mean ± standard deviation (obtained for two independent samples)
NA: Data not available, unstable emulsion

Figure 4.29 shows the concentration of lipid hydroperoxides (μmol L^{-1}) as a function of casein/oil ratio. Each point in the chart represented the mean of two duplicate emulsions

and there are two subsamples in the mean value of each duplicate. The error bars are obtained from the standard deviation of the corresponding means.

The two curves in the Figure 4.29 represented the concentration of lipid hydroperoxides at 72 hours and 30 days after preparation. For the seven samples that remained stable during 30 days storage, the concentration of lipid hydroperoxides decreased with time. The decrease in the concentration of lipid hydroperoxides likely occurred due to changes in protein configuration and the increase in the thickness of the interfacial layer that protects the oil surface. The rate of oxidation is also associated with the oil composition. Canola oil mainly contains unsaturated fatty acids: oleic and linoleic acids, which increase the reactivity of the oil phase with prooxidants; thus the reduction in hydroperoxide concentrations over time can also indicate that the propagation step of the lipid oxidation mechanism described in section 2.3.2 proceeds rapidly during the first 72 hours due to the unsaturated character of the lipid phase. In addition, the low concentration of lipid oxidation products in emulsions 9 and 10 (larger protein/oil ratio) is consistent with studies conducted in oil-in-water emulsions were the concentration of lipid hydroperoxides decreased as the total content of protein increased (section 2.3.3). Figure 4.29 also revealed that there is not a clear relationship between the content of lipid hydroperoxides and casein/oil ratios. Moreover from the results of mean droplet size, some emulsions with small droplet size, such as emulsion 5, 6, 8 had larger amounts of lipid hydroperoxides than other emulsions also with small droplet size like emulsions 9 and 10. Therefore, from these studies, the lipid oxidation stability of emulsions seems to be unaffected by droplet size.

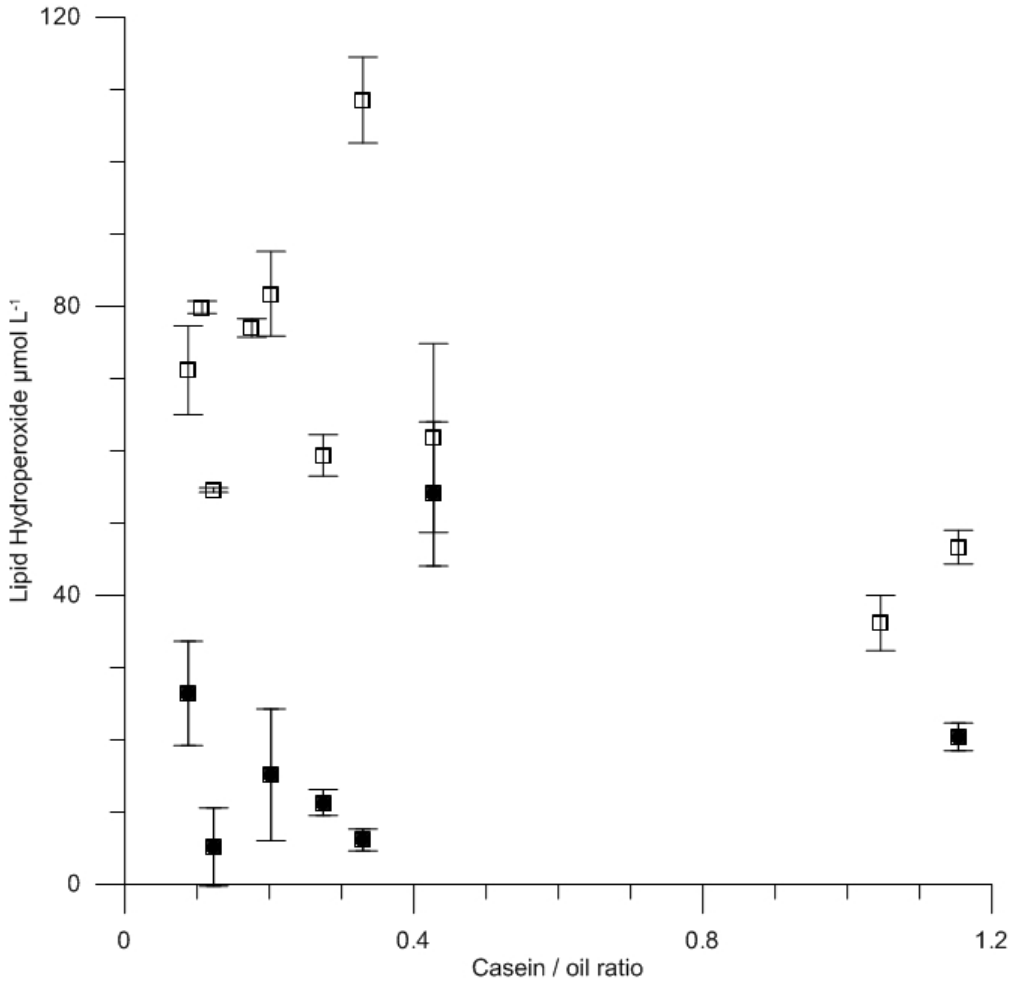

Figure 4.29 Lipid hydroperoxide concentration as a function of casein/oil ratio for emulsions made with canola oil at 72 hours (□) and 30 days after preparation (■). Error bars are obtained from the standard deviation of the corresponding means of two independent samples.

4.3.2. Sodium Caseinate-Coconut Oil-Ethanol System

The results of concentration of lipid hydroperoxides for the 10 samples evaluated are shown in Table 4.8. It can be seen that for all samples after 72 hours the concentration of lipid oxidation products was low (less than 10 µmol L^{-1}), but it increases by several orders of magnitude after 30 days storage. In other words, the formation of hydroperoxides increases over time. For example for emulsion 1, the concentration of lipid hydroperoxides

increases from 6.2 μmol L^{-1} at 72 hours to 21 μmol L^{-1} at 30 days. For other emulsions, the increment in the concentration of lipid hydroperoxides was less marked, like emulsion 9, where the concentration of lipid hydroperoxides was 2 μmol L^{-1} at 72 hours and increased to 5.9 μmol L^{-1} at 30 days. Also, comparing the concentration of lipid hydroperoxides obtained for emulsions made with canola oil versus emulsions made with coconut oil at 72 hours, it can be seen that the extent of lipid oxidation was lower in emulsions made with coconut oil, which was expected due to the saturated character of coconut oil.

The low concentration of lipid hydroperoxides also leads to an increase in the standard deviation of the values reported in Table 4.8 because the values are close to the lower limit of concentrations of hydroperoxides used for the construction of the calibration curve. For the linear regression model applied the error associated with the deviation of the values with the model is high at the lower and upper limits.

Table 4.8 Lipid hydroperoxide concentrations of emulsions made with coconut oil after 72 hours and 30 days of storage at 26°C.

72 hours after preparation		30 days after preparation	
Sample	Lipid Hydroperoxide [1] μmol L^{-1}		Lipid Hydroperoxide μmol L^{-1}
1	6.2 ± 0.3	21.4 ± 5.8	
2	3.1 ± 2.7	25.1 ± 14.1	
3	1.4 ± 0.5	4.3 ± 1.0	
4	6.8 ± 0.8	7.8 ± 4.2	
5	7.7 ± 4.5	10.6 ± 3.7	
6	4.3 ± 4.6	3.2 ± 3.5	
7	6.1 ± 5.4	14.8 ± 10.5	
8	1.0 ± 1.3	NA	
9	2.0 ± 1.7	5.9 ± 0.8	
10	2.5 ± 1.0	NA	

[1] Mean ± standard deviation (obtained for two independent samples)
NA: Data not available, unstable emulsion

Figure 4.30 shows the concentration of lipid hydroperoxides (μmol L^{-1}) as a function of casein/oil ratio for the system sodium caseinate-coconut oil-ethanol. Like for emulsions prepared with canola oil, each point in the chart represented the mean of two duplicate emulsions and there are two subsamples in the mean value of each duplicate. The error bars are obtained from the standard deviation of the corresponding means.

It can be seen in Figure 4.30 that the curve representing the concentration of lipid hydroperoxides at 72 hours had lower values than the curve at 30 days and that there is not a lineal correlation between lipid hydroperoxides and casein/oil ratios. Lower amounts of lipid hydroperoxides were expected due to the content of saturated fatty acids in coconut oil. The increase in lipid oxidation over time may indicate that the interaction of alkyl radicals (L*) and peroxyl radicals (LOO*) in the interfacial layer is favored. Decker et al. (2010) proposed that during storage, lipid oxidation products would increase because lipid hydroperoxides became more polar than the unsaturated lipid where they came from, so that lipid hydroperoxides will tend to move from the oil droplet to the interfacial layer and consequently they will be exposed to prooxidant attack.

It is interesting to notice that emulsions 6, 8, 9 and 10 had similar values in droplet size but showed differences in lipid hydroperoxides concentration at 72 hours. This points out that the influence of droplet size became less important for the oxidation stability of emulsions as reported for some studies conducted in emulsions stabilized by proteins (Lethuaut et al., 2002; Ries et al., 2010)

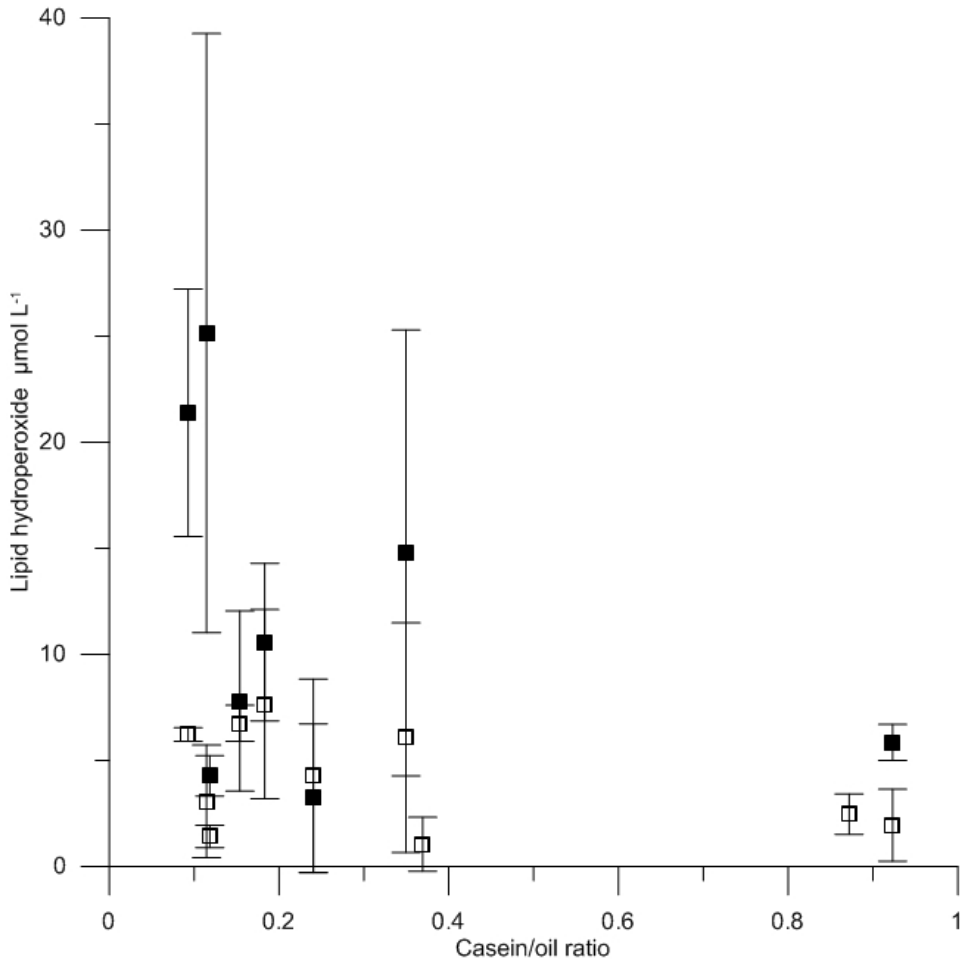

Figure 4.30 Lipid hydroperoxide concentration as a function of casein/oil ratio for emulsions made with coconut oil at 72 hours (□) and 30 days after preparation (■). Error bars are obtained from the standard deviation of the corresponding means of two independent samples.

It should be noticed that for both systems the oils used are refined, which implies itself a low content of free fatty acids, trace metals and tocopherols (Chaiyasit et al., 2007). Since both oils were supplied by local stores, it is also possible that they contained synthetic antioxidants such as BHA (butylated hydroxyanisole) or BHT (tertiary butylated hydroxytoluene). With regards to tocopherols and others antioxidants (BHT and BHA), they can retard the rate of hydroperoxide formation (see section 2.3.4). On the other hand,

free fatty acids and trace metals such as iron enhance the formation of alkyl radicals (L*) that can further promote oxidation (Waraho et al., 2011). Therefore, in addition to the large influence of the size distribution of oil droplets on the surface area of oil, the minor components mentioned above may have a positive or negative effect on the oxidation behavior of the emulsions.

4.3.3. Discussion on Lipid Oxidation

The analytical method used for the determination of lipid hydroperoxides is based on a spectrometric determination of the oxidation of the ferrous ion by the presence of peroxides (Shantha & Decker, 1994). This assay was initially developed to measure the concentration of lipid hydroperoxides in oils (Shantha & Decker, 1994) and then was modified to measure the lipid hydroperoxides in emulsions (Hu et al., 2003). For this purpose, the lipid phase is separated from the continuous phase by using an organic solvent to dissolve the lipid phase which is then separated by centrifugation. A fixed amount of the supernatant is collected and transferred into another organic solvent and the assay is performed. The amount of supernatant taken to react with the ferrous ion is assuming that the emulsion is totally comprised of lipid according to the original paper (Shantha & Decker, 1994). However, in the case of emulsions, only a certain amount of emulsion is lipid. In order to evaluate the effect of changes in emulsions composition on the determination of lipid hydroperoxides, the volume fraction of oil in the 10 samples calculated from equation 3 was used as a correction factor for the lipid oxidation results, so that concentrations of oxidation products is corrected for the amount of oil in the emulsion. The volume fraction of oil includes the corresponding correction in the density of the continuous phase due to the addition of ethanol as described in section 4.2.4. Thus, the concentrations of lipid hydroperoxides were re-calculated as $LOOH\ (\mu molL^{-1}) =$

$LOOH\left(\frac{1}{\phi_{oil}}\right)$ and plotted versus casein/oil ratio. Figure 4.31 shows the calculated lipid hydroperoxide concentration as a function of the casein/oil ratio for emulsions made with canola and coconut oils. The plots show that the trend in the concentration of lipid hydroperoxides changes due to the correction factor. Figure 4.31 indicates that the concentration of lipid hydroperoxides increases as the casein/oil ratio increases while in Figures 4.29 and 4.30 the concentration of lipid hydroperoxides showed a tendency to decrease as the casein/oil ratio increased.

In emulsions stabilized by proteins, authors of studies have remarked that the mechanism of lipid oxidation in oil in water emulsions is sensitive to the composition of the continuous phase (Chaiyasit et al., 2007; Waraho et al., 2011). Thus the rate at which oxidation proceeds may also be influenced by the presence of ethanol. However related studies, where the isolated effects of ethanol on the oxidation stability of sodium caseinate stabilized emulsion have been explored, are not available and therefore the explanations given for the changes in lipid oxidation due to the presence of ethanol are limited. Taking into consideration the results of research projects that had evaluated the oxidation stability of protein stabilized emulsions when the range of pH of the continuous phase is near to 7 so that droplets are negatively charged (Chaiyasit et al., 2007; Waraho et al., 2011), it seems possible that changes in the polarity of the continuous phase when ethanol is added may also produce droplets that are negatively charged and therefore the interaction between cationic metals and anionic lipids is enhanced so that the formation of lipid hydroperoxides is favored. Nevertheless, the influence of ethanol on the oxidation stability is not directly explainable in a facile manner, other factor such as protein content, and thickness of the interfacial layer have an impact on the generation of peroxyl radicals (LOO*) and therefore in the rate of lipid oxidation. As was mentioned in section 2.3, thicker barriers protect the oil droplets against the attack of prooxidants. It has been discussed

that emulsions containing ethanol have a large protein surface coverage which in turn increases the thickness of the interfacial layer. Therefore, it is possible that the rate of lipid oxidation in emulsions containing ethanol is delayed at high ethanol contents.

In summary, it is not clear which of the factors mentioned above have a major impact on the lipid oxidation mechanism, thus it is difficult to forecast a lipid oxidation rate for a given emulsion composition. Moreover, the lipid oxidation test has shown some limitations of use in emulsions containing ethanol.

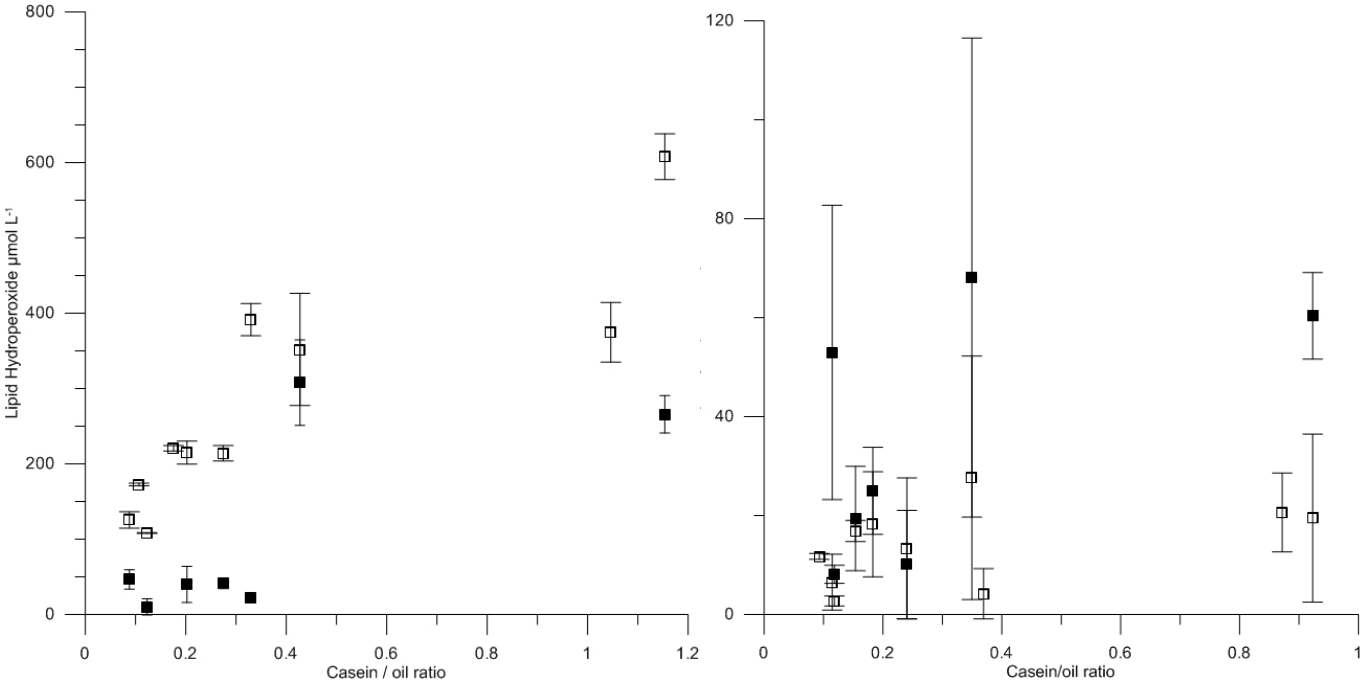

(a) (b)

Figure 4.31 Calculated lipid hydroperoxide concentration considering a correction factor due to the changes in oil volume fraction for emulsion made with canola oil (a) and with coconut oil at (b) 72 hours (□) and 30 days after preparation (■). Error bars are obtained from the standard deviation of the corresponding means of two independent samples.

5. Conclusions

In this project, the phase diagrams for the systems: sodium caseinate-canola oil-ethanol and sodium caseinate-coconut oil-ethanol were generated and the region of emulsion stability was established. The region of emulsion stability for emulsions made with canola oil was slightly larger than for emulsions made with coconut oil; the difference was found at high oil contents (~ 60%wt) where emulsions made with coconut oil were unstable towards creaming and phase separation. In general, the range of emulsion composition for the stable region was limited to concentrations of sodium caseinate in solution between 32-68 %wt, oil concentrations in the range of 10-53 %wt and ethanol contents from 8 to 32 %wt. The main unstable behaviors observed in the region of emulsion stability during storage for 30 days were: phase separation, creaming and neck plug formation. Neck plug formation seems sensitive to emulsion compositions as supported from the stability observations where the thickness of the plug formed at the surface of the emulsion was relatively higher in emulsions made with large amounts of oil (> 30 %wt).

The influence of ethanol in altering the rheological behavior was discussed in terms of the best model fitted to the shear flow curves at 72 hours and 30 days after preparation. Emulsions in the region of emulsion stability were classified as Newtonian fluids, and the viscosity values were highly dependent on the amount of ethanol added, a result also observed by Dickinson & Golding (1998). As ethanol content increased with the respective changes in casein/oil ratio, a decrease in viscosity was observed. Further reduction in ethanol concentrations and increments in oil concentrations produced an increase in viscosity although emulsions remained as Newtonian fluids. The driving mechanism presented to describe the influence of ethanol on the rheological behavior was based on the influence of ethanol in altering the properties of casein micelles, that is, collapse of the k-casein layer and changes in hydrophobic interactions. These changes lead to an

increase in protein-protein interactions and enhance migration of casein micelles from the continuous phase to the interfacial layer. The overall result is an increase in the thickness of the interfacial layer and a reduction in the number density of unadsorbed casein (Radford et al., 2004). The reduction in the number density of unadsorbed casein leads to a decrease in the strength of the depletion flocculation process. Since flocculation is the mechanism responsible for non-Newtonian flow behavior, the retarding of flocculation leads to emulsions exhibiting a Newtonian behavior.

From the results of droplet size distribution, a dependence between droplet size and ethanol content was postulated. Plots on the phase diagram lines indicated the changes in the mean droplet size occurred as ethanol and casein/oil ratios changed. Emulsions with large droplet sizes, which correspond to emulsions made with ethanol contents > 20 %wt, were located on the right hand side of the region of emulsion stability. Emulsions with small droplet sizes, corresponding to emulsions made with low amounts of ethanol, < 20 %wt, were located on the left hand side of the region of emulsion stability. Also the large value of mean droplet diameter obtained at 72 hours and the unimodal distribution obtained for emulsions that were unstable during storage time, was attributed to Ostwald ripening as reported in studies conducted to evaluate the stability of sodium caseinate stabilized emulsions (Hemar & Horne, 1999; Radford et al., 2004)

The results of emulsion characterization provided evidence that ethanol led the changes observed in emulsion stability. It was suggested that there is a redistribution of casein micelles between the continuous phase and the oil-in-water interface as ethanol is added. Depletion flocculation caused by the exclusion of casein micelles from the interstitial space created between two adjacent droplets was observed to depend on ethanol content and emulsion composition. Using the results of droplet size, and considering the increase in surface coverage as ethanol increases that has been reported by Radford et al. (2004), it

was possible to generate a phase diagram that shows the minimum concentrations of unadsorbed casein needed to generate an osmotic pressure gradient that will potentially induce depletion flocculation. This analysis was useful for understanding the influence of ethanol on the reduction of the concentration of unadsorbed casein in the continuous phase. The phase diagram was used to explain the zone of emulsion stability found at high ethanol levels (i.e., emulsion composition in the range of emulsions 7 and 9). The explanation was that the high level of ethanol promotes protein migration to the interfacial layer, and consequently less protein remains in the continuous phase, which in turn reduces the osmotic pressure gradient and therefore decreases the strength of depletion flocculation (Radford et al., 2004). From the theoretical model of depletion flocculation, the calculation of the maximum depletion interaction energy (U_D) was made for a large range of emulsion compositions within the region of emulsion stability. The results supported the statement that depletion interaction is reduced as ethanol content increases and that emulsions made with high levels of protein and low levels of ethanol had high depletion interaction energies.

The results of concentration of lipid hydroperoxides obtained from the two systems provide evidence that the oil distribution on the oil surface influences the production of hydroperoxides during storage. Canola oil, which contains long chains of unsaturated fatty acid, showed more reactivity to oxidation at 72 hours compared to coconut oil. However the fact that there was not a clear correlation between casein/oil ratio and concentration of hydroperoxides suggested that regardless of the type of oil, emulsions characteristics such as protein surface coverage and the presence of ethanol in the continuous phase may affect the formation of oxidative products. The discussion presented in terms of the adequacy of the analytical assay used in this work pointed out that the method seems unsatisfactory for high casein/oil ratios. Thus, more studies are needed to evaluate a

potential effect of ethanol in the production of lipid hydroperoxides and to confirm the limitation of the analytical method when the determination of lipid hydroperoxides is conducted in emulsions made with high oil fractions.

References

Agboola, S., & Dalgleish, D. (1996). Effects of pH and ethanol on the kinetics of destabilization of oil-in-water emulsions containing milk proteins. Journal of the Science of Food and Agriculture, 72(4), 448-454.

Asakura, F., & Oosawa, S. (1954). Surface tension of high-polymer solutions. Journal of Chemical Physics, 22, 1255.

Banks, W., & Muir, D. (1985). Effect of alcohol content on emulsion stability of cream liqueurs. Food Chemistry, 18(2), 139-152.

Banks, W., Muir, D., & Wilson, A. (1981). Extension of the shelf-life of cream-based liqueurs at high ambient-temperatures. Journal of Food Technology,16(6),587-595.

Belda, R., Herraez, J.V., & Diez, O. (2004). Rheological and Thermodynamic analysis of the binary system (water/ethanol): Influence of concentration. Physics and Chemistry of Liquids, 42 (5), 467-479.

Berli, C.L.A, (2008). Rheology and phase behavior of aggregating emulsions related to droplet-droplet interactions. Brazilian Journal of Chemical Engineering, 24 (2) 203-210.

Berli, C. L. A., Quemada, D., & Parker, A. (2002). Modelling the viscosity of depletion flocculated emulsions. Colloids and Surfaces A: Physicochemical and Engineering Aspects, 203(1-3), 11-20.

Berlin, E., & Pallansch, M. J. (1968). Densities of several proteins and L-amino acids in the dry state. The Journal of Physical Chemistry, 72(6), 1887-1889.

Bouchoux, A., Debbou, B., Gesan-Guiziou, G., Famelart, M. -., Doublier, J. -., & Cabane, B. (2009). Rheology and phase behavior of dense casein micelle dispersions. Journal of Chemical Physics, 131,16.

Casanova, H., & Dickinson, E. (1998). Rheology and flocculation of oil-in-water emulsions made with mixtures of αs_1-casein + β-casein. Journal of Colloid and Interface Science, 207(1), 82-89.

Chaiyasit, W., Elias, R.J., McClements, D.J. & Decker, A.E. (2007). Role of physical structures in bulk oils on lipid oxidation. Critical Reviews in Food Science and Nutrition, 47, 299-317.

Chantrapornchai, W., Clydesdale, F. M., & McClements, D. J. (2001). Influence of relative refractive index on optical properties of emulsions. Food Research International, 34(9), 827-835.

Cho, J.Y, Alamed, J., McClements, D.J, & Decker, E.A (2003) Physical location and prooxidants activity of iron in oil-in-water emulsions. Journal of Food Science, 68, 1952-1957.

Dahbi, L., Alexander, M., Trappe, V., Dhont, J. K. G., & Schurtenberger, P. (2010). Rheology and structural arrest of casein suspensions. Journal of Colloid and Interface Science, 342(2), 564-570.

Dalgleish D.G., Srinivasan, M. & Singh, H. (1995). Surface properties of oil-in-water emulsions droplets containing casein and tween 60. Journal of Agricultural and Food Chemestry, 43, 2351-2355.

Dalgleish, D.G. & Law, J.R. (1988). Sodium Caseinates-Composition and properties of different preparations. Journal of the Society of Dairy Technology, 41 (1), 1-4.

Dauphas, S., Amestoy, M., Llamas, G., Anton, M., & Riaublanc, A. (2008). Modification of the interactions between β-casein stabilised oil droplets with calcium addition and temperature changing. Food Hydrocolloids, 22(2), 231-238.

De Kruif, C. G. (1998). Supra-aggregates of casein micelles as a prelude to coagulation. Journal of Dairy Science, 81(11), 3019-3028.

De Kruif, C. G. (1999). Casein micelle interactions. International Dairy Journal, 9(3-6), 183-188.

Decker, E.A, Alamed, J., & Castro, A.I. (2010) Interaction between polar components and the degree of unsaturation of fatty acids on the oxidative stability of emulsions. Journal of American Oil Chemists Society, 87, 771-780.

Dewan, R. K., Chudgar, A., Mead, R., Bloomfield, V.A., & Morr, C.V. (1974). Molecular weight and size distribution of bovine milk casein micelles. Biochimica et Biophysica Acta (BBA), 2, 313-321.

Dickinson, E. (1999). Caseins in emulsions: Interfacial properties and interactions. International Dairy Journal, 9(3-6), 305-312.

Dickinson, E. (2001). Milk proteins interfacial layers and the relationship to emulsion stability and rheology. Colloids and Surfaces, 20, 197-210.

Dickinson, E. (2009). Hydrocolloids as emulsifiers and emulsion stabilizers. Food Hydrocolloids, 23(6), 1473-1482.

Dickinson, E.(1997). Properties of emulsions stabilized with milk proteins: Overview of some recent developments. Journal of Dairy Science, 10, 2607-2618.

Dickinson, E., & Golding, M. (1997). Depletion flocculation of emulsions containing unadsorbed sodium caseinate. Food Hydrocolloids, 11(1), 13-18.

Dickinson, E., & Golding, M. (1997b). Rheology of sodium caseinate stabilized oil-in-water emulsions. Journal of Colloid and Interface Science, 191(1), 166-176.

Dickinson, E., & Golding, M. (1998). Influence of alcohol on the stability of oil-in water emulsion containing sodium caseinate. Journal of Colloid and Interface Science, 197,133-141.

Dickinson, E., & Woskett, C. M. (1988). Effect of alcohol on adsorption of casein at the oil—water interface. Food Hydrocolloids, 2(3), 187-194.

Dickinson, E., Golding, M., & Povey, M. J. W. (1997). Creaming and flocculation of oil-in-water emulsions containing sodium caseinate. Journal of Colloid and Interface Science, 185(2), 515-529

Dickinson, E., Narhan, S. K., & Stainsby, G. (1989). Stability of alcohol-containing emulsions in relation to neck-plug formation in commercial cream liqueurs. Food Hydrocolloids, 3(2), 85-100.

Dickinson, E., Narhan, S. K., & Stainsby, G. (1989b). Factor affecting the properties of cohesive cream formed from cream liqueurs. Journal of the Science of Food and Agriculture , 48 (2), 225-239.

Dickinson, E., Radford, S. J., & Golding, M. (2003). Stability and rheology of emulsions containing sodium caseinate: Combined effects of ionic calcium and non-ionic surfactant. Food Hydrocolloids, 17(2), 211-220.

Dickinson, E., Ritzoulis, E., Yamamoto, Y., & Logan, H. (1999). Ostwald ripening of protein-stabilized emulsions: effect of trasglutaminase crosslinking. Colloids and Surfaces, 12, 139-146.

Donnelly, W., (1987). Ethanol stability of casein solutions as related to storage stability of dairy-based alcoholic beverages. Journal of Food Science, 52 (2), 389- 393.

Elysée-Collen, B. & Lencki, R., (1996). Protein ternary phase diagrams.2.Effect of ethanol ammonium sulfate, and temperature on the phase behavior of (S)-Ovalbumin. Journal of Agricultural and Food Chemistry, 44, 1658-1663.

Euston, S. R., & Hirst, R. L. (1999). Comparison of the concentration-dependent emulsifying properties of protein products containing aggregated and non-aggregated milk protein. International Dairy Journal, 9(10), 693-701.

Euston, S.R., & Mayhill, P.G. (2001). Time and temperature-dependent changes in the adsorbed layer on caseinate-stabilized emulsion droplets. Food Research International, 34, 369-376.

Fang, Y., & Dalgleish, D. G. (1993). Dimensions of the adsorbed layers in oil-in-water emulsions stabilized by caseins. Journal of Colloid and Interface Science, 156(2), 329-334.

Farrer, D., & Lips, A. (1999). On the self-assembly of sodium caseinate. International Dairy Journal, 9, 281-286.

FDA (Food and Drug Administration in United States) List of Food Aditive Status Part ihttp://www.fda.gov/Food/FoodIngredientsPackaging/FoodAdditives/FoodAdditiveListings/ucm091048.htm

Fleer, G.J, Scheutjens, B., Vincent, B. (1984). The stability of dispersions of hard spherical particules in the presence of nonadsorbing polymer. ACS symposium series, 240, 245-263.

Fredrick, E., Walstra, P., & Dewettinck, K. (2010). Factors governing partial coalescence in oil-in-water emulsions. Advances in Colloid and Interface Science, 153(1-2), 30-42.

Griffin, M., & Griffin, W. (1985). A simple turbidimetric method for the determination of the refractive- index of large colloidal particles applied to casein micelles. Journal of Colloid and Interface Science, 104(2), 409-415.

Gustone, F., (2008). Oils and Fats in the Food Industry, Ed.,Wiley-Blackwell; pp 2.

Hemar, Y., & Horne, D. (1999). A diffusing wave spectroscopy study of the kinetics of Ostwald ripening in protein-stabilised oil/water emulsions. Colloids and Surfaces B: Biointerfaces, 12, 239-246.

Hemar, Y., Pinder, D. N., Hunter, R. J., Singh, H., Hébraud, P., & Horne, D. S. (2003). Monitoring of flocculation and creaming of sodium-caseinate-stabilized emulsions using diffusing-wave spectroscopy. Journal of Colloid and Interface Science, 264(2), 502-508.

Holt, C., & Horne, D., (1996). The hairy casein micelle: Evolution of the concept and its implications for dairy technology. Netherlands Milk and Dairy Journal, 50 (2), 85-111.

Horne, D. (1984). Steric effects in the coagulation of casein micelles by ethanol. Biopolymers , 23, 989-993.

Horne, D. (1985). Steric stabilization and casein micelle stability. Journal of Colloid and Interface Science, 111(1), 250-260.

Horne, D. (1987). Ethanol stability of casein micelles-a hypothesis concerning the role of calcium phosphate. Journal of Dairy Research, 54 (3), 389-395.

Horne, D. (1998). Casein interactions: Casting light on the black boxes, the structure in dairy products. International Dairy Journal, 8(3), 171-177.

Horne, D. (2006). Casein micelle structure: Models and muddles. Current Opinion in Colloid and Interface Science, 11, 148-153.

Horne, D., & Davidson, C., (1986). The effect of environmental conditions on the steric stabilization of casein micelles. Colloid and Polymer Science, 264, 727-734.

Horne, D., & Muir, D. (1990). Alcohol and Heat Stability of Milk Protein. Journal of Dairy Science, 73 (12), 3613-3626.

Hu, M., McClements, D. J., & Decker, E. A. (2003). Lipid oxidation in corn oil-in-water emulsions stabilized by casein, whey protein isolate, and soy protein isolate. Journal of Agricultural and Food Chemistry, 51(6), 1696-1700.

Husband, F.A.; Wilde, P.J.; Mackie, A.R., Garrood, M.J. (1997). A comparison of the functional and interfacial properties of β-casein and dephospohorylate β-casein. Journal of Colloid and Interface Science, 195, 77-85.

Jenkins, P., Snowden, M. (1996). Depletion flocculation in colloidal dispersions. Advances in Colloid and Interface Science, 68, 57-96.

Kellerby, S. S., McClements, D. J., & Decker, E. A. (2006). Role of proteins in oil-in-water emulsions on the stability of lipid hydroperoxides. Journal of Agricultural and Food Chemistry, 54(20), 7879-7884.

Kim, H. -., Decker, E. A., & McClements, D. J. (2004). Influence of free protein on flocculation stability of β-lactoglobulin stabilized oil-in-water emulsions at neutral pH and ambient temperature. Langmuir, 20(24), 10394-10398.

Lampi, A.M., Kataja, L., Eldin, A.K., & Vieno, P. (1999). Antioxidant activities of α- and γ-tocopherols in the oxidation of rapesedd oil triacylglycerols. Journal of the American Oil Chemists Society, 76 (6), 749-755.

Lethuaut, L., Métro, F., & Genot, C. (2002). Effect of droplet size on lipid oxidation rates of oil-in-water emulsions stabilized by protein. Journal of the American Oil Chemists Society, 79, 425-430.

Lifshitz, I.M & Slyozov, V.V.(1961). The kinetics of precipitation from supersaturated solid solutions. Journal of Physics and Chemistry of Solids, 2, 35-50.

Lucey, A..J., Srinivasan, M., Singh, H. & Munro, P.A. (2000). Characterization of commercial and experimental sodium caseinates by multiangle laser light scattering and size-exclusion chromatography. Journal of Agricultural and Food Chemistry, 48.1610-1616.

Lynch, A., & Mulvihill, D. (1997). Effect of sodium caseinate on the stability of cream liqueurs. International Journal of Dairy Technology, 50 (1), 1-7.

Malvern Instruments Ltd., (2007). Mastersizer 2000 user manual. England; Chapter 9,pp 9-5.

Mao, Y., Cates, M. E., & Lekkerkerker, H. N. W. (1995). Depletion force in colloidal systems. Physica A: Statistical and Theoretical Physics, 222(1-4), 10-24.

Marangoni, A. G., & Lencki, R.W., (1998). Ternary phase behavior of milk fat fractions. Journal of Agricultural and Food Chemistry, 46 (10), 3879-3884.

McClements, D.J. 2004. Food Emulsions: Principles, practices, and techniques, CRC Press United States of America.

McClements, D.J. (2007). Critical review of techniques and methodologies for characterization of emulsion stability. Journal of Food Science and Nutrition, 47 (7), 611-649.

Medina-Torres, L., Calderas, F., Gallegos-Infante, J. A., González-Laredo, R. F., & Rocha-Guzmán, N. (2009). Stability of alcoholic emulsions containing different caseinates as a function of temperature and storage time. Colloids and Surfaces A: Physicochemical and Engineering Aspects, 352(1-3), 38-46.

Mezdour, S., & Korolczuk, J. (2010). Particle size distribution of sodium caseinate in water-ethanol solutions. MILCHWISSENSCHAFT-Milk Science International, 65,2, 148-150.

Mezdour, S., Brule, G., & Korolczuk, J. (2006). Physicochemical analysis of casein solubility in water-ethanol solutions. LAIT, 86(6), 435-452.

Mimouni, A., Deeth, H. C., Whittaker, A. K., Gidley, M. J., & Bhandari, B. R. (2009). Rehydration process of milk protein concentrate powder monitored by static light scattering. Food Hydrocolloids, 23(7), 1958-1965.

Min, D.B., & Boff, J.M. (2002). Lipid oxidation of edible oil in Food Lipids: Chemistry, Nutrition, and Biotechnology, Eds: Akoh,C.C and Min, D.B. Ed: CRC Press.

Mohan, S., & Narsimhan, G. (1997). Coalescence of protein-stabilized emulsions in high-pressure homogenizer. Journal of Colloid and Interface Science, 192, 1-15.

Morr, C.V., Lin, S. H., Dewan, R.K & Bloomfield, V.A (1973). Molecular weights of fractionated bovine milk casein micelles from analytical ultracentrifugation and diffusion measurements. Journal of Dairy Science, 56, 415-418

Muir, D., & Banks, W. (1986). Technical note: Multiple homogenization of cream liqueurs. Journal of Food Technology, 21 (2), 229-232.

Noskow, S.Y., Lamoureux, G., & Roux, B. (2005). Molecular dynamics study of hydration in ethanol-water mixtures using a polarizable force field. Journal of Physical Chemistry B, 109, 6705-6713.

O'Kennedy,B. (2001).Stability of sodium caseinate to ethanol. MILCHWISSENSCHAFT-Milk Science International, 56 (2), 680-684.

Pantzaris, T.P., & Basiron, Y. (2000). The lauric (coconut and palmkernel) oils in Vegetable Oil in Food Technology, Gunstone, D., Ed.; CRC Press; pp182.

Parkinson, E. L., & Dickinson, E. (2004). Inhibition of heat-induced aggregation of a β-lactoglobulin-stabilized emulsion by very small additions of casein. Colloids and Surfaces B: Biointerfaces, 39(1-2), 23-30.

Perry, R,H & Green, D,W. 1997. Perry's Chemical Engineers' Handbook, McGraw-Hill United States of America.

Pierre, A. (1989). Milk stability in ethanolic solutions. Journal of Dairy Research, 56, 521-527.

Pitkowski, A., Durand, D., & Nicolai, T. (2008). Structure and dynamical mechanical properties of suspensions of sodium caseinate. Journal of Colloid and Interface Science, 326(1), 96-102.

Predel, B., Hoch, M., & Monte, P. (2004). Phase diagrams and heterogeneous equilibria, a practical introduction, Springer Germany; pp 143-145.

Przybylski, R., & Mag, T. (2000). Canola/rapeseed oil in Vegetable Oil in Food Technology, Gunstone, D., Ed.; CRC Press; pp111.

Radford, S. J., Dickinson, E., & Golding, M. (2004). Stability and rheology of emulsions containing sodium caseinate: Combined effects of ionic calcium and alcohol. Journal of Colloid and Interface Science, 274(2), 673-686.

Radford, S.J. & Dickinson, E. (2004). Depletion flocculation of caseinate-stabilised emulsions: what is the optimum size of the non-adsorbed protein nano-particles?.Colloids and Surfaces A: Physicochemical and Engineer Aspects, 238, 71-81.

Ries, D., Ye, A., Haisman, D., & Singh, H. (2010). Antioxidant properties of casein and whey proteins in model oil-in-water emulsions. International Dairy Journal, 20, 72-78.

Robson, E., & Dalgleish, D.G. (1987). Interfacial Composition of Sodium Caseinate Emulsions. Journal of Food Science, 52 (6), 1694-1698.

Schwartz, H., Ollilainen, V., Piironen, V.,& Lampi, A.M. (2008). Tocopherol,tocotienol and plant sterol contents of vegetables oil and industrial fats. Journal of Food Composition and Analysis, 21, 152-161.

Shantha, N. C., & Decker E.A. (1994). Rapid, sensitive, iron-based spectrophotometric methods for determination of peroxide values of food lipids. Journal of AOAC International, 77(2), 421-424.

Silva, C., Sanaiotti, G., Lanza, M., Follegatii-Romero, L., Meirelles, J., Batista, E. (2010). Mutual solubility for systems composed of vegetable oil + ethanol + water at different temperatures. Journal of Chemical Engineer Data, 55, 440-447.

Sperry, P.R. (1984). Morphology and mechanism in latex flocculated by volume restriction. Journal of Colloid and Interface Science, 99 (1), 97-108.

Srinivasan, M., Singh, H., & A. Munro, P. (1999). Adsorption behavior of sodium and calcium caseinates in oil-in-water emulsions. International Dairy Journal, 9(3-6), 337-341.

Sugiarto, M., Ye, A., Taylor, M.W., Harjinder, S. (2010). Milk protein-iron complexes: Inhibition of lipid oxidation in an emulsion. Journal of Dairy Science and Technology, 90, 87-98.

Thurgood, J., Ward, R., & Martini, S. (2007). Oxidation kinetics of soybean oil/anhydrous milk fat blends: A differential scanning calorimetry study. Food Research International, 40(8), 1030-1037.

Tuinier, R., & De Kruif, C.G. (1999). Phase behavior of casein micelles/exocellular polysaccharide mixtures: Experiment and theory. Journal of Chemical Physics, 10 (18), 9296-9304.

Vasquez, G., Alvarez, E., & Navaza, J. (1995). Surface tension of alcohol + water from 20 to 50°C. Journal of Chemical & Engineering Data, 40, 611-614.

Vincent, B. (1990). The calculation of depletion layer thickness as a function of bulk polymer concentration. Colloids and Surfaces, 50, 241-249.

Vrij, A. (1976) Polymers at interfaces and the interactions in colloidal dispersions. Pure and Applied Chemistry, 48, 471-483.

Wagner, C. (1961). Ostwald Rippening (Ostwlad-Reifung). Zeitshrift fur Elecktrochemie, 65, 581-591.

Walz, J. Y., & Sharma, A. (1994). Effect of long range interactions on the depletion force between colloidal particles. Journal of Colloid and Interface Science, 168(2), 485-496.

Waraho, T., McClements, D. J., & Decker, E. A. (2011). Mechanisms of lipid oxidation in food dispersions. Trends in Food Science & Technology, 22(1), 3-13.

Ye, A. (2008). Interfacial composition and stability of emulsions made with mixtures of commercial sodium caseinate and whey protein concentrate. Food Chemistry, 110(4), 946-952.